NOTICE

The quality of this microform is heavily dependent upon the quality of the original thesis submitted for microfilming. Every effort has been made to ensure the highest quality of reproduction possible.

If pages are missing, contact the university which granted the degree.

Some pages may have indistinct print especially if the original pages were typed with a poor typewriter ribbon or if the university sent us an inferior photocopy.

Previously copyrighted materials (journal articles, published tests, etc.) are not filmed.

Reproduction in full or in part of this microform is governed by the Canadian Copyright Act, R.S.C. 1970, c. C-30.

AVIS

La qualité de cette microforme dépend grandement de la qualité de la thèse soumise au microfilmage. Nous avons tout fait pour assurer une qualité supérieure de reproduction.

S'il manque des pages, veuillez communiquer avec l'université qui a conféré le grade.

La qualité d'impression de certaines pages peut laisser à désirer, surtout si les pages originales ont été dactylographiées à l'aide d'un ruban usé ou si l'université nous a fait parvenir une photocopie de qualité inférieure.

Les documents qui font déjà l'objet d'un droit d'auteur (articles de revue, tests publiés, etc.) ne sont pas microfilmés.

La reproduction, même partielle, de cette microforme est soumise à la Loi canadienne sur le droit d'auteur, SRC 1970, c. C-30.

Canada

Load Distribution Characteristics of A Slab-on-girder Bridge Model At Ultimate

by

Ezeedin Galuta

A thesis
submitted to the University of Ottawa in
fulfillment of the thesis requirements
for the degree of
Master of Applied Science
in
Civil Engineering

Ottawa, Ontario
March, 1988

ISBN 0-315-46775-4

UNIVERSITÉ D'OTTAWA
UNIVERSITY OF OTTAWA

Abstract

This thesis is concerned with the overload behavior of a composite continuous slab-on-girder bridge model consisting of four steel girders supporting a cast-in-place reinforced concrete deck . The purpose of this thesis was not to develop any method of post-elastic design and analysis, but rather to explore certain aspects of the post-elastic behavior to determine how they might affect the responses at ultimate limit state . Progressive plastification of the bridge under increasing load were studied, as well as actual collapse due to excessive deflection and rotation .

A nonlinear finite element program "ADINA" was used to study the load distribution characteristics, nonlinear behavior, and to develop the load distribution factors for the ultimate limit state which include load redistribution in both tansverse and longitudinal directions .

Acknowledgements

The auther wishes to express his gratitude to his supervisor, Dr. M.S. Cheung . His continuous guidance, helpful suggestions, and encouragement during the course of study is sincerely appreciated . Also I would like to thank Mr. H. Hachem for his help in using ADINA .

The author is also indebted to the computer center and Vanier library for their cooperation.

Dedication

To my parents.

Nomenclature

A_g	Area of the steel girder.
A'_s	Area of the reinforcing steel in the slab .
A_w	Area of the web of the steel girder.
B	Actual width of slab overhang .
B_e	Effective width of slab overhang .
b	Half bridge width .
b_e	Effective total width of concrete slab .
b_f	Total width of concrete slab .
C_f	A correction factor used to adjust the D value .
D	Transverse load distribution factor .
D_d	Design elastic load distribution factor .
D_x	The longitudinal flexural rigidity per unit width .
D_y	The transverse flexural rigidity per unit length .
D_{xy}	The longitudinal torsional rigidity per unit width.
D_{yx}	The transverse torsional rigidity per unit length .
D_1	The coupling rigidity per unit width .
D_2	The coupling rigidity per unit length .
d	overall heigth of steel girder .
E	Modulus of elasticity .
E_c	Modulus of elasticity of concrete .
E_s	Modulus of elasticity of steel .
F_y	Yield stess of steel .
f	Load factor .

f'_c	Compressive strenght of concrete .
f_y	Yield stess of reinforcing steel .
G	Shear modulus .
H	The effective torsional rigidity .
h	Clear depth between flanges .
I	Moment of inertia of a section .
J	Torsional inertia of a section .
L	Span length .
M	Longitudinal moment at a section .
M^+	Positive or sagging moment at a section .
M^-	Negative or hogging moment at a section .
M_g	Moment resisted by one girder .
M_p	Simple plastic moment of a section.
M_y	Yield moment of a section.
S	Girder spacing .
t	Thickness of the flange .
w	Thickness of the web .
α, θ	charaterizing parameters for load distribution .
μ	A parameter defined in section 2.4 .
ν	Poisson's ratio .
ψ	Longitudinal distribution factor.

Contents

List of Figures

List of Tables

Chapter 1

INTRODUCTION

For more than thirty years now, composite slab-on-girder bridges have been one of the most popular bridge types in the short to medium span range. A large number of these bridges were built in Ontario and the rest of North America with rapid expansion of the infrastructure over this period. In that time span, however, legal load limits have increased significantly, to the point where in some cases they are greater than the loads for which these bridges were designed. Although the generally satisfactory performance of these structures indicate that they have sufficient capacity to support these service loads, current analytical methods used in bridge design often indicate a level of safety against failure less than the minimum acceptable by today's design standards.

In the field of bridge design, current practice is to use elastic method of

analysis to determine the distribution of force effects, while the capacities are set equal to the ultimate resistances of the various components which imply inelastic behavior. In addition, the capacity of the structure is normally limited to that load at which the first section reachs its capacity based on these elastic strength calculations. A reserve of capacity between first yield and complete collapse will usually exist. In a highly redundant structure such as a multi-span continuous composite slab-on-girder bridge, the magnitude of that reserve capacity could be significant. If post-elastic methods were available to determine the magnitude of this strength reserve, the ultimate capacities of many of these old structures would no longer be in question. We could confidently leave them in service for many more years at considerable savings. Significant savings could also be realised in the design of new structures by exploiting some of this post-elastic strength reserve. As a result, a more uniform level of safety prior to collapse would apply to different structures leading to better overall economy.

The present AASHTO specification criteria for wheel load distribution in highway bridge does not provide a uniform and consistent approach for determination of transverse load distribution factors in a broad range of commonly utilized short and medium span highway bridge structures. The AASHTO load distribution factors are different for different bridge types. This may be due to the absence of some significant parameters(bridge width-span ratio, bending and torsional moments of inertia of girders, composite and non-composite behavior, stiffness and spacing of diaphragms, boundary conditions, etc...) in the equations that are being used .

The introduction of limit states design philosophy and the ever growing demand for higher permissible loads for overload vehicles or special permit vehicles necessitates a thorough investigation of the behavior and live load distribution characteristics of bridges beyond the working stress range. Evaluation of the live load moment at ultimate utilizing elastic load distribution factors is neither realistic nor logical, as the distribution factors should reflect the actual structure/load response at that stage, such as nonlinear behavior and load redistribution due to yielding. At the ultimate state, the transverse distribution of vehicle loads could be significantly different from that to the serviceability limit state. At present, many codes which require consideration of the ultimate limit state, still permit linear elastic analysis for this limit state. The main reason for this apparent discrepancy is the lack of experimental results and easy to apply methods of analysis which can account for the nonelastic behavior of bridges at the ultimate limit state. However, the true behavior of the bridge and its distribution characteristics at ultimate are critical and important to a bridge designer, especially when assessing and up-grading existing bridges.

Although several authors have studied load distribution characteristics at ultimate loads in the past, their studies were mainly restricted to AASHTO truck load and the AASHTO code (Heins and Kuo [37]). Also the most recent study based on the OHBDC was carried out by Cheung, Ng, and Gradner [40].

This thesis presents only the results of analytical study of the load distribution characteristics at ultimate for a large scale continuous slab-on-girder bridge model which includes load redistribution in both longitudinal and transverse direction, non-linear behavior. Since slab-on-girder bridges resist loads primarily through flexure, only the redistribution of moments was examined. The behavior of the bridge model and load distribution factors reported in this thesis were based on simulated OHBDC truck loading (OHBDC 1983).

Chapter 2

LITERATURE REVIEWS

2.1 Limit States Design vs. Working Stress Design

The popularity of LSD over WSD is based on its more uniform level of safety and hence greater economy. In the WSD method, force effects in a structure under specified loading are calculated using elastic methods of analysis. The individual members are designed so that the maximum stresses due to these force effects do not exceed an allowable stress derived from the yield stress of the material. This allowable stress would normally vary with the type of force effect being resisted. The ratio of yield stress to the allowable stress provides a factor of safety against failure under an

overload while satisfactory performance under the specified service loads is ensured since the material is kept well within the elastic regime. However, the actual factor of safety against collapse will likely be much higher than this ratio since structural elements possess a strength reserve between first yield and failure. The magnitude will vary with type of force effect being resisted but it can be significant in flexural members. It will also vary with the proportions of the structural elements as they determine the ability of the member to withstand progressive plastification between first yield and the plastic moment while avoiding secondary failures such as buckling and crushing. Other factors which affect the magnitude of this strength reserve are the shape of the member, the material properties and workmanship. There may be a further reserve of strength between failure of the first member and collapse of the structure depending on the degree of redundancy and the ability of the members to withstand plastic rotations leading to the formation of a plastic collapse mechanism.

Not only can the true resistance vary considerably from those determined by an allowable stress design, so may the actual loading vary from the design loading. Specified loads are only estimates of the loads the structure may resist in its life. The actual loads vary with the same probability distribution and may well exceed the specified loads the aforementioned factor of safety is also intended to compensate for that possibility in WSD. However, different types of loads have different probability distributions : live loads have much wider distributions than dead loads. Since the ratio of live load to dead load varies between structures, so does the level of safety.

It is apparent that this variability of resistance and loads results in a highly non-uniform level of safety amcng structures designed using WSD. Although an acceptable probability of failure suggests that minimum levels of safety as provided by WSD are satisfactory , some structures are over designed and, hence, are uneconomical.

Limit state design is based on the principle that the structure must perform satisfactorily at different limit states. At the serviceability limit states (SLS) the structure must be able to support the anticipated service loads without excessive deformations, cracking, etc., or susceptibility to fatigue failure. The structure would normally behave elastically at these load levels.

The Ultimate Limit State(ULS) ensures that the probability of failure is sufficiently small. This is achieved by applying load factors which are derived from the distributions of the loads such that the probability of exceeding the factored loads within a specified return period is acceptably low. Since different load types have different distributions, they will also have different load factors.

The resistance of the structural members at the ULS is the maximum resistance that can be expected. Depending on the force effect being considered, the resistance will vary with the dimensions of the section, bracing and end-fixity, as well as material properties. In the case of flexure, the resistance could range anywhere up to the full plastic moment or more, although it could well be less than the theoretical yielding moment. In any case, this resistance may be reduced by performance factors to account for uncertain-

ties in calculating the member resistance due to the variability of material properties, dimensions, workmanship,..etc. Even the type of failure plays a role: the tensile resistance of a steel member can be predicted for more accurately than the shear resistance of a concrete section. An allowance may also be inclined for inaccuracies in the method of analysis used.

It is interesting to note that different LSD codes specify different load and performance factors for apparently similar circumstances. Part of the reason is that code writers have considerable flexibility when choosing to include variable quantities in a performance factor or a load factor. Another reason is that those codes which also specify different design loads.

Regardless, the combination of load factors and performance factors are intended to provide satisfactory performance under service loads and an acceptable low probability of failure at ULS. It should be obvious that the probability of failure can never be reduced to zero, but economically feasible structures can be built with acceptably low probabilities of failure. The level of safety in LSD structures is bound to be more uniform than in WSD structures.

2.2 Inelastic Method in Bridge Design

2.2.1 Resistance To Plastic Design :

Although the LSD philosophy has gained acceptance, the use of plastic analysis is not widespread in bridge design outside of yield line theory for slabs. This has led to the inconsistency of using elastic analysis to predict the distribution of load effects in a structure while the capacities are based on ultimate resistances which imply inelastic behaviour. The strength calculation based on an elastic analysis normally limit the capacity of the structure to the load at which the first section reaches its capacity. In an indeterminate structure, there is usually a strength reserve between the failure of the first section and collapse of the structure. The magnitude of that strength reserve will depend on the degree of redundancy and the loading configuration as it affects the relative ratios of force effects to capacities at the critical sections. How much of that strength reserve that can be mobilized will depend on the ability of the structure to redistribute the force effects up to collapse.

In the case of slab-on-girder bridges, the principle force effect is flexure. A hinge forms at a section once the flexural capacity is reached . In a multi-span continuous bridge, longitudinal redistribution of moments will occur under increasing load if the hinge can rotate at or above the plastic moment. It will continue until sufficient hinges have formed to form a mechanism in

that member.

However, in a multi-girder bridges, the transverse slab will likely continue to support the 'failed' member, redistributing load transversely to the other as yet unfailed longitudinal members. It is likely that the longitudinal and transverse redistribution will occur simultaneously. It may be possible to continue loading until the structure or a portion of it fails due to formation of a collapse mechanism. Again, it will depend on the plastic rotation capacities of the various members.

In any case, the strength between the first hinge and collapse may be significant, and will be highly variable between different structural types. In that respect, even LSD yields variable factors of safety when capacities are based on elastic methods. Plastic analysis is necessary, basing ULS on collapse of the structure, if truly uniform levels of safety are to be achieved.

2.2.2 AASHTO Inelastic Analysis Provisions:

It is often argued that any economies which may be realized by exploiting these strength reserves would not offset the additional time and expense of the required plastic analysis. Some codes allow designers to include some of the benefits of plasticity without the inherent work of a plastic analysis by permitting a limited redistribution of the elastic bending moments. Within the LSD option, AASHTO allows a maximum 10% reduction of the negative moments over supports, accompanied by an appropriate increase in

the maximum positive moments for continuous steel beams with compact sections.

AASHTO defines a compact section as one that is able to reach the simple plastic moment and rotate at near constant moment during redistribution. The simple plastic moment for a naked beam and a composite section are calculated using the assumed stress distribution shown in Figure(2.1).

When calculating the simple plastic moments from the stress distribution in Figure(2.1), the full width of the slab may not be effective in resisting the moment due to elastic shear lag: the shear stress may not dissipate uniformly through the slab, resulting in a peaked distribution of slab stresses over the girder. The effective width is that width of slab over which the peak stress will give the same net force as the actual stress distribution. AASHTO limits the effective width to the least of (i) one-fourth the span of the girder, (ii) the distance center to center of the girders, or (iii) twelve times the slab thickness. These limits are based on the elastic behaviour of composite beams, but are assumed to be also applicable, if not more conservative, at the ULS .

The 10% redistribution of elastic bending moments is applicable at the maximum load level, or ULS. It may also be admissible at the overload level of AASHTO, Which represents the infrequent passage of heavy vehicles equal to 1.67 times the design vehicle. This is a serviceability limit state with the criteria being that no objectionable permanent deformation occur. These are prevented by limiting the flange stresses to 80% of the

yield stress, F_y ,in non-composite sections under the redistributes moments, and 95% of F_y in composite sections under the original moment distribution. However, these limits effectively prevent any redistribution in either case. For the non-composite sections, the allowed 'redistribution' of elastic bending moments effectively increases the allowable flange stress to $0.89F_y$ at a negative bending section under the elastic moments, and something less than $0.8F_y$ at the positive bending section.

2.2.3 Provisions for Inelastic Analysis in Canadian Codes :

Since the CSA's "Design of Highway Bridges" has not yet adopted the LSD option for steel bridges, there are no provisions for longitudinal redistribution of bending moments. Nor does the OHBDC [2] make any allowance for plastic distribution. No non-linear analytical methods may be used without approval except in special areas such as yield-line theory for slabs. The OHBDC still classifies compact section is one that can reach the simple plastic moments but need not have adequate rotational capacity to allow for any redistribution. The slenderness and bracing limits are consequently less restrictive than those for an AASHTO compact section . For composite sections in positive bending, only the lateral spacing requirements for the compression flange are assumed to be satisfied by the shear connection between girder and slab; the slenderness limits are not explicitly waived. Capacities are still calculated using the fully plastic stress distributions of

Figure(2.1), but the effective slab width are given by [2] :

$$\frac{B_e}{B} = 1 - \left(1 - \frac{L}{15B}\right)^3 \leq 1 \qquad (2.1)$$

Where :

B, B_e = slab dimensions as shown in figure (2.1).

L = equivalent span length in positive or negative as appropriate.

To further clarify the difference between an AASHTO compact section and an OHBDC compact section, reference is made to the CSA's "steel structures for buildings-limit states design"[5]. Although this code is not applicable to bridge design, the classification of steel sections is universal. Here a class 1 or plastic design section will reach the plastic moment and allow subsequent redistribution. A class 2 or compact section will reach the plastic moment but need not allow any redistribution.

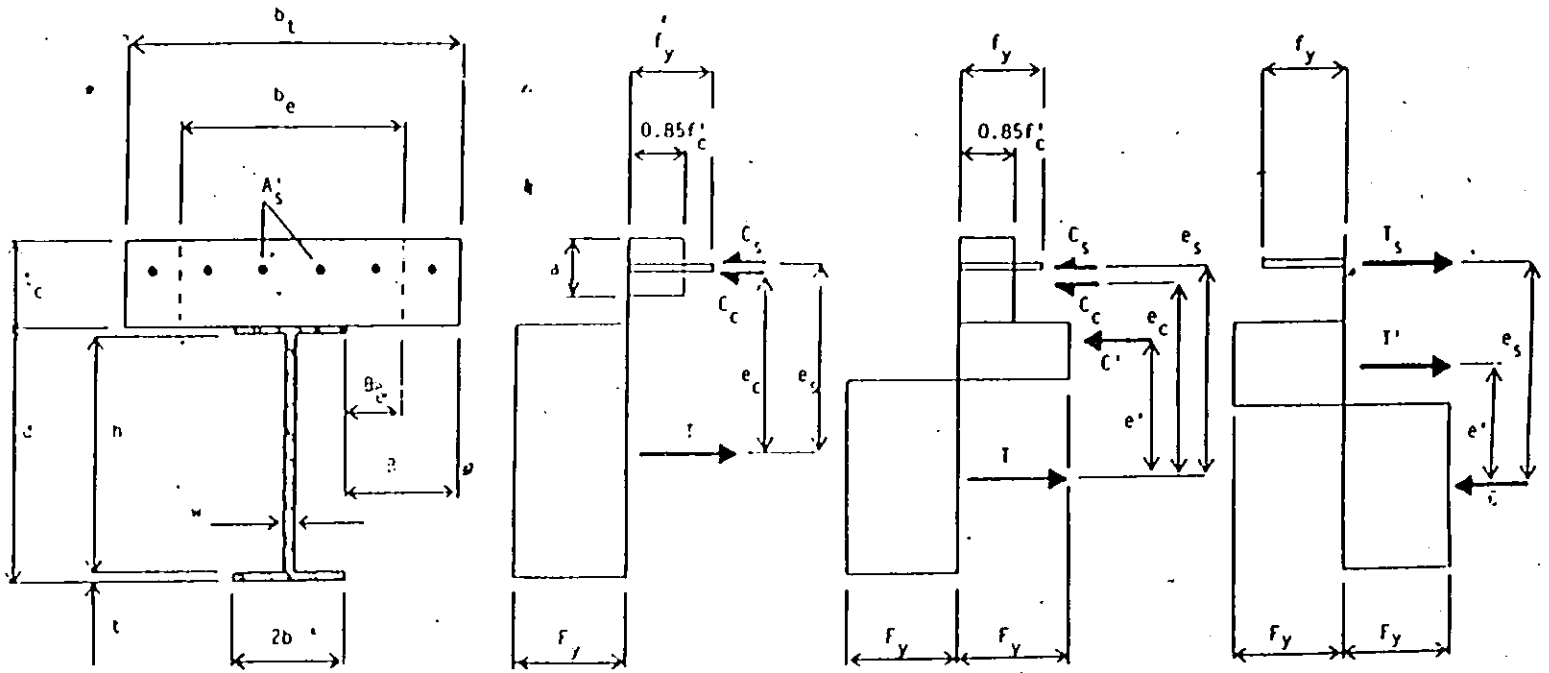

Figure 2.1: Composite cross section: Dimensions and capacity calculations.

2.3 Methods of Analysis

Within a time span of approximately 30 years, the science of bridge analysis has undergone major change. Following the advent of the digital computer, and the consequent development of analytical techniques based upon its use, the bridge designer has available today a number of powerful analytical tools in the so-called refined methods of analysis, including the following:

- The direct stiffness methods .
    1. The orthotropic plate method
    2. The grillage analogy method.
    3. The folded plate method.
    4. The finite element methods including its finite strip formulation
- Finite Difference Method .
- Semi-continuum Method .

These refined methods are by now well established for the analysis of load distribution in bridge of various types. It is important to realize that most of the refined methods have limitations as to the kinds of bridge superstructures which they are capable of representing. For example, the usual grillage analogy and the orthotropic plate methods are suitable for the analysis of bridges in which load distribution takes place mainly through flexure and

torsion in the longitudinal and transverse directions, with deflection due to shear being negligibly small.

2.3.1 Orthotropic plate theory :

In applying the orthotropic plate theory to bridge analysis, the bridge deck treated as a plate. The rigidities of the longitudinal beams are assumed to be uniformly distributed throughout the deck in the directions perpendicular to the respective members. Thus, the actual discontinuous structure of the deck is represented by an idealized substitute orthotropic plate, reflecting the characteristic properties of the actual system. The deformations and stresses can be computed by means of the ordinary theory of elastic plates. The elastic properties of an orthotropic plate are defined by the rigidity coefficients:

$$D_x = \frac{E_x t^3}{12(1-\nu^2)} \tag{2.2}$$

$$D_y = \frac{E_y t^3}{12(1-\nu^2)} \tag{2.3}$$

$$D_{xy} = \frac{G_{xy} t^3}{12} \tag{2.4}$$

$$H = \frac{1}{2}[D_x \nu + D_y \nu + 4D_{xy}] \tag{2.5}$$

Where :

D_x = The flexure rigidity of the plate in the x direction.

D_y = The flexure rigidity of the plate in the y direction.

D_{xy} = The torsional rigidity of the plate in the x direction.

H = The effective torsional rigidity.

t = Plate thickness.

The non-homogeneous differential equation giving the relationship between the deflection and the loading of an orthotropic plate, often referred to as Huber's equation is:

$$D_x \frac{\partial^4 w}{\partial x^4} + 2H \frac{\partial^4 w}{\partial x^2 \partial y^2} + D_y \frac{\partial^4 w}{\partial y^4} = p(x, y) \tag{2.6}$$

where w is the deflection of the middle surface of the plate at any point (x, y) and $p(x, y)$ is the loading intensity at any point, expressed as a function of the coordinates x and y. The general solution of equation (2.6) consists of superposition of two solutions:

$$W = W_h + W_p \tag{2.7}$$

where :

W_h is a general solution of the corresponding homogeneous differential equation:

$$D_x \frac{\partial^4 w}{\partial x^4} + 2H \frac{\partial^4 w}{\partial x^2 \partial y^2} + D_y \frac{\partial^4 w}{\partial y^4} = 0. \tag{2.8}$$

and W_p is a particular solution of the homogeneous equation (2.6). The solution of the homogeneous equation is most difficult and often impossible. Generally, such solution can be only given as infinite series. For example, in the case of a plate simply supported along the edges x=0 and x=1 and subject to any boundary conditions along the edges y= constant, "Lévy" suggested that solution for the homogeneous equation may be represented in the general form:

$$W_h = \sum_{n=1}^{\infty} Y_n \sin \frac{n\pi x}{L} \tag{2.9}$$

where L is the span in the x direction, Y_n is a function of the variable y. Three different expressions for Y_n are obtained for the following three basic cases :

1. $H^2 > D_x D_y$
2. $H^2 = D_x D_y$
3. $H^2 < D_x D_y$

The particular solution may be expressed as:

$$W_p = \frac{1}{D_x} \sum_{n=1}^{\infty} \left(\frac{L}{n\pi}\right)^4 p(x) \tag{2.10}$$

Where $p(x)$ is the loading represented by a Fourier series. When the deflection surface, w, of the orthotropic plate and the value of the constants have been determined, the bending moment at any point of the plate can

be found out by:

$$M_x = -D_x \left(\frac{\partial^2 w}{\partial x^2} + \nu \frac{\partial^2 w}{\partial y^2} \right) \tag{2.11}$$

$$M_y = -D_y \left(\frac{\partial^2 w}{\partial y^2} + \nu \frac{\partial^2 w}{\partial x^2} \right) \tag{2.12}$$

2.3.2 Grillage Analogy Method :

A wide variety of bridge types may be idealized as a grillage, where the real structure is represented by a series of beam elements in both the longitudinal and transversal directions, as shown in Figure (2.2) . The longitudinal stiffnesses of the slab are concentrated in the longitudinal beams while the transverse stiffnesses are concentrated in the transverse beams. Ideally the beam stiffness should be such that when the prototype slab and equivalent grillage are subjected to identical loads, the two structures should deflect identically and the moments, shear forces and torsions in any grillage beam should equal the resultants of the stresses on the cross section of the part of the slab the beam represents. Some rules have to be followed while doing the grillage idealization:

1) Place grillage beams coincident with lines of design strength, i.e. parallel to prestress or component beams, along edge beams , along lines of strength over bearing ...etc.

2) Place edge grillage members closely to the resultant of the vertical shear flow at edge of the deck.

3) The total number of longitudinal member can be varying from four to twenty or so depending on the bridge geometry and the loading conditions.

4) The spacing between transverse members should be sufficiently small for loads distributed along longitudinal members to be represented with reasonable accuracy by a number of point loads acting at the intersection points of the beams.

5) The transverse and longitudinal member spacing should be reasonably similar to permit sensible statical distribution of loads.

6) Simply supported decks at skew angles less than 20 degree can usually be analyzed with grillage having right supports. Once such an idealization of the structure has been established the analysis of the resulting grillage becomes very easy.

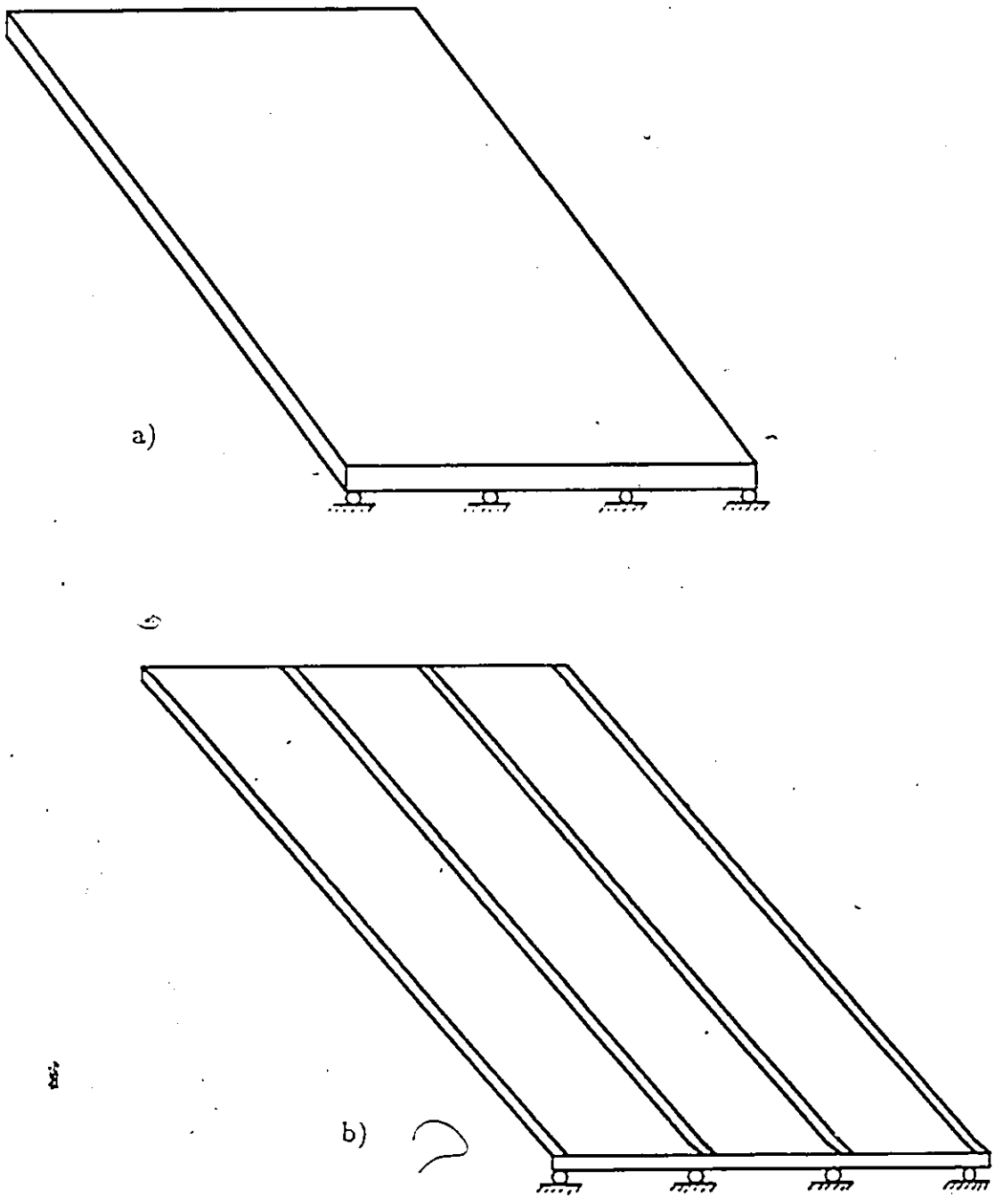

Figure 2.2: a) Prótype deck and b) Equivalent grillage.

2.3.3 Folded Plate Method :

The behaviour of a folded plate may be considered to consist of the action of a series of transverse one-way strip supported elastically at the ridges by a series of interconnected plate beams spanning longitudinally between the end diaphragms. The slab strips only transmit shears and moments in the transverse direction, while the plate beams only transmit forces in their plane. The analysis is not straightforward because the slab system is assumed elastically supported by the plate system.

Yitzhaki [11], suggested a solution technique called the method of particular loadings. In this method of particular loading the structure, under the action of the externally applied loads, is analyzed first assuming the slab system to be rigidly supported by the plate system and the displacements thus set up in the plate system by these ridge loads are calculated. These plate displacements lead to relative joint displacements, as defined in Figure (2.3), which set up additional 'sway' moments in the transverse slab system. A subsequent correction analysis is carried out to take these additional moments into account, and the final results are obtained by superposition of the individual parts of the analysis.

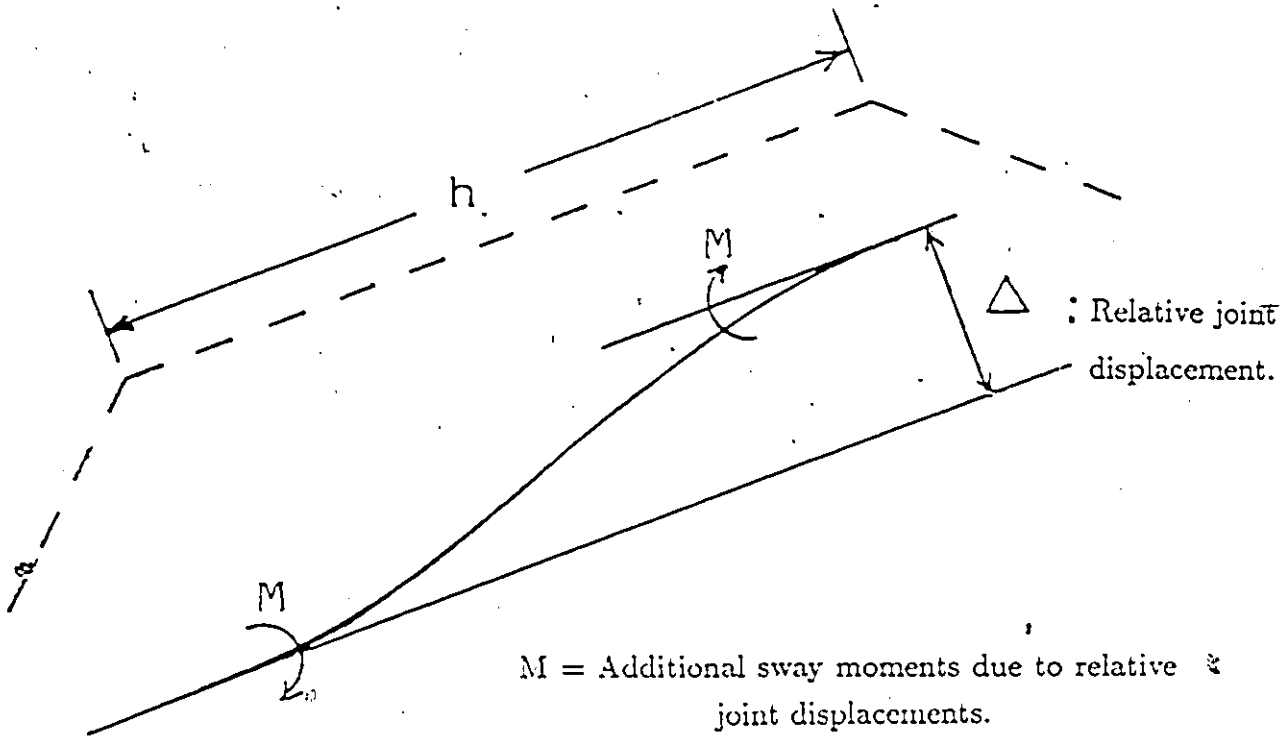

Figure 2.3: Relative joint displacements.

2.3.4 Finite Element Method :

The finite element method is one of the most powerful analytical techniques based on the direct stiffness approach. The fundamental concept of the finite element method is that any structure is made up of elements; therefore, the general behavior of a structure can be determined by considering the behavior of its components (elements). The assembly of the elements is done by mathematically enforced continuity conditions at the element node points (points where the elements are joined to each other or to a boundary). The minimum total potential energy theorem is used to develop the relationship between unknown nodal displacement parameters and the applied loading. A two-way polynomial function is usually used to represent the displacement function of the structure. A set of overall stiffness equation can be obtained based on the chosen displacement function. The nodal displacement parameters are then solved from the equations [12,13].

Some aspects of the method which have significant influence on the bridge analysis is discussed below. A structure can be modelled using one, two, or three-dimensional elements or combination of these elements. There are two main types of one-dimensional elements namely bar element and beam element. Bar element can take only axial tension or compression, see Figure (2.4). However, beam element has bending strength with respect to principal axes of bending as well as axial strength.

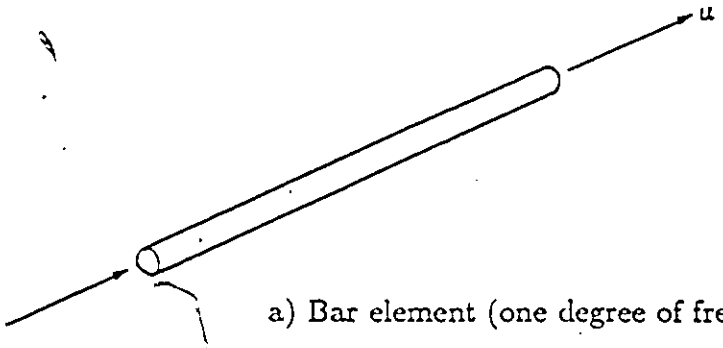

a) Bar element (one degree of freedom at each node).

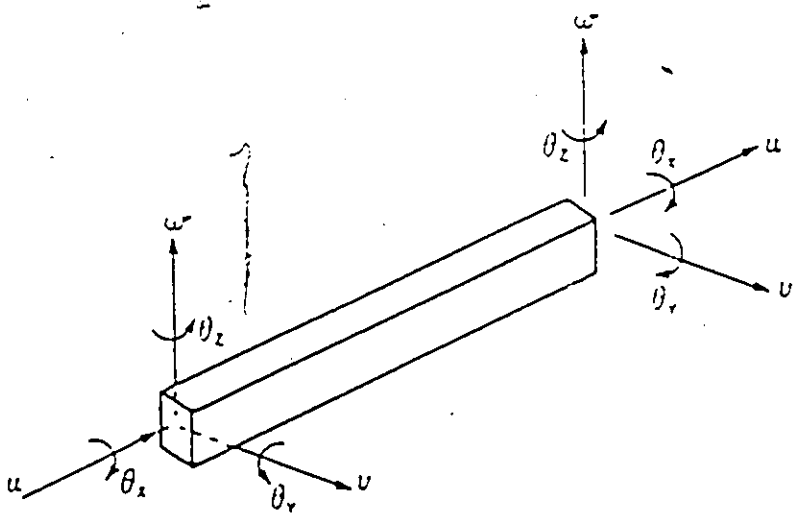

b) Beam element (six degrees of freedom at each node).

Figure 2.4: One dimensional elements .

In two-dimensional elements, if the nodes are allowed to have displacements only in their own plane, the element is termed a membrane element. Alternatively, the element may be used to simulate plate bending action by specifying three degree of freedom at each node as shown in Figure 2.5(c).

Three-dimensional solid elements are seldom used in the analysis of bridge decks . Solid elements are used more often for the analysis of nuclear reactor and complex soil structures. The simplest elements consists of tetrahedra or hexahedra with nodes at the corners as shown in Figure 2.6. If the mesh is fine, the nodes need only have three degree of freedom for displacement in the three dimensions. More sophisticated elements have additional nodes in addition to those at the corners, with more degree of freedom at each node.

In selecting the element type for a particular model, some factors such as element accuracy, reliability and simplicity, as well as computational cost must be taken into consideration. Element size should be chosen in such a way that they are well proportioned. Degrees of freedom are assigned only to those displacements and rotation which can be resisted by elements connected to the node.

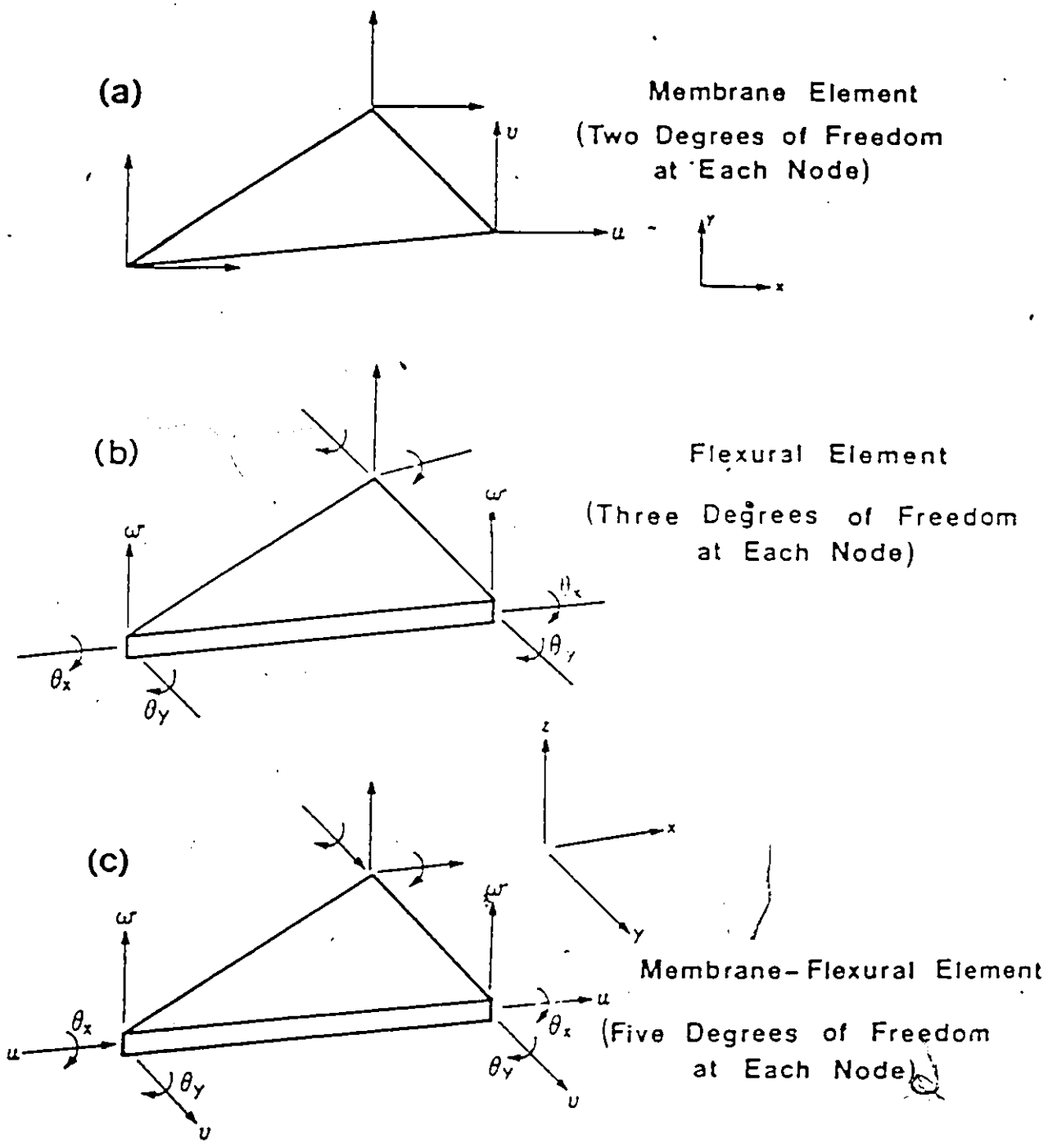

Figure 2.5: Typical triangular elements .

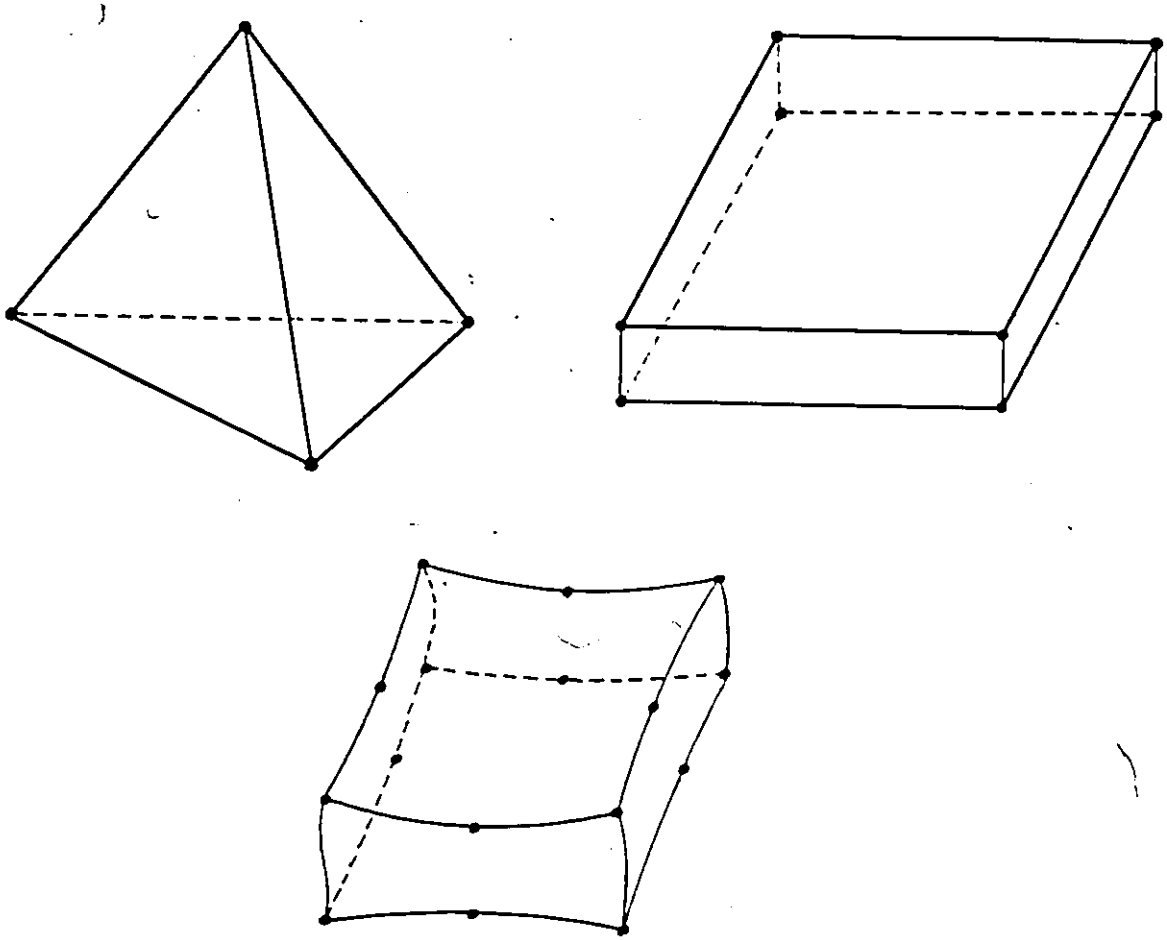

Figure 2.6: Three-Dimensional solid elements.

2.3.5 Finite Strip Method :

Bridge decks can be analyzed with a simple and economic type of finite element called a finite strip. The method introduced by Y.K. Cheung [6] is very similar to folded plate analysis. The structure is assumed, as in Figure(2.7) to be made up of finite elements called 'strips' which extend from one end of the deck to the other. The strips are connected by nodes which also run from one end to the other. A displacement function, in terms of the nodal displacement parameters, is chosen to represent the displacement field and consequently the strain and strain field within each strip. Stiffness matrix and load matrices are then obtained based on the chosen displacement function.The stiffness and load matrices of all the strips are assembled to form a set of overall stiffness equations. Then nodal displacements can be solved from these equations. Therefore, the choice of displacement function for a strip is the most critical part of the analysis.

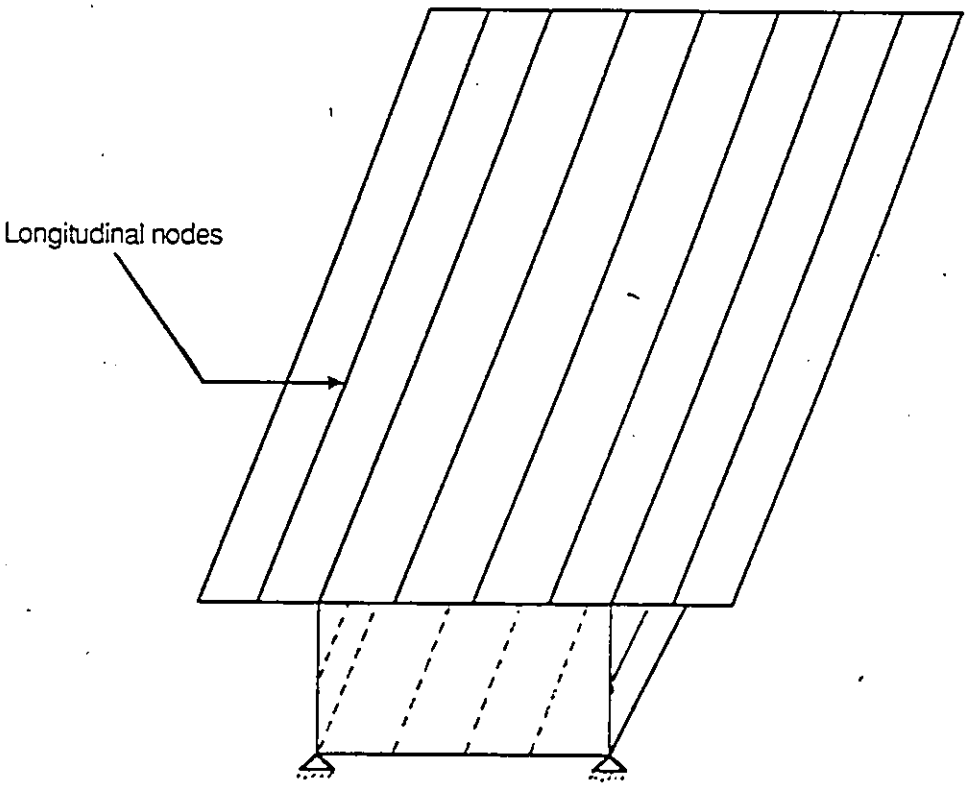

Figure 2.7: Finite strip model of box girder.

2.3.6 Finite Difference Method :

In this method the bridge deck is subdivided into a grid of plate elements. The governing equations for the orthotropic plate elements are expressed in terms of the unknown deflections at the grid intersections. Different formulations are required for different boundary conditions. The results are a set of simultaneous equations, which can be solved for the unknown deflections, from which the force effects at the intersection points can then be calculated. The resulting deflection pattern approximates the actual curved profile with a series of linear segments, and the accuracy of the section will depend on the fineness of the grid. A detailed discussion of the finite difference method can be found in Cusens and Pama [7].

Although computer programs using the finite difference method to solve the governing equations for orthotropic plates have allowed the analysis of many bridge configurations which otherwise would have been too difficult or time consuming, they are still only applicable to those bridges which can realistically be idealized as orthotropic plates. This is not always possible, and in other cases the bridge is better idealized in different fashions.

2.3.7 Semi-continuum Method :

The semi-continuum method is well suited to the analysis of girder bridges. The longitudinal elements are idealized as discrete members while the transverse slab is represented by a continuous medium. Hendry and Jaeger[10] first developed the method for analyzing bridges with negligible torsional stiffnesses. Jeager and Bakht [8] expanded on the method to take account of the torsional stiffnesses in both the longitudinal and transverse directions.

The method provides a more rational model of the slab-on-girder than either the orthotropic plate theory, which idealizes it as a continuous medium in both directions, or the grillage analogy, which uses discrete members in both directions. Although the method would appear to be a hybrid of the other two, its formulation is relatively unique. The vertical deflection and longitudinal twist of the longitudinal members are expressed as harmonic series. For each harmonic the deformation patterns for each longitudinal girder are the same but with different amplitudes. The vertical load and torque functions associated with these deformations are similarly expressed as harmonics. The different deflections, slopes and twists of adjacent girders at some longitudinal portion result in the bending and twisting of an associated strip of the transverse medium. The amplitudes of the longitudinal deflection and twist functions at each harmonic remain unknown. For a bridge with N-girders, these 2N unknowns are found by solving the 2N simultaneous equations resulting from equilibrium of moments, and the relative deflections and twists between the N-girders. Alternatively, the so-

solution can be generated in the form of distribution coefficients for the total longitudinal and torsional moments from which the other force effects can be determined. In either case a solution is found for each harmonic and the results summed over a sufficient number of harmonics depending on the loading conditions and the accuracy required. Jeager and Bakht [8] have shown the method yields fairly rapid convergence for loading under a series of wheel loads.

The results of this method have been verified against those of a grillage analysis. The semi-continuum method has the advantage over the grillage analysis of requiring less computer storage and execution time, and is therefore better suited for applications on personal computers. As developed the semi-continuum method is only applicable to single span, simply supported right bridges, although continuity over intermediate supports could be accommodated by application of the force method. However, as it is fairly new in its current state, the method has not yet been expanded to consider other geometries, boundary conditions or internal releases.

2.4 Load Distribution Factor Theory

The evaluation of the load response of bridges requires consideration of the interaction of all parts of the system, i.e. girder, slab, and diaphragms. Loads on a highway bridge are distributed transversely to the main longitudinal girder by the floor system, which consists of the deck slab and supporting members. The interaction between the different components of a highway bridge is difficult to determine, thus the complete structural analysis of a bridge is a complex undertaking.

For the purpose of designing new bridges or evaluating existing ones, most codes (AASHTO 1977; CSA 1978; OHBDC 1983) provide empirical or semi-analytical rules for transverse load distribution. Currently both AASHTO and CSA-S6 specifications permit a simplified method according to which the live load longitudinal moments or shears for a longitudinal girder can be obtained by treating the girder as a beam and subjecting it to one line of wheels of the design vehicle, the weights of which are multiplied by a load fraction ($\frac{S}{D}$). S is equal to the spacing of girders, and D is a factor accounting for the degree of load distribution in the bridge.

The concept of the factor D can be explained with reference to Figures (2.8) and (2.9) which show the transverse distribution of longitudinal moments at a cross-section due to a vehicle on a slab-on-girder bridge. The total live load moment M_y that the girder under the vehicle should be required to sustain, is equal to the area under curve shown hatched in Figure

(2.9). If the intensity of the maximum longitudinal moment is $M_{x(max)}$, and the girder spacing is equal to S, then this area is approximately equal to $SM_{x(max)}$. Thus:

$$M_g = SM_{x(max)} \tag{2.13}$$

Now assume that the unknown quantity $M_{x(max)}$, can be obtained by a factor D which is given by :

$$D = \frac{M}{M_{x(max)}} \tag{2.14}$$

Where M is one-half the total moment due to one vehicle, or, in other words, the moment due to one line of wheels at the section under consideration. Substituting the value of $M_{x(max)}$ from equation (2.13) into equation (2.14), we get:

$$M_g = \frac{MS}{D} \tag{2.15}$$

Thus, if the value of D is known for a bridge, the maximum live load moment in S of the bridge can be obtained as a fraction $\frac{S}{D}$ of the beam bending moment due to one line of wheels, i.e., half the design vehicle. The Ontario Highway Bridge Design Code (OHBDC 1983) adopted more refined load distribution schemes which are functions of material and geometric properties of the bridge. It also provides values of D, but these depend upon the values of α and θ, and also upon the total number of lanes in the bridge and the number of lanes occupied by the design live loadings. (α, θ are torsional and flexural parameters of the bridge and are defined in reference ,OHBDC 1983). The D values are given for bridges having 3.3 meter lanes in the form of contours in the $\alpha - \theta$ space. The design D values,

D_d for bridges having lane widths other than 3.3 meters, are obtained as follow:

$$D_d = D\left[1 + \frac{\mu C_f}{100}\right] \tag{2.16}$$

The correction factor C_f is obtained from a set of charts and μ is given by:

$$\mu = \frac{Lane\ width\ in\ meters - 3.3}{0.6} \tag{2.17}$$

The development background and the details of this method are given by Bakht et al [20]. It should be pointed out that D values given in current OHBDC were developed entirely based on linear elastic analysis.

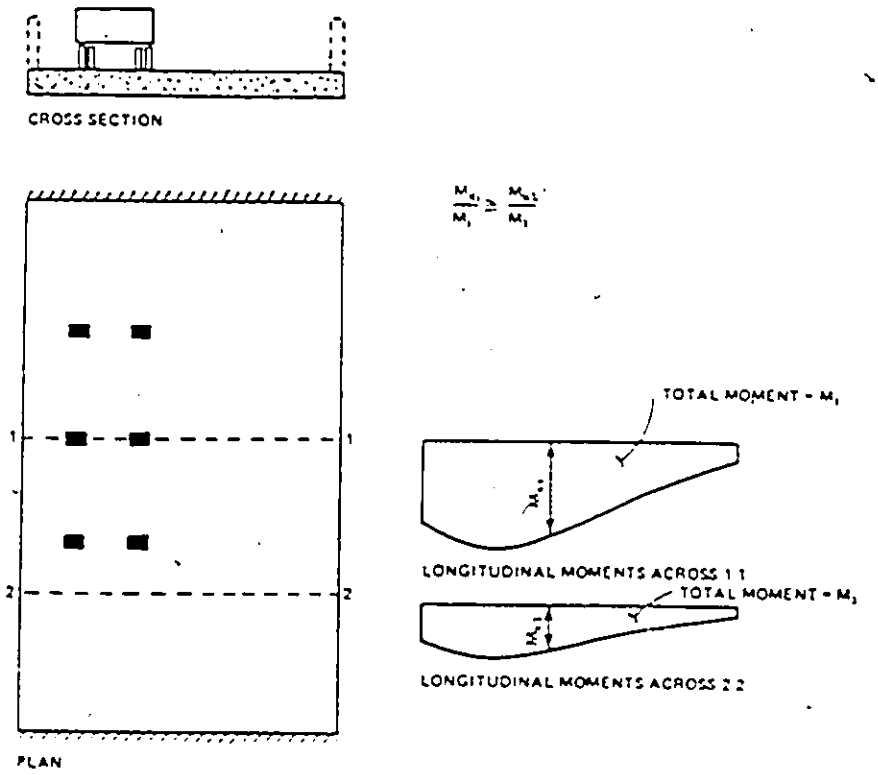

Figure 2.8: Distribution patterns for longitudinal moments.

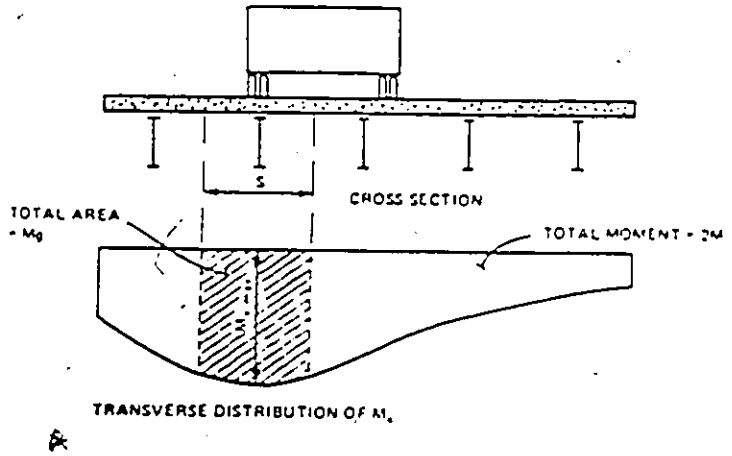

Figure 2.9: Longitudinal moment distribution across a transverse section.

2.5 Research into the Post-Elastic Behaviour of Slab-on-girder Bridges

A considerable volume of research, both analytical and experimental, has been done over the past three decades into the post elastic and ultimate behaviour of composite beams and slab-on-girder bridges. It is not intended to describe the development of the general methods of plastic analysis and design here, but rather to concentrate on those works which are applicable to slab-on-girder bridges. The conclusions reached by the researchers will be emphasized rather than their methods except where those methods have a direct bearing on those used in this study.

2.5.1 Single Span, Simply Supported Beams

Early tests by Chapman [28] were some of the first to explore the post elastic behaviour of composite sections. With the positive bending capacity based on the rectangular stress blocks of Figure (2.1), composite sections have relatively large span factors, in the order of 1.5 compared to 1.15 for naked steel sections, composite beams seemed appropriate candidates for the ultimate strength design methods which were gaining attention at that time.

Preliminary tests on simply supported continuous beams suggested that this theoretical ultimate moment could be attained provided that adequate

shear connection was supplied. It was also observed that for a section with a relatively large slab compared to the steel section, the neutral axis at ultimate load was well within the slab, and failure was marked by crushing of the slab only after considerable strain hardening had occurred in the bottom flange of the steel beam. As the relative size of the slab decreased, the location of the plastic neutral axis moved toward or into the girder.

Chapman proposed that a section where the plastic neutral axis is located well within the steel section may not be able to reach the ultimate moment since failure would occur by crushing of the concrete before the steel section could yield throughout. This was not expected to be a problem in building design where the girders are not large relative to the slab. It may be more critical in bridge design. Chapman also hypothesized that the location of the plastic neutral axis served as a measure of the ductility of a sagging hinge as well as its ability to reach the simple plastic moment. Plastic ductility would be a requirement in an indeterminate structure where the sagging hinge would have to rotate plastically at or above the simple plastic moment to form a collapse mechanism.

Chapman and Balakrishnan [29] investigated the effects of shear connection and interface slip on the ultimate bending capacity of composite sections. They varied the number and distribution of shear stud connector in a series of experimental tests. They found that a minimum number of connectors were required to attain the maximum moment based on the rectangular stress distribution of Figure (2.1) but beyond that additional connectors

served only to reduce the interface slip between slab and girder. Slip has no significant effect on the ultimate bending capacity in this range. The authors also recommended that compression steel in the slab not be included in calculating the plastic moment capacity since small amounts had little effect and larger amounts would have to be tied against buckling.

Baranard and Johnson [30] reported on an analytical study of the moment curvature relationship for composite beams in positive bending. A computer was used to locate points on the curve using the actual stress-strain relationships for the constituent materials and integrating the resulting stress across the section at an assumed curvature. Six composite beams were tested to failure to check the analytical results. Dimensions were chosen which allowed the effects of neutral axis location and the degree of yielding in the steel at ultimate moment to be examined. These verified the validity of computer program which was then used to model a wider range of sections. From the experimental and analytical models it was concluded that sections where the steel has not fully yielded before unloading due to concrete crushing would be subjected to a rapid loss of capacity. This is because the behaviour of concrete, in the declining portion of its stress-strain curve, governs.

A brittle failure such as this would be suitable in a plastic design where plastic ductility is required. However, it was also concluded that the use of the simpler rectangular stress blocks, and assuming that the steel was always fully yielded, generally gave ultimate moment capacities within 5%

of the more precise values calculated from the computer program. This ultimate moment was more sensitive to the maximum allowable concrete strain than the shape of the concrete stress-strain curve.

An analytical study by Yam and Chapman [31] also considered the effects of various parameters on the ultimate bending capacity of composite sections, including shear connection, slab depth, strain hardening, span lengths, and loading configuration. Rather than assuming rectangular stress blocks, an iterative technique was used to converge on the precise distribution of stresses at the critical sections to coincide with an assumed bending moment distribution. For the range of parameters considered the sections always reached theoretical ultimate positive moment provided the shear connection was adequate.

2.5.2 Multi-Span Continuous Beams

Having established that the rectangular stress blocks of Figure (2.1) provided a reliable estimate of the ultimate sagging moment capacity of a composite section, research then turned to plastic design of continuous composite beams. In most indeterminate structures this would require that the section not only should have ultimate flexural capacities, but also that the hinge should sustain that moment while undergoing plastic rotation. Some indication of the plastic ductility of a sagging hinge was provided in the earlier test on simply supported single span beams, but more extensive testing on continuous beams was required.

Barnard and Johnson [32] reported on a series of tests of four three-span continuous composite beams. Span configurations were varied to study rotations at sagging and hogging hinges. Slab reinforcement and shear stud spacing were also varied. Based on their observation, the authors classified the plastic hinges in a composite beam as their strain softening or strain hardening depending on whether the concrete slab was in compression or tension respectively. For the compact section tested, the strain hardening hinges in the hogging moment regions possessed significant rotation capacity at or above the simple plastic moments calculated using the rectangular stress blocks of Figure (2.1), ignoring the concrete in tension but including the slab reinforcement. Their behaviour appeared to be governed by the strain hardening properties of the steel. The hinges in the sagging moment regions were classified as strain softening since their behaviour appeared to

be governed by the declining portion of the stress-strain curve of the concrete slab, at least for the sections tested which were squat, compact girders with relatively narrow slabs. These hinges did not display significant rotation capacity, and those tested beams which formed strain softening hinges first failed to support the simple plastic load. Their failure was marked by crushing of the concrete before enough rotation could occur to redistribute the moments and form a collapse mechanism.

The preliminary conclusion from these tests was that plastic design was suitable for structures of composite construction if the sagging hinges were the last to form. Although the ability of these sagging sections to reach the plastic moment had been established, the ductility of these hinges was now becoming suspect. However, Mallick and Chattopadhyay [33] tested two and three span continuous composite beams to failure, and found, in general, that all hinges had sufficient ductility to form collapse mechanism. The only exception was a three span beam loaded in the outside spans requiring a uniform plastic moment across the middle span at the plastic collapse load, which would be rare in most cases. In all the test specimens, the plastic neutral axis was located in the slab. This would support Chapman's [28] earlier hypothesis that only composite sections where the plastic neutral axis is in the slab would be able to reach the ultimate sagging moment and sustain it through enough rotation to form a mechanism. Up to this point, most of the concern with the post-elastic behaviour of composite beams was with the ductility of the sagging hinge. This was in spite of the fact that the sagging plastic moment capacity, M_{ps}, is generally

larger than the hogging plastic moment, M_{ph}, because the slab is effective in compression but not in tension. It was assumed that since the composite section in negative bending was essentially a naked beam, it would have the same plastic rotational characteristics as a naked beam. These have already been established in extensive research such as those reported by Lay [34] and Lukey and Adams [35]. They determined that failure was usually caused by local buckling at the hinge, and this was dependent on the slenderness of the flange and web. Slenderness limits had been established for compact section suitable for plastic design. Bracing requirements were also established to prevent lateral buckling during plastic rotation.

2.5.3 Experimental and Analytical Studies of Composite Bridge Decks

Up to this point, only post-elastic behaviour of individual composite beams has been reviewed. The post-elastic behaviour of a multi-girder composite bridge would be more complex since it involves more redundancies and requires both transverse and longitudinal redistribution of bending moments. Some of the earliest physical tests on multi-girder bridges were performed by Lash and Nagaraja [36] in 1970.

They reported on the testing to failure of twelve scale model slab-on-girder bridges. The bridges had concrete rather than steel longitudinal girders, but the failure mechanism may still provide some insight into the plastic behaviour of steel bridges. All the test specimens were models of a 60 ft, single span, two lane structure with two or four longitudinal girders. Other variables included the presence of internal diaphragms, the type of loading and the number of lanes loaded. In addition to the experimental test, the authors analyzed the bridges under various assumed failure mechanisms to arrive at minimum upper bound estimates of the collapse loads.These mechanism included flexural hinges in the girders, flexural and torsional hinges in the diaphragms, and yield lines in the slab. The test loads generally exceeded the theoretical values, although the failure mechanisms were similar to those predicted. Longitudinal yield lines along the torsionally stiff concrete girders were typical. Steel I-beams have much lower torsional stiffnesses, and the slab in a slab-on-steel-girder bridge would not likely de-

velop as large transverse bending moments along them. Longitudinal yield lines are less likely to occur in steel bridges except under specific loading conditions.

Heins and Kuzweil [37] performed an analytical study of different failure mechanisms in slab-on-girder bridges. They considered local failures of the slab due to yield lines mechanisms within an area bounded by longitudinal girders, support lines and free edges, and global collapse mechanisms consisting of hinge lines which involve all girders at sections of maximum moments. Girder spacing and span lengths were varied, as were the relative flexural capacities of the slab in the orthogonal directions and of the girders in positive and negative bending. It was concluded that the design of the slab would generally be ignored by serviceability requirmenets, not the ultimate limit state, and that global failure mechanisms would be the most likely to occur. The authors noted that yield line theory normally underestimates the strength of concrete slabs due to membrane action and strain hardening of the steel, thereby further reducing the likelihood of local slab failures.

Heins and Kuo [38] performed an analytical study of single span multi-girder composite bridges to determine the transverse distribution of live load applicable at the ultimate limit state, which they defined as the formation of the first sagging hinge in accordance with AASHTO provisions. Although no plastic rotation of that hinge nor subsequent transverse redistribution of moments was considered, some redistribution would occur

between first yield and the formation of the hinge. The authors believed that live load distribution factors based on elastic behaviour such as those defined in AASHTO and OHBDC which are described in sections 2.2.2 and 2.2.3 respectively, may be too conservative, and that uniform distribution of load results from the yielding.

A finite difference technique was used to solve the differential equations of the equivalent orthotropic plates for bridges with various girder span and aspect ratios. At each load increment, iterations were performed to converge on the equilibrium force effects with declining member stiffnesses. More uniform distributions of load were noted as the first hinge formed, and the authors proposed a method to calculate the appropriate distribution factors at ULS based on the number of girders and the number of design lanes. However, the effects of relative flexural and torsional stiffnesses in the longitudinal and transverse directions were not considered. Wegmuller [39] investigated the same post-yielding behaviour of simply supported single span composite bridges using a slightly different analytical technique. Instead of an orthotropic plate idealization, he used a finite element model which subdivided the slab and girders into layered elements. Under incremental loading, an iterative procedure was again used to converge on the appropriate element stiffnesses corresponding to an equilibrium set of deformations. Stiffnesses were modified to account for concrete cracking and crushing, yielding of the steel girder. Loads up to 27% higher than first yield were considered, but the emphasis was on the immediate post-cracking behaviour rather than the ULS or beyond to an actual collapse mechanism.

In that range, however, an improvement in the transverse distribution of longitudinal bending moments was noted.

Improved transverse distribution of load in the post-elastic range was also the purpose of scale model bridge tests performed by Botzler and Colville [40]. A two span and three span model were included, both with three compact longitudinal girders composite throughout. Loading consisted of a single concentrated point load over the middle girder at center of one span, the middle span in the three span model. Loading was increased until yielding has occurred in both the sagging and hogging regions with moments redistributed from the loaded section. From the load deflection plots, however, the models were not unloading at this point and the formation of a collapse mechanism did not seem imminent. Based on measured strains the transverse distribution of sagging moments at the loaded section was more uniform than at elastic load levels. Moments were also being redistributed longitudinally, but apparently only along the loaded centre girder since the transverse distributions of hogging moments at the support sections became more concentrated in the post-elastic range. Had loading increased beyond this, however, transverse redistribution may have occurred at the hogging sections as well, progressing towards a collapse mechanism.

The results of another experimental test to determine the load distribution factors at ULS were reported by Cheung et al [41] in 1986. A scale model of a single span simply supported slab-on-girder bridge was loaded with scaled Ontario Highway Bridge Design (OHBD) vehicles in one or two of the

three lanes, increased proportionally to failure. There were six longitudinal girders with compact rolled sections. The interior girders were most heavily loaded, and between first yield and full plasticization of the most heavily loaded girder, the transverse distribution became more peaked with that girder carrying a larger proportion of the load. Subsequently, moments were redistributed transversely and the distribution improved. However, at the highest load level for which results were reported, the distribution was still more concentrated than the elastic distribution, contrary to what would be expected. The nature of the failure was not made clear, but it was obviously not due to the formation of a collapse mechanism consisting of a single sagging hinge line, otherwise the transverse distribution of moments would have been more uniform.

Chapter 3

ANALYTICAL PROCEDURE

A finite element analysis was carried out using the ADINA program [1], to analyze the bridge model. Both elastic and non-elastic behavior of the steel girders of the bridge were taken into consideration in the finite element idealization. The element type that is used throughout the model is an isoparametric thick shell element with nine nodes. Only material nonlinearity was considered in the analysis. In the plastic region the Von Mises yield criterion with isotropic strain hardening was used. For ADINA, the load is given as a function of time defining the time history point by point. Within each load increment an equilibrium iteration is performed if desired. The finite element model idealized the concrete deck as linear elastic shell elements, and the steel diaphragms as three-dimensional elastic shell elements, and the steel girder as three-dimensional elastic/plastic shell elements. Details of the finite element idealization are shown in Figure 3.3.

3.1 Bridge Geometry

The analysis was undertaken on a reduced scale model of a highway bridge that spans the Red River near Ste-Agathe, Manitoba. The model shown in Figure (3.1), was made to a 0.354 scale which reduced the overall size to approximately 16.186 m. long and 3.220 m. wide .

The bridge model consisted of four $W15 \times 10$ steel beams with steel diaphragms and a cast-in-place concrete deck of thickness of 62.5 mm. The four girders were spaced at each 900 mm, and connected transversely by ten C-beams acting as diaphragms. Three diaphragms were located at each support, and two of them were equally spaced at each span, as shown in Figure(3.2). The bridge model has span lengths of 4.856 m, 6.474 m, and 4.856 m. The total width of the bridge model was 3.22 m.

Taking advantage of symmetry about the transverse center line, a finite element mesh of 1659 nodes was used to model the bridge model. 312 shell elements were selected to represent the girders and slab. The finite element idealization for the bridge model is shown in Figures 3.3, 3.4, 3.5, and 3.6 .

3.2 Material Properties of the Slab-on-girder Bridge Model :

3.2.1 Girders

The 0.354 scale factor permitted to use the standard $W10 \times 15$ steel beams to model the $W36 \times 10^4$ steel beams used in the prototype. The structural steel is of type CSA G40.12 with a specified minimum yield stress of 304 MPa, and a modulus of elasticity of 2×10^5 MPa. To provide for composite action, $\frac{3}{8}in$ long channel acting as shear connectors $C1.5 \times 1.7$ were welded to the upper surface of the flange. The shear connectors were not structurally redesigned for this bridge model but were only scaled from the prototype. Dimensions of the girder are shown in Figure (3.2).

3.2.2 Concrete Deck

The properties of the concrete used for the bridge model deck were determined by Y. Symko [25] : Concrete control cylinders of 3×6 *inches* were made for every half section cast in order to determine the compressive strength and the modulus of elasticity . Values of elastic modulus were determined from longitudinal strain measurements on the compression cylinders. The average modulus values were found to be 6., 7.8, 5.1, 6.7 and 6. (in terms of 10^6 psi) and the average ultimate cylinder strengths

6900, 7400, 6400, 7200 and 6800 psi, respectively .

3.2.3 Reinforcing Steel

The structural action of the slab is essentially one-way. The load is carried by the slab in the direction perpendicular to the traffic. Steel was provided in longitudinal direction as temperature and shrinkage reinforcement. The reinforcement layout is shown in Figure (3.2). The tensile and compressive steel ratios shown in Figure (3.2) are given for a doubly reinforced slab resisting positive and negative moments occurring between and at the steel beams respectively.

The main reinforcement has tensile steel ratio varying from 0.0198 to 0.0314 and the compressive steel ratio from 0.0071 to 0.0316. For longitudinal reinforcement, the small steel ratio was 0.006.

3.2.4 Bridge Bearing

The girders of the bridge model were simply supported at one end. At that end, there is no longitudinal movement but only rotation. At the opposite end and at interior piers, the girders are supported on a rocker and rollers to permit both rotation about supports and longitudinal displacement. Details of the hinged and rocker-roller bearing are outlined in Figure (3.2).

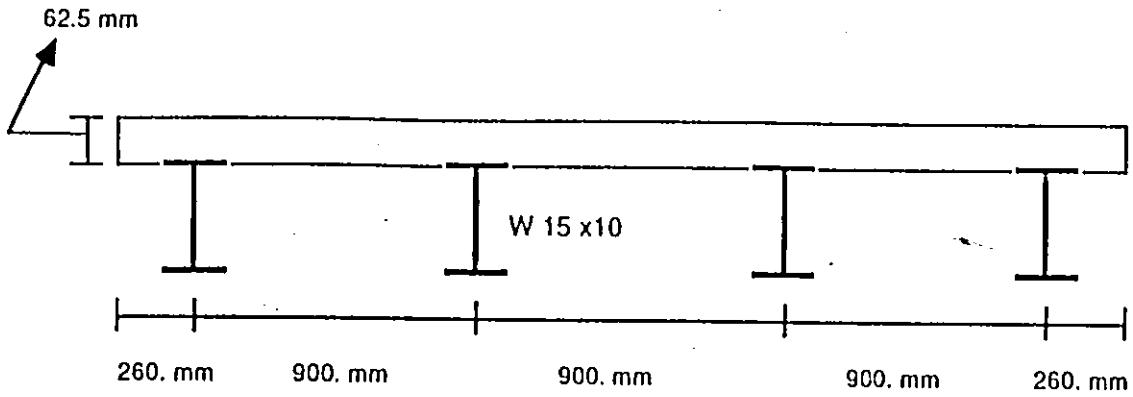

Transverse section.

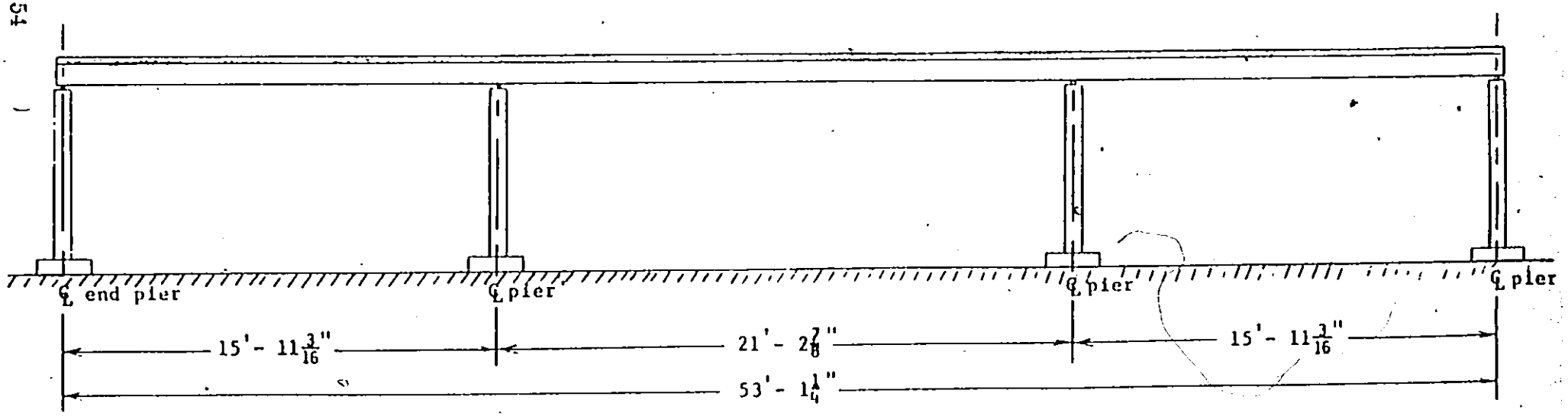

Elevation.

Figure 3.1: The 0.354-scale model bridge.

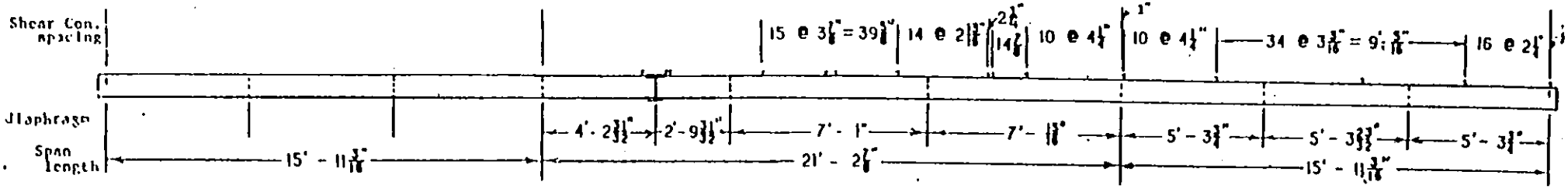

a) Longitudinal steel beams scale $\frac{3}{16}$" = 1'

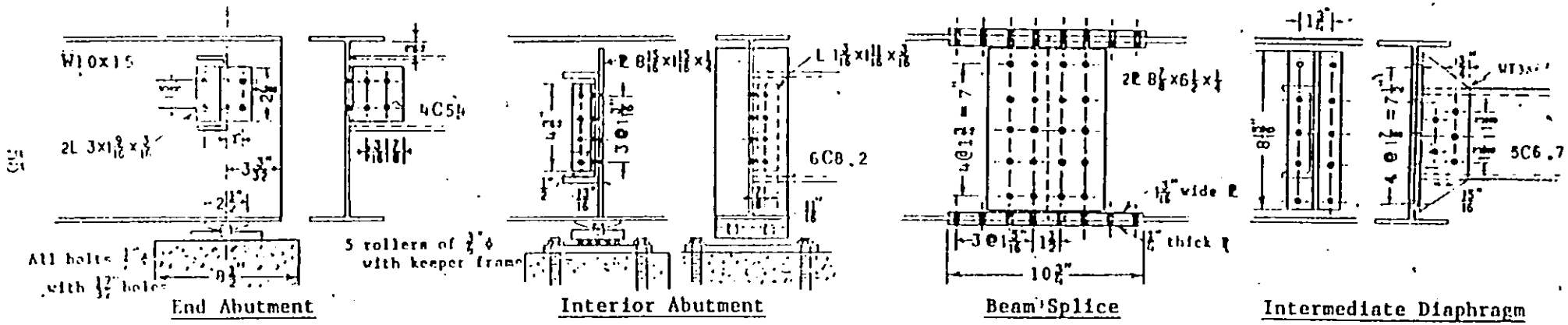

b) Details scale $\frac{1}{8}$" = 1"

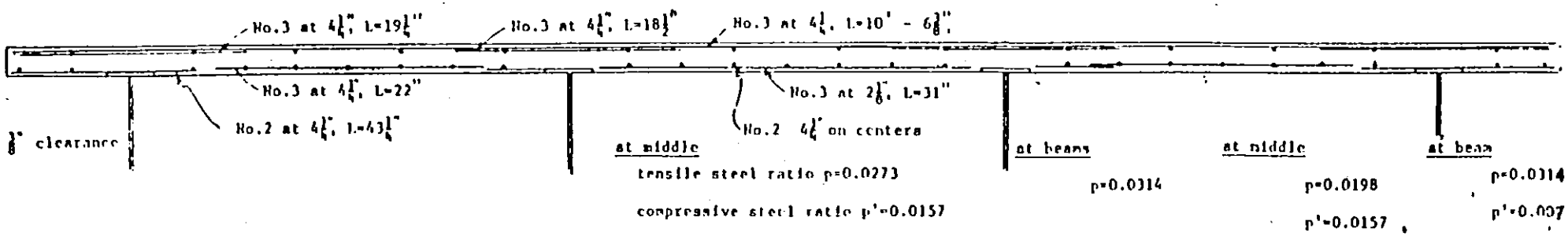

c) Reinforcement of deck

Figure 3.2: Structural details of model

3.3 Bridge Loading

3.3.1 Load System

Two types of loads were applied to the bridge model. The first type consisted of two point loads moving across the centerline of the bridge span.In moving the load across the centerline of the bridge, the loads were positioned directly above the interior girders, to determine the effect of intermediate diaphragms. The second type of loading consisted of the OHBDC truck load scaled down to fit the model and positioned to produce the following:

1. The maximum negative longitudinal moment.
2. The maximum positive longitudinal moment at the middle span.
3. The maximum positive longitudinal moment at the end span.

The position of the loads in the longitudinal direction are shown in Figure (3.7). Three lanes loaded always govern the design of a three lane bridge at the ULS in an elastic analysis. The truck loads distributed transversely over the girders. The transverse positions of the OHBDC vehicles are shown in Figure (3.8). In a design problem, the design vehicles would be positioned at any transverse position within each lane so as to maximize the force effect under consideration. This would require that transverse positions

Section 2.4, designers would normally use simplified methods to determine the largest elastic force effect in an interior and an exterior girder, then design all girders for the worst case. However, in a post-elastic analysis, the transverse redistribution that can occur will depend on the elastic distribution of moments, which depends on the transverse positions of the loads. Obviously, a multitude of combinations of transverse positioning could be considered. To keep the time and expense of this analysis within a reasonable limit, only one transverse position of the truck was included .

3.3.2 Scale OHBDC Load

The load scale factor was calculated so that the bending stresses produced in the prototype by the actual loads would be equal to the bending stresses produced in the model due to the scale load. The scale load factor was calculated to be 0.094 ($\frac{1}{10.63}$). The OHBDC truck load is shown in Figure (3.9 a). This loading was simplified by combining the two 140 kN load into one 280 kN load. This simplified loading was then moved longitudinally (from left to right) along the prototype bridge until the position of maximum moment was found (positive moment govern). The applied loads were then reduced by the load scale factor (0.094), and the spacing of the loads were reduced by the geometric scale factor (0.354) to get the model scale truck load as shown in Figure (3.9 c). The loading in Figure (3.9 c) was further simplified. The 5.64 kN load was eliminated to create only three lines of load. The other three loads were increased by (7.18%)

in order to produce the same maximum moment with three loads as was produced with the original four loads, see Figure (3.9 d). This adjustment of the loads increased the maximum value of the shear by only 5%.

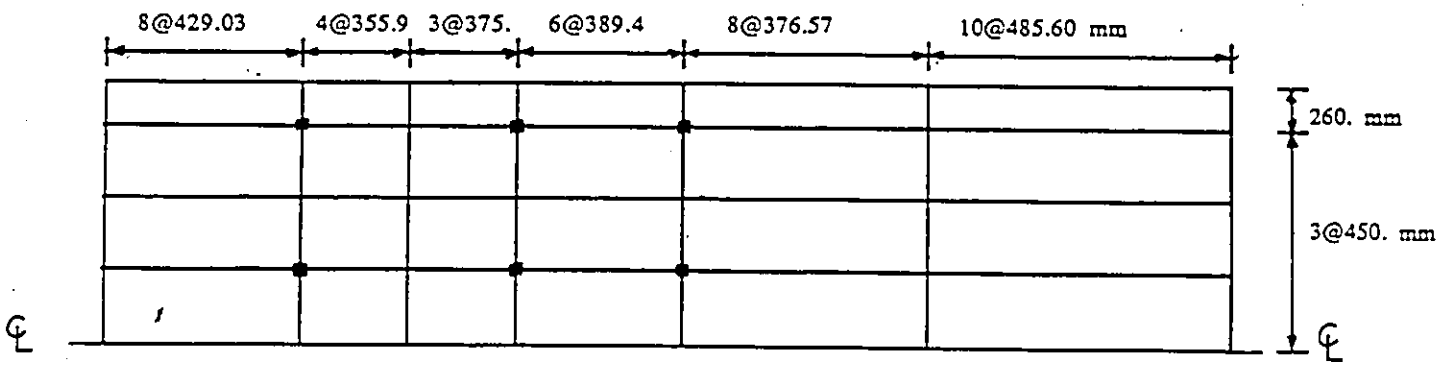

a) Finite element model-concrete slab elements.

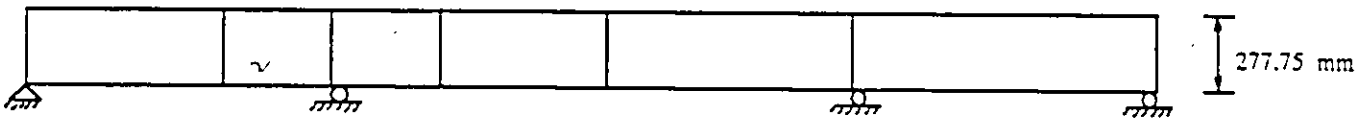

b) Finite element model-web elements.

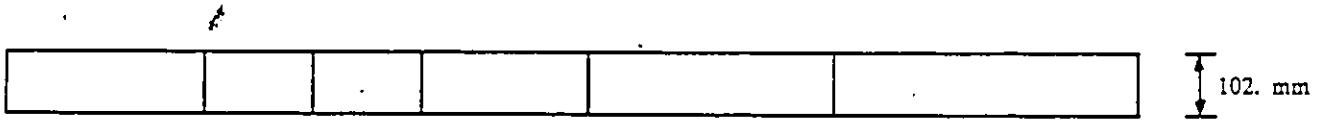

c) Finite element model-bottom flange elements.

Figure 3.3: Finite element mesh of the bridge model for NTC.

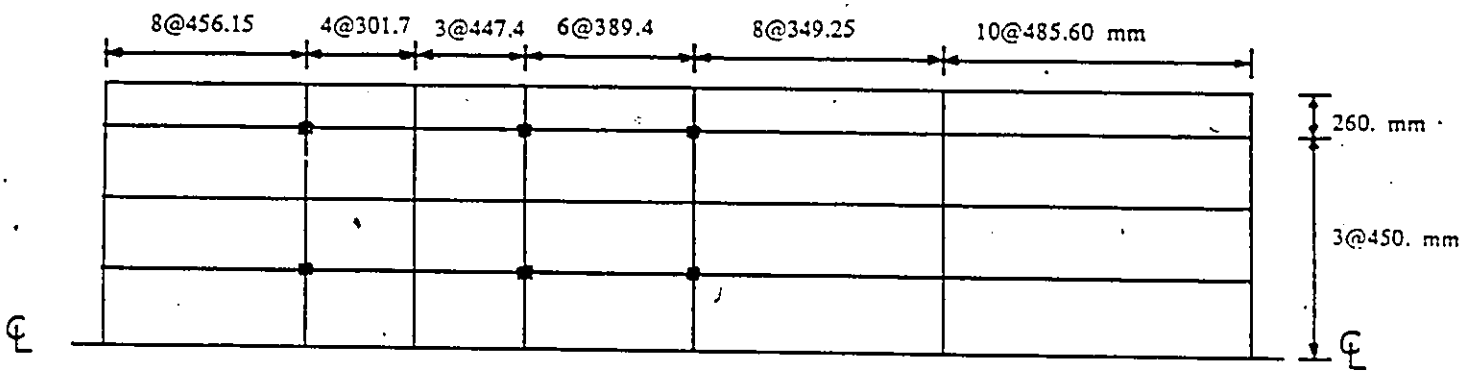

a) Finite element model-concrete slab elements.

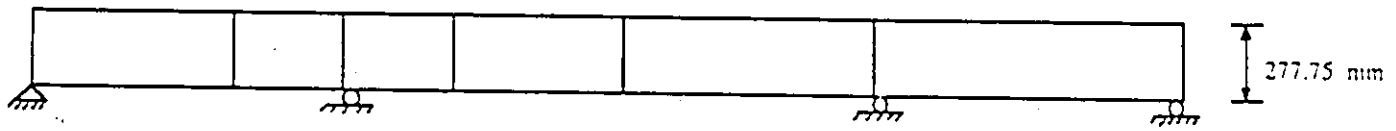

b) Finite element model-web elements.

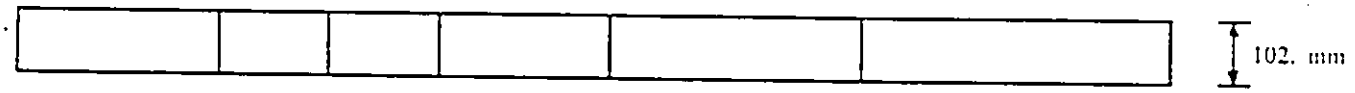

c) Finite element model-bottom flange elements.

Figure 3.4: Finite element mesh of the bridge model for PTC.

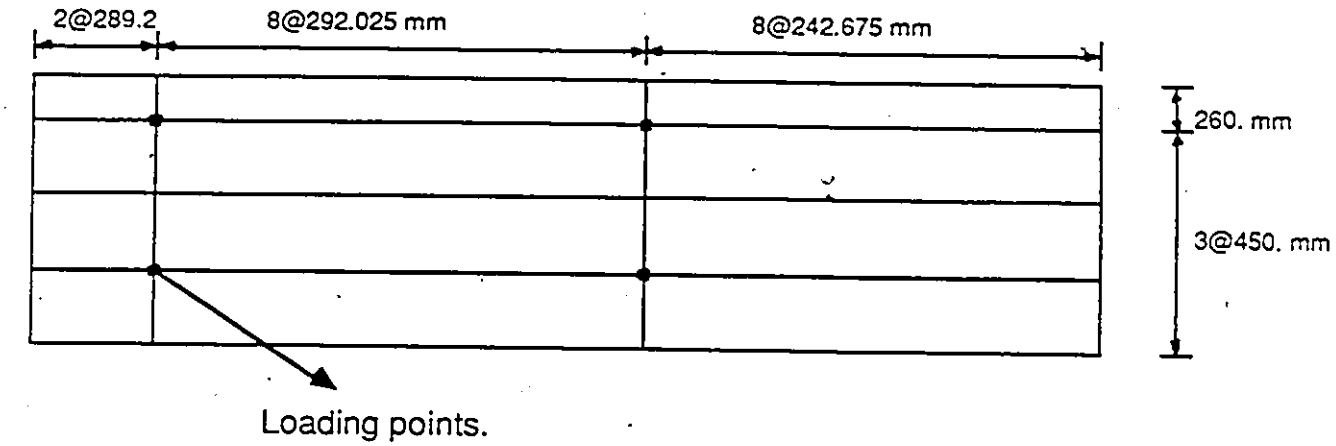

a) Finite element model-concrete slab elements.

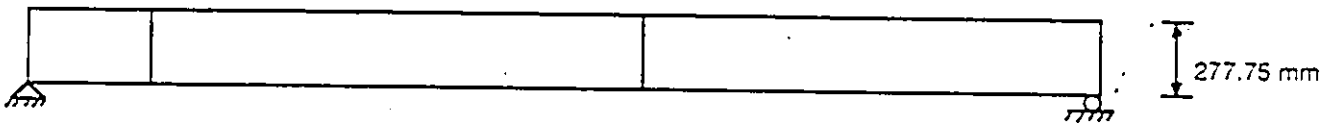

b) Finite element model-web elements.

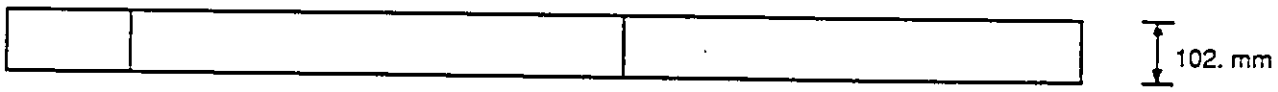

c) Finite element model-bottom flange elements.

Figure 3.5: Finite element mesh of the bridge model for PTS-3L & PTS-1L.

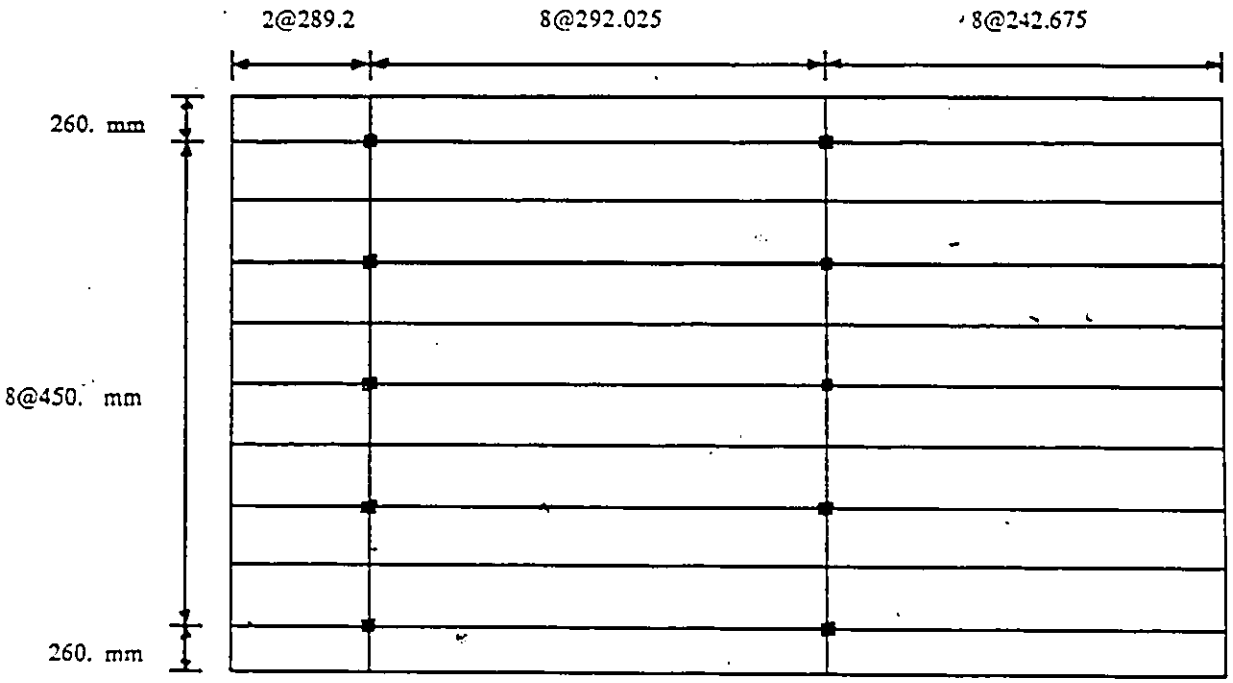

a) Finite element model-concrete slab elements.

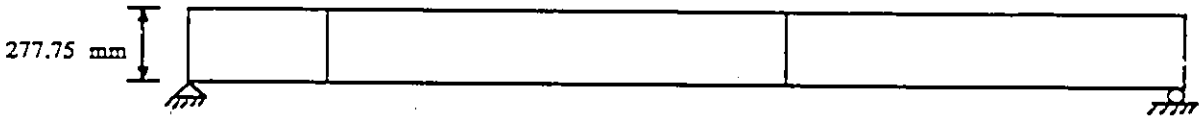

b) Finite element model-web elements.

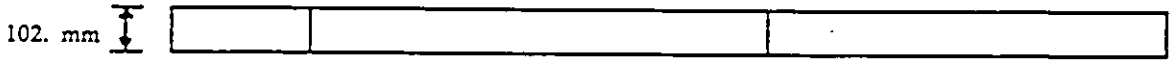

c) Finite element model-bottom flange elements.

Figure 3.6: Finite element mesh of the bridge model for PTS-2L.

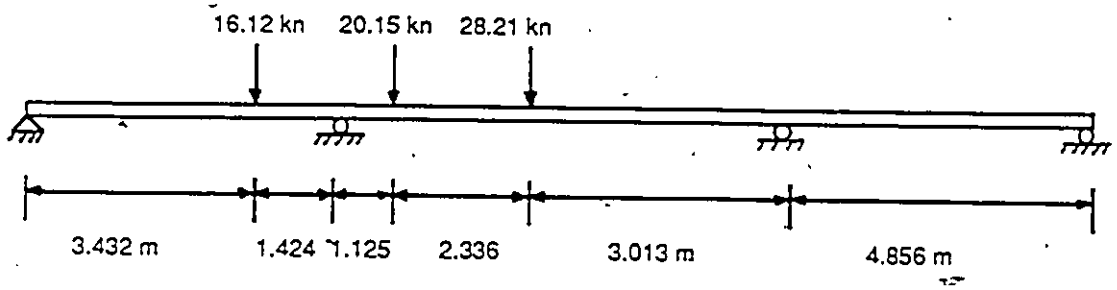

a) Longitudinal position of scaled OHBDC load for the NTC.

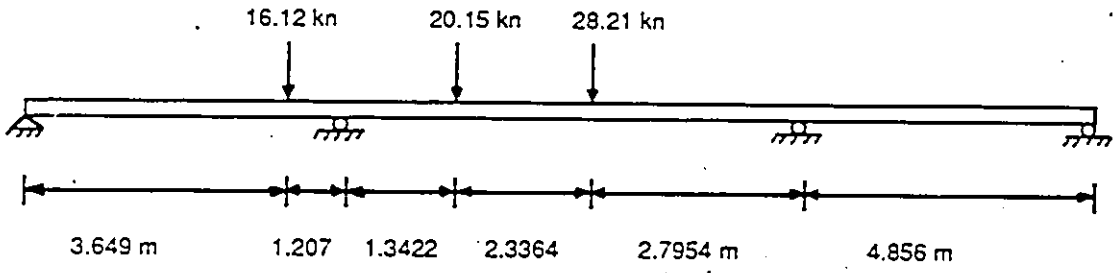

b) Longitudinal position of scaled OHBDC load for the PTC.

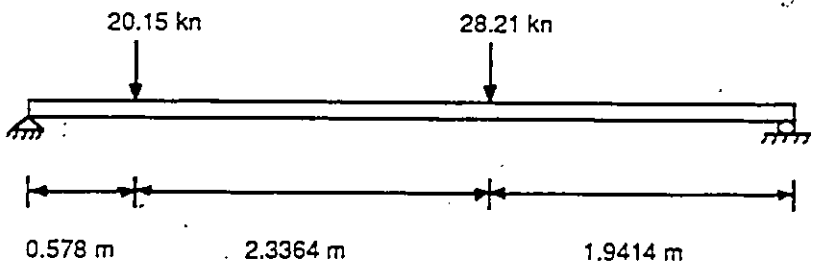

c) Longitudinal position of scaled OHBDC load for the PTS.

Figure 3.7: Position of the load in the longitudinal direction.

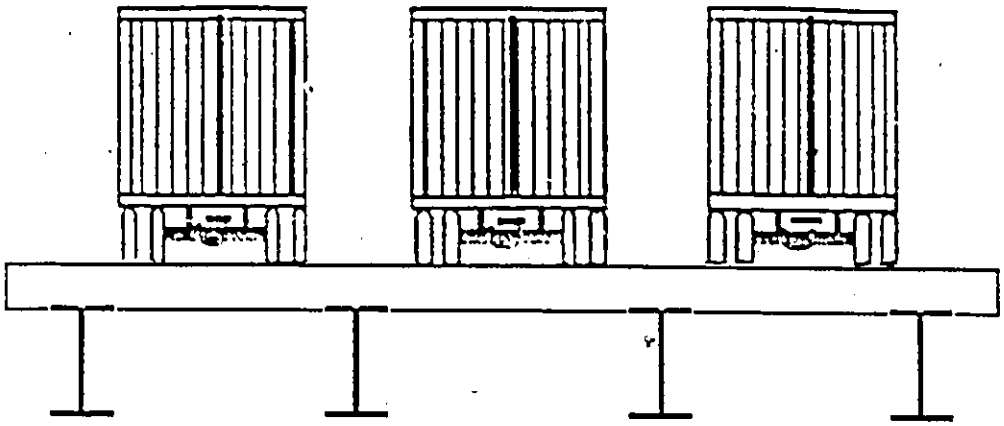

a) Three lanes loaded.

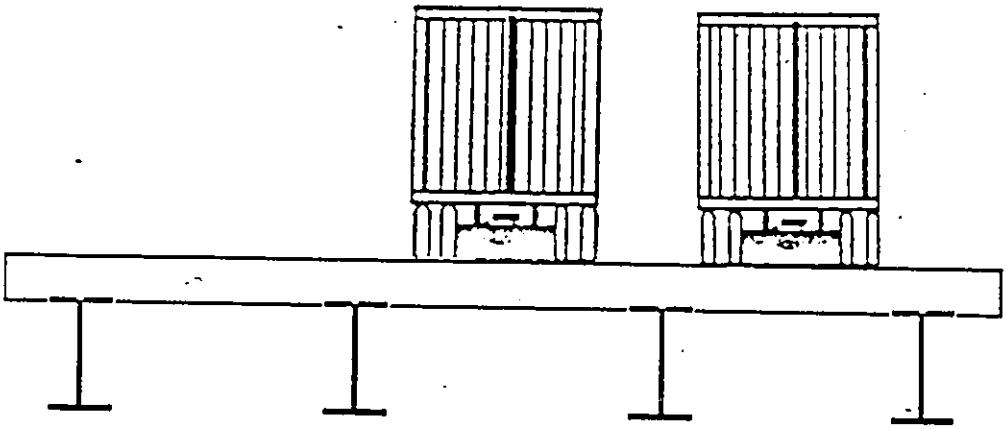

b) Two lanes loaded.

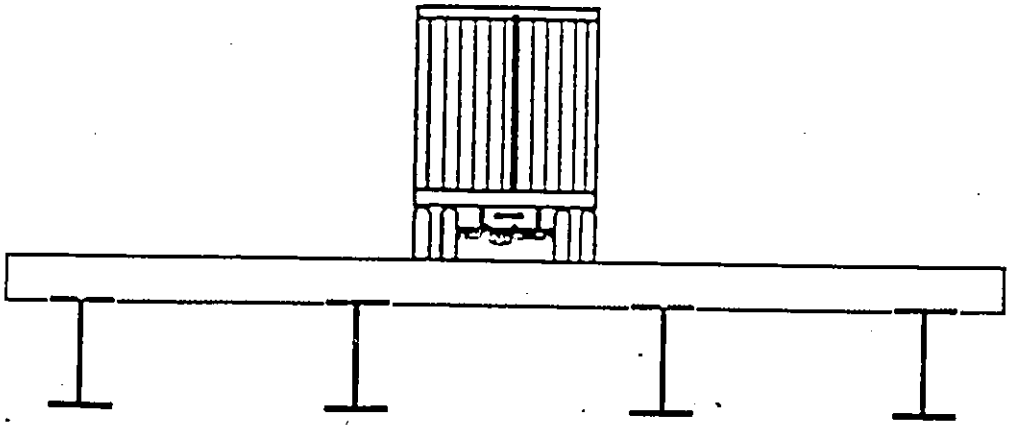

c) One lane loaded.

Figure 3.8: Transverse Truck Positions Considered.

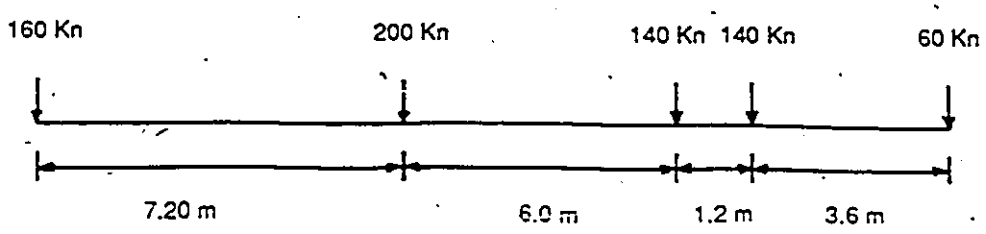

a) OHBDC Truck Load.

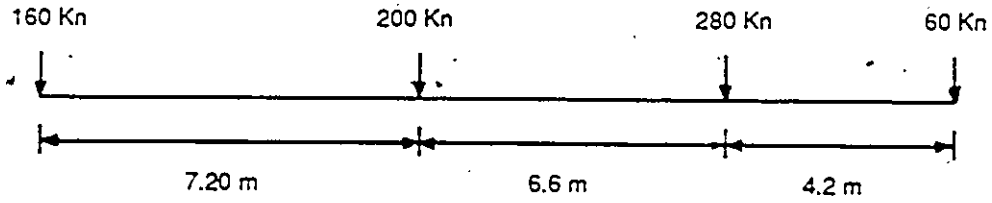

b) Simplified OHBDC Truck Load.

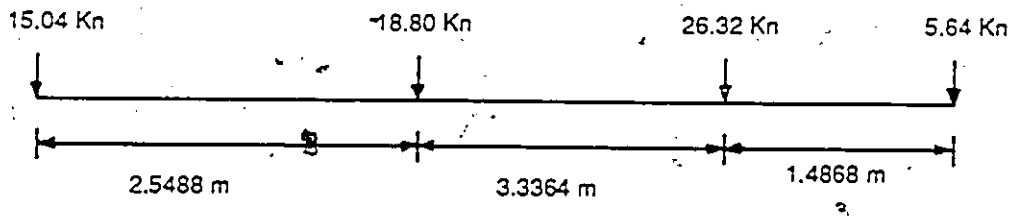

c) Model Scale Truck Load.

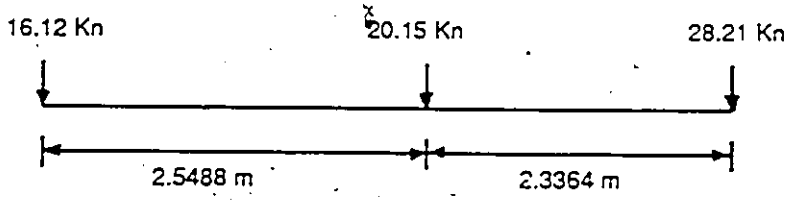

d) Actual Model Scale Truck Load.

Figure 3.9: OHBDC Scale Truck Loading.

3.4 Failure Criteria

It has been established that the bridge could fail due to a variety of reasons. The largest possible failure load would be associated with a plastic collapse mechanism. This occurs when enough hinges form to render the structure or a portion of it unstable. At the point of collapse, all the hinges are free to rotate while still resisting their simple plastic moments. However, it is possible that a hinge will have exhausted its plastic rotational capacity before a mechanism can form. If it unloads faster than the moment can be redistributed to other parts of the structure the load will not reach the simple plastic collapse load. Ductility of a sagging hinge depends on the degree of strain hardening in the tension flange of the steel girder before the slab concrete crushes. Various geometric and material properties influence this ductility[17]. Hogging rotation capacity depends on slenderness ratio and lateral bracing much the same as for naked steel beams, although the slenderness requirements for the web are severe because the slab reinforcement in a composite section will put more of the web into compression at the plastic moment than in a naked section [18]. Alternatively non-compact sections can be assumed to have sufficient hogging rotational capacity at a reduced effective moment according to Autostress Design Methods. High vertical shear could also cause a failure prior to the formation of a collapse mechanism, or could cause a reduction in the flexural capacity at hogging hinges over interior supports. The effect of a shear failure on the plastic collapse behavior of the bridge in question was not considered explicitly

because the shear capacities can be increased more or less independently of the flexural capacities by thickening the web. This could still influence the redistribution characteristics in that the thicker web improves the rotation capacity of a hogging section.

3.4.1 Numerical Verification

In order to show the validity of ADINA that was used in the analysis to develop the load distribution factors, a bridge analyzed experimentally by Dorton [19] and analytically by Bakht and Cheung [20] using OHBDC, was chosen to verify the computer solution presented in this thesis .

The structure selected was slab-on-girder bridge with six girders. The design details of the bridge is shown in Table(3.1). also the cross section of the bridge is shown in Figure (3.10) . Using simplified method given in the OHBDC . The calculation steps in arriving at D_{design} , are :

$$D_x = \frac{EI}{S} = \frac{E(56.29 \times 10^5)}{236.2} = 23829.62E \qquad (3.1)$$

$$D_y = \frac{Et^3}{12} = \frac{E(19.05)^3}{12} = 576.11E \qquad (3.2)$$

Neglecting the contribution of the steel beams to the torsional inertia,

$$D_{xy} = D_{yx} = \frac{Gt^3}{6} = \frac{E(19.05)^3}{12(1+.15)} = 500.96E \qquad (3.3)$$

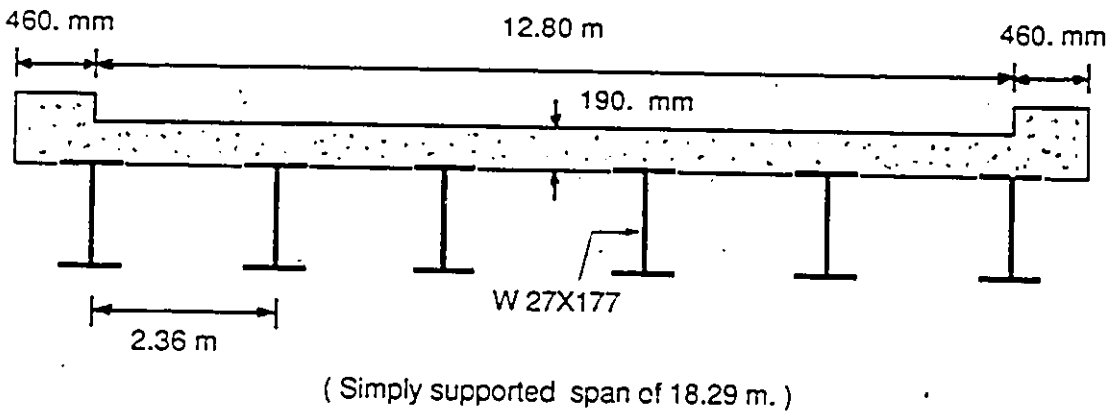

Figure 3.10: Cross section of a slab-on-girder bridge.

Table 3.1: Design details of the bridge and material properties

Bridge span length	=	18.29 m.
Bridge width	=	13.72 m
Spacing of beams	=	2.36 m
Slab thickness	=	190 mm.
Number of beams	=	6
Yield stress of beams	=	300 MPa
Modulus of elasticity of steel	=	20×10^3 MPa
Modulus of elasticity of concrete	=	26.5×10^3 MPa
Poisson's ratio	=	0.15

$$D_1 = D_2 = \nu D_y = 0.15(576.11)E = 86.42E \tag{3.4}$$

$$\alpha = \frac{1}{2}\left[\frac{D_{xy} + D_{yx} + D_1 + D_2}{(D_x D_y)^{0.5}}\right] \tag{3.5}$$

$$\alpha = \frac{1}{2}\left[\frac{500.96 + 500.96 + 86.42 + 86.42}{(23829.62 \times 576.11)^{0.5}}\right] = 0.16 \tag{3.6}$$

$$\theta = \frac{W}{2L}\left[\frac{D_x}{D_y}\right]^{0.25} = \frac{1371.53}{2 \times 1828.71}\left[\frac{23829.62}{576.11}\right]^{0.25} = 0.95 \tag{3.7}$$

The lane width is 4.27 m , therefore,

$$\mu = \frac{4.27 - 3.3}{0.6} = 1.6 > 1 \tag{3.8}$$

Use $\mu = 1$.

From the charts (3-7.1.2.1 b) given in OHBDC [2], the values of D and c_f are 1.98 m and 6.8% respectively, therefore ,

$$D_{design} = 1.98\left(1 + \frac{1 \times 6.8}{100}\right) = 2.12m. \tag{3.9}$$

This value is compared with the value obtained from ADINA using elastic analysis as shown in Table 3.2 .

Table 3.2: Comparison of distribution factors obtained by ADINA, OHBDC, and reference[20]

Method	D_{design}	
	meters	feet
OHBDC	2.12	6.96
ADINA	2.20	7.72
Testing[20]	2.43	7.97

Approximately 3.6% difference of D value between the finite element method and OHBDC method. This percent could be further reduced by increasing the number of elements.

Chapter 4

RESULTS AND DISCUSSION

The results for the seven separate analyses are presented in this chapter. They are listed below and labeled as the following:

- NTC
  1. Maximum negative moment in the continuous span bridge.
  2. Diaphragms are not included.
  3. Transverse hinges included in the analysis.
- PTC
  1. Maximum positive moment in the continuous span bridge.
  2. Diaphragms are not included.
  3. Transverse hinges included in the analysis.

4. Longitudinal hinges included in the analysis.

- PTS-3L

1. Maximum positive moment in the simply supported bridge.
2. Diaphragms are not included.
3. Transverse hinges included in the analysis.
4. Three lanes loaded.

- PPS1

1. Maximum positive moment due to point load in the continuous span bridge.
2. Diaphragms are included.
3. Transverse hinges are included.

- PPS2

1. Maximum positive moment due to point load in the continuous span bridge.
2. Diaphragms are not included.
3. Transverse hinges are included.

- PTS-2L

1. Maximum positive moment in the simply supported bridge.
2. Diaphragms are not included.

3. Transverse hinges included in the analysis.

4. Two lanes loaded.

- PTS-1L

1. Maximum positive moment in the simply supported bridge.
2. Diaphragms are not included.
3. Transverse hinges included in the analysis.
4. One lane loaded.

4.1 Critical States:

As mentioned in section 2.5 , the plastic collapse is not the only possible mode of failure in an elasto-plastic analysis. Rapidly increasing deflection subsequent to a significant decline in stiffness would be another critical state, even though the structure is technically stable .

There are other stages in the post-elastic loading that may also be critical with respect to changing behavior . Due to the loading configuration and the geometry of the bridge model , the first hinge to form was a sagging hinge, even in that case where the vehicle was positioned to maximize negative bending moment. The beginning of post-elasticity with the formation of the first hinge is one such state. According to OHBDC specifications, this would represent the capacity of the bridge at ULS for the specific loading configuration.

In summary, there are four states in the elasto-plastic loading when the behavior of the structure may become critical. The four critical states are defined as follows :

1. Formation of the first sagging hinge.
2. Formation of the first hogging hinge.
3. Significant reduction in the overall stiffness of the structure, followed by rapidly increasing deflection.
4. Failure at the ultimate load.

In all the analyses the four critical states in sequence at distinct load stages,

4.2 Transverse Distribution:

Transverse distribution of moments could be expressed numerically by the load distribution factor, D. This value, which has unit of length, is used in the ratio $\frac{S}{D}$, where S is the girder spacing, to calculate the fraction of the load effects due to one wheel line of the design vehicle to be carried by one girder. The transverse distribution factors calculate as follow:

$$D = \frac{M}{M_g}\left(\frac{S}{2n}\right) \tag{4.1}$$

where, n is the number of lanes loaded. The load distribution factor for the most heavily loaded interior and exterior girders at the critical sections and at each critical state are tabulated in Tables 4.1 to 4.7. The larger the value of D, the less load that girder will carry. At the elastic stage and the formation of the first hinge the exterior girders usually have D values larger than the interior girders. The closer the values of D across a section, the better (i.e. the more uniform) the transverse distribution of load. Consequently, as the moments are redistributed transversely, the D values for the interior girders increase while those for the exterior girders decrease.

In Figures 4.10 to 4.14, the moment ratio for each girder at the three stages is plotted, where the moment ratio is given by the live load moment in each girder divided by the total live load moment across the section ($\frac{M_g}{M}$). For

bulk of the load is carried by the interior girders in an elastic distribution (i.e. elastic stage). At stage two (elasto-plastic), the transverse distribution of the moments begins to improve, reaching the uniform distribution at ultimate .

The transverse distributions for that analysis where both lanes where loaded, NTS-2L, is shown in Figure (4.13). In this case, the elastic distribution has the most of the moments carried by the girders G2, G3, and G4, with a larger proportion resisted by the girders G3 and G4. The exterior girder G1 furthest from the load resists only a small moment in the opposite sense to the others . In the post-elastic range, the transverse distribution improves among the two most heavily loaded girders (G3 and G4). The girders G1 and G2 also resist an increasing proportion of the moment and the redistribution was not achieved at any section.

For the case where one lane was loaded (PTS-1L), the load initially is carried primarily by the interior girders in the elastic stage . However, as the load increases causing yielding of the interior girders, the distribution of the moments begin to change. At the elasto-plastic and ultimate stages, the transverse distribution of the moments begin to improve as shown in Figure (4.14).

For the Tables 4.1 to 4.7, the distribution factors for all the cases are nearly constant under low magnitude of load (elastic stage). This value is a function of the elastic stiffness of the slab and the girder as well as the loading configuration. The distribution factors start to decrease when first

yield occurs at the interior girders. This trend continues until the section becomes fully plastic. Then, any further increase of external load will be distributed to the external girders until sufficient number of plastic hinges have developed to form a collapse mechanism. Table 4.1 also shows that the total moment is distributed both transversely and longitudinally as the load increases.

4.3 Longitudinal Distribution:

The longitudinal distribution of live load bending moment for the PTC at each load step, is shown in Figure (4.1). This represents the distribution of the total longitudinal moments summed over each of the four girders . The maximum positive and negative moments are indicated by M^+ and M^- respectively.

The distribution at the formation of the first hinge is elastic. The longitudinal distribution factor, ψ, is given by :

$$\psi = \frac{M_n^-}{M_1^-}\left(\frac{f_1}{f_n}\right) \tag{4.2}$$

where :

M_1^-, M_n^- = the total negative moment at the first and n^{th} states respectively.

f_1, f_n = the live load factors at the first and n^{th} states respectively.

This is the ratio of the elasto-plastic hogging moment to the elastic moment at an equivalent load multiple. The expression $100(1-\psi)$ yields the percent redistribution of moments from the hogging region to the sagging region . A negative value corresponds to net redistribution from the sagging region to the hogging region (*i.e.* $\psi > 1$). The values of longitudinal distribution factors are shown in Table (4.1).

Table (4.1), shows small amount of longitudinal redistribution achieved for the PTC analyzes loaded to maximize positive bending, 0.2% to 15.2% by stage.two, and up to 19.4% by failure.

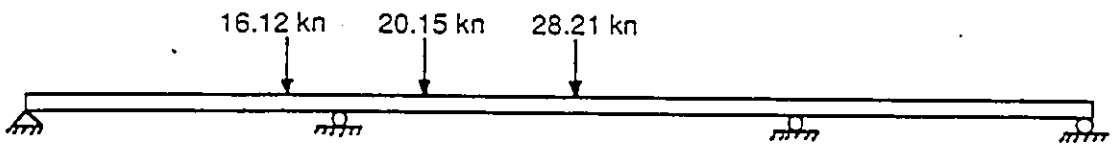

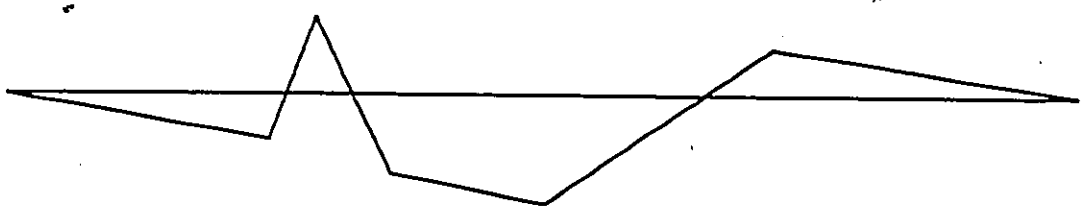

State 1 : First hinge forms (elastic moments)

M = 492.89 kn.m
Ψ = 1.

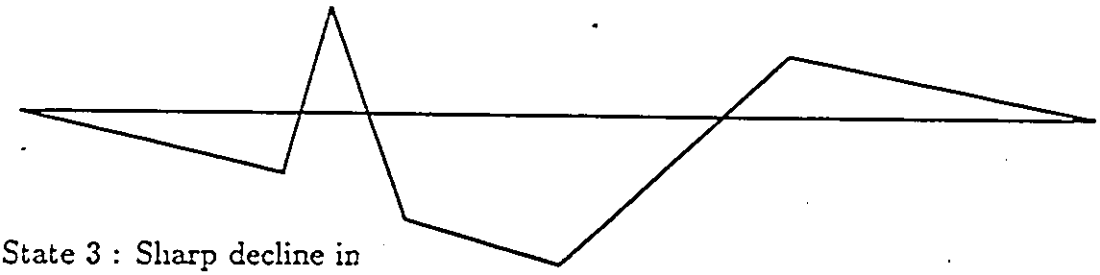

State 3 : Sharp decline in stiffness .

M = 750.61 kn.m
Ψ = 0.9089

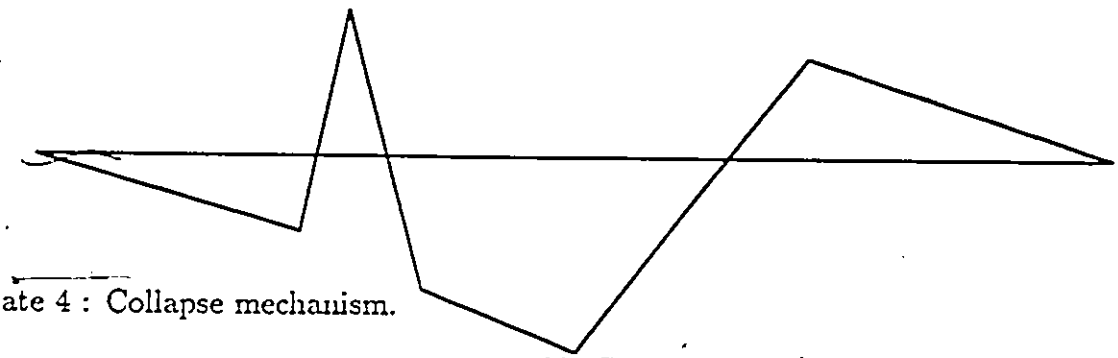

State 4 : Collapse mechanism.

M = 744.132 kn.m
Ψ = 0.8604

Figure 4.1: Longitudinal moment distribution, case PTC .

4.4 Load vs. Deflection

The nonlinear behavior of a bridge is perhaps most easily revealed when the load-deflection curve of some suitable point is plotted . For this bridge, the maximum deflection at the mid-span for both exterior and interior girders are plotted against the load for all the analysis in Figures (4.3) to (4.9). In each case analyzed, it is seen that these curves have, of course, a linear portion in the beginning. When plastification starts, deflection increase more rapidly. After a certain load level these curves again seem to have an almost linear but still rising portion . In Table (4.4), the maximum deflection for exterior girder in the case of PPS1 is more than that in the case of PPS2 by 10% in the elastic stage. This percentage decreased up to 0.2% at the ultimate.

The collapse caused by plastic hinge action is usually indicated by a horizontal portion in the load-deflection curve. The corresponding load level is then taken as the plastic load. In this case, an estimation for the limit load can be determined by the intersection of the two tangents to the load deflection curve .

4.5 Effect of Diaphragms

In the cases of PPS1 and PPS2, two point loads were applied on the mid-span of each of the interior girders to determine the effect of the diaphragms . The initial yielding of the girders was predicted at a load of 275 kN. Some typical results are presented in Table (4.4) to illustrate the effect of diaphragms on the transverse distribution of bending moments and the deflection at the mid-span . The data presented in Table (4.4) indicate that the diaphragms improves the distribution factors by 0.2% in the elastic stage. This percentage increased up to 2% at the ultimate . The result also serves to indicate the general non-uniform distribution of bridge response when load is applied in a relatively concentrated mode. It should be emphasized that with increasing load across the section(more lane loaded), the distribution of moments becomes much more uniform.

4.6 Number of Lanes Loaded

For the three lane bridge analyzed, two conclusions can be made regarding the effect of the number of lanes loaded.

First, one and two lane loading would not govern the design of the bridge at ULS regadless of whether capacity is based on elastic strength calculation, plastic collapse, or any of the intermediate states identified as being critical.

Second, three lane loading generally will govern the design of the bridge at ULS and it is possible to achieve a collapse mechanism . This would be contingent on sufficient capacity in the slab to allow complete transverse redistribution. With one and two lane loaded, however, the formation of a collapse mechanism is highly improbable based on the significant decrease in stiffness and rapidly increasing deflection which were predicted before any substantial transverse redistribution was achieved .

In practice, the truck can occupy any location across the bridge, therefore, one and two lanes loading cases will be important when assessing an existing bridge.

4.7 Load Multiples and Strength Reserve :

The load multiples or (load factors) are presented graphically in Figure (4.2), from which certain observations are easily made. First, for a given longitudinal positioning of the vehicles the load factors for a continuous span bridge are more than those for simple-span bridge at each critical state . In Figure (4.2) it can be seen that the ultimate load capacity for the one and two lanes loaded (PTS-1L and PTS-2L) is higher than that for the three lanes loaded (PTS-3L) . Also in a comparison of NTC vs. PTC, the load factor at critical state one (formation of the first hinge) is less when the vehicles are positioned to maximize negative rather than positive moments, but at all other cases the load factors for the positive bending case govern.

This indicates that when dealing with moving loads, the strength reserve between the formation of the first hinge (i.e elastic failure) and the plastic collapse of the bridge is given by the minimum plastic collapse load factor divided by the minimum elastic failure load factor, which may not necessarily be for the same load position. For example, it would be 7.44 (PTC, state four) divided by 4.8 (NTC, state one), yielding a strength reserve of 1.55 .

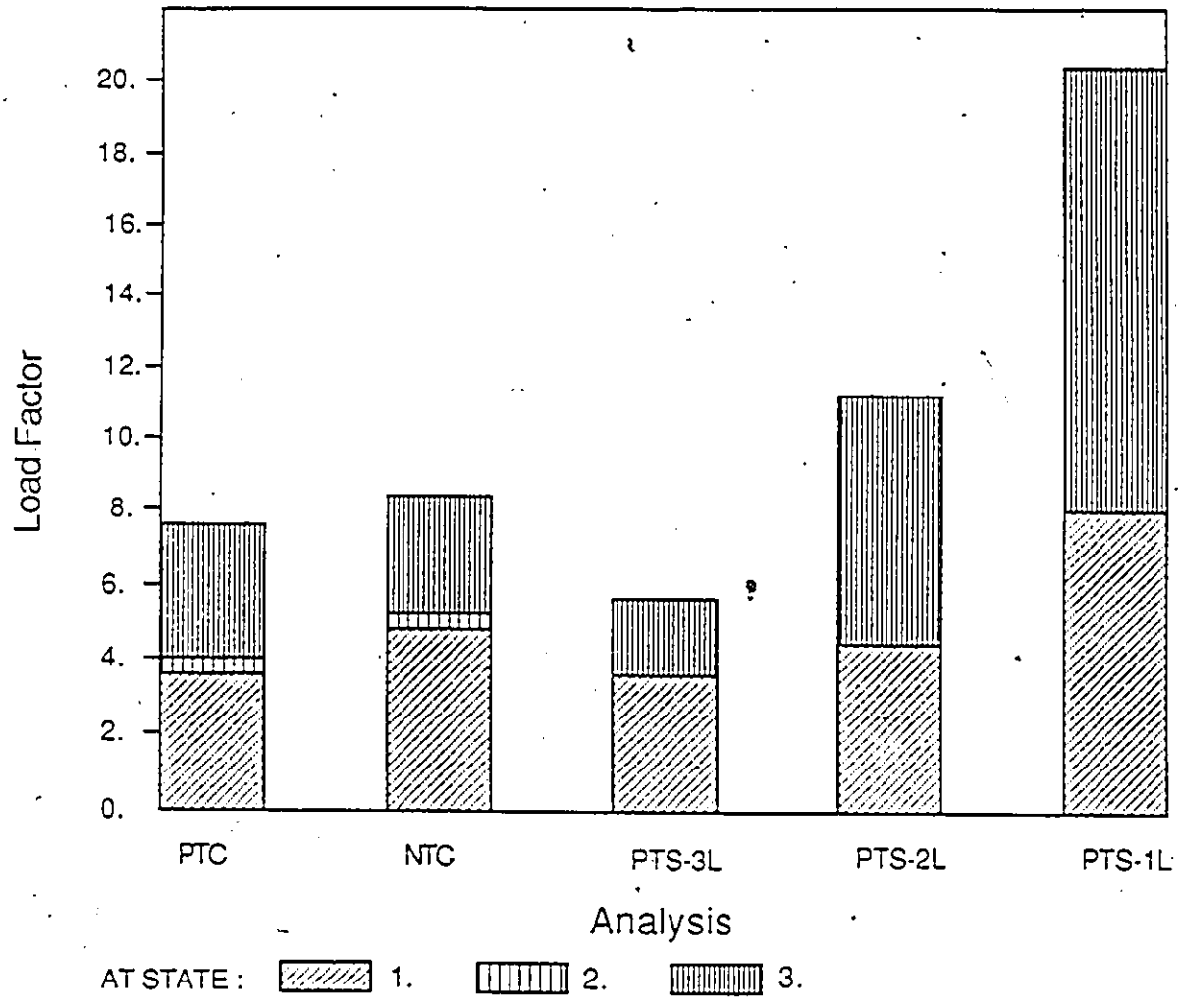

Figure 4.2: Load multiples at critical states.

Table 4.1: Moments and Load Distribution Factors for PTC

Load factor	Moment (kN.m)		D (m)		ψ (m)
	Exterior	Interior	Exterior	Interior	
1.0	29.185	35.317	0.6630	0.5479	–
2.0	58.371	70.635	0.6630	0.5479	–
3.82*	111.525	134.923	0.6630	0.5479	1.
4.0	116.726	140.844	0.6620	0.5486	0.9981
4.6	134.573	160.657	0.6581	0.5513	0.9948
5.2	153.633	178.901	0.6493	0.5576	0.9912
5.8	173.933	192.168	0.6315	0.5715	0.9783
6.4	184.576	190.727	0.6100	0.5903	0.9089
7.0	192.116	190.800	0.5979	0.6020	0.8479
7.44**	195.599	191.467	0.5937	0.6065	0.8064

1* first yielding started at the interior girder

2** both exterior and interior girders are yielded

Table 4.2: Moments And Load Distribution Factors For NTC

Load Factor	Moment (kN.m)		D (m)	
	Exterior	Interior	Exterior	Interior
1.	28.986	34.970	0.6619	0.5487
4.	115.948	139.881	0.6619	0.5487
4.8*	140.980	165.237	0.6516	0.5559
5.2	155.165	178.360	0.6448	0.5610
5.6	169.955	187.818	0.6315	0.5715
7.2	233.442	248.078	0.6188	0.5823
7.6	236.732	246.832	0.6128	0.5848
8.	242.189	245.404	0.6039	0.5961
8.4**	245.901	240.585	0.5935	0.6066

Table 4.3: Moments And Load Distribution Factors For PTS-3L

Load Factor	Moment (kN.m)		D (m)	
	Exterior	Interior	Exterior	Interior
1.	33.177	40.206	0.6636	0.5476
2.	66.356	80.411	0.6635	0.5476
3.	99.532	120.617	0.6636	0.5476
3.8*	127.111	152.651	0.6603	0.5498
4.	133.925	160.084	0.6586	0.5510
4.2	142.821	170.458	0.6581	0.5514
4.4	150.764	176.840	0.6519	0.5557
4.6	158.469	183.225	0.6469	0.5595
4.8	166.610	188.014	0.6385	0.5658
5.0	175.753	190.522	0.6252	0.5767
5.2	186.161	201.400	0.6246	0.5773
5.4	189.553	204.580	0.6238	0.5780
5.6	192.841	200.450	0.6118	0.5886
5.8	193.979	192.893	0.5983	0.6017
5.93**	189.329	190.578	0.6019	0.5980

Table 4.4: Deflection and Load Distribution Factors for PPS1 and PPS2

Load Factor	Girder	Deflection (mm)		D (m)	
		PPS1	PPS2	PPS1	PPS2
0.25	Ext.	2.40	2.19	3.049	3.065
	Int.	3.64	3.89	1.274	1.277
0.50	Ext.	4.81	4.37	3.048	3.065
	Int.	7.27	7.78	1.273	1.278
0.75	Ext.	7.20	6.56	3.049	3.066
	Int.	10.91	11.66	1.274	1.278
1.00*	Ext.	9.60	8.75	3.046	3.064
	Int.	14.55	15.55	1.277	1.274
1.50	Ext.	13.49	14.32	2.834	2.918
	Int.	24.05	26.06	1.319	1.302
2.00	Ext.	23.04	21.41	2.521	2.589
	Int.	36.51	39.65	1.400	1.380
2.50	Ext.	36.85	35.67	2.300	2.352
	Int.	55.77	60.52	1.478	1.458
2.75	Ext.	48.14	47.41	2.218	2.303
	Int.	69.34	75.66	1.515	1.498
2.80	Ext.	50.87	50.57	2.214	2.640
	Int.	72.68	79.43	1.516	1.479
2.82**	Ext.	52.11	51.99	2.215	2.265
	Int.	74.15	81.01	1.516	1.480

Table 4.5: Moments And Load Distribution Factors For PTS-2L

Load Factor	Moment (kN.m)				D (m)			
	G1	G2	G3	G4	G1	G2	G3	G4
1.	5.836	21.342	35.359	34.738	3.750	1.026	0.6190	0.6300
2.	11.676	42.674	70.714	69.492	3.750	1.026	0.6190	0.6299
4.*	23.352	85.341	141.413	139.076	3.750	1.026	0.6192	0.6296
6.	37.447	135.733	201.103	208.255	3.500	0.9656	0.6518	0.6294
7.	54.544	163.586	212.858	220.325	2.687	0.8958	0.6885	0.6651
8.	83.339	177.426	209.755	215.425	1.852	0.8699	0.7358	0.7164
10.	148.844	192.541	240.237	240.678	1.243	0.9609	0.7701	0.7687
11.	171.893	208.565	260.927	259.301	1.179	0.9717	0.7767	0.7815
11.18**	176.379	212.346	264.861	265.810	1.173	0.9742	0.7810	0.7811

Table 4.6: Moments And Load Distribution Factors For PTS-1L

Load Factor	Moment (kN.m)		D (m)	
	Exterior	Interior	Exterior	Interior
1.	7.322	16.450	2.922	1.301
2.	14.645	32.902	2.922	1.301
8.	58.590	131.621	2.922	1.301
8.2*	60.063	134.697	2.918	1.301
12.	91.035	189.881	2.777	1.331
14.	121.558	205.635	2.422	1.432
16.	142.671	198.440	2.152	1.547
18.	168.873	211.239	2.026	1.619
20.	181.670	215.190	1.966	1.660
20.42**	185.084	217.646	1.958	1.665

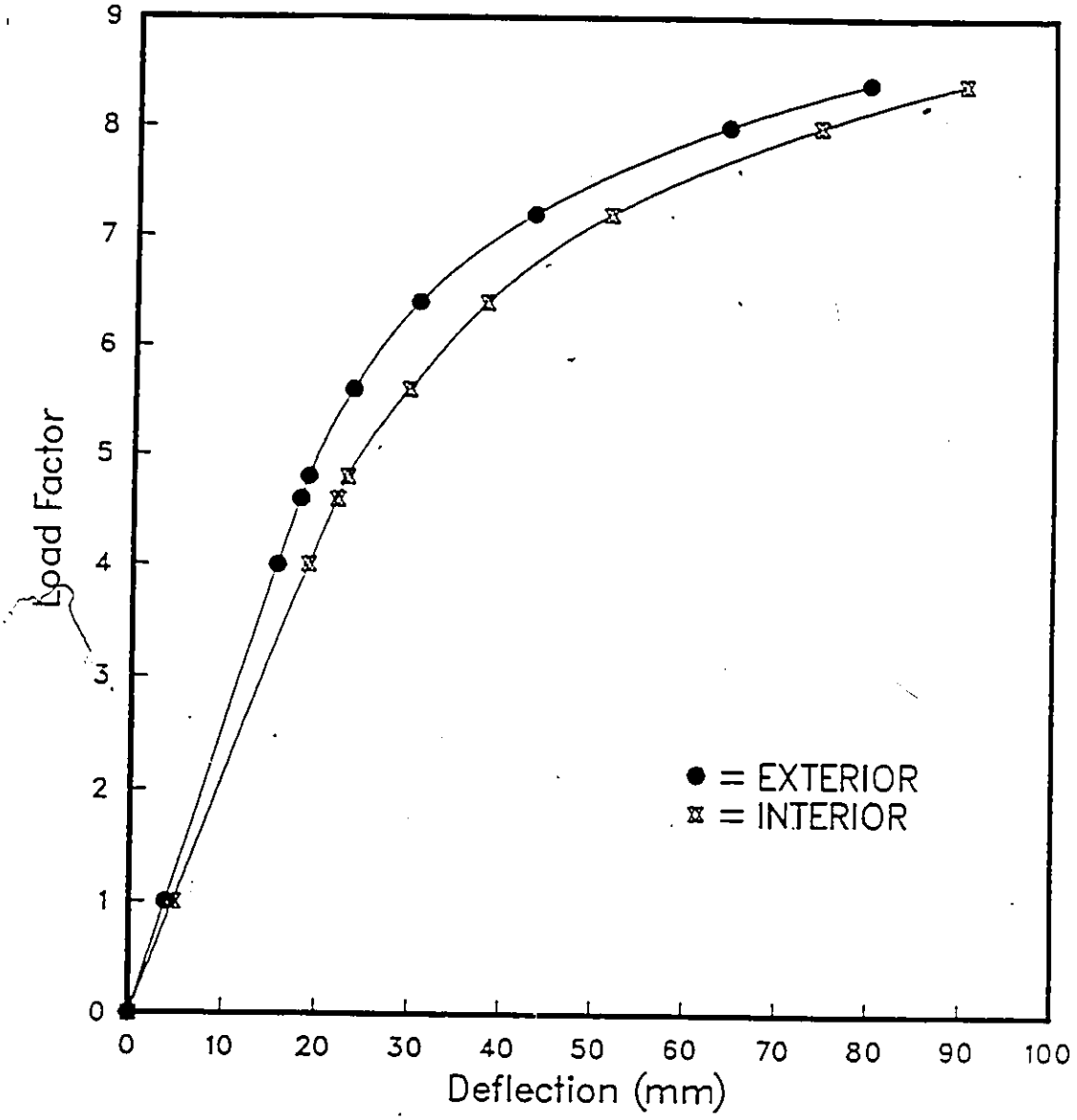

Figure 4.3: Load vs Maximum Deflection, case NTC.

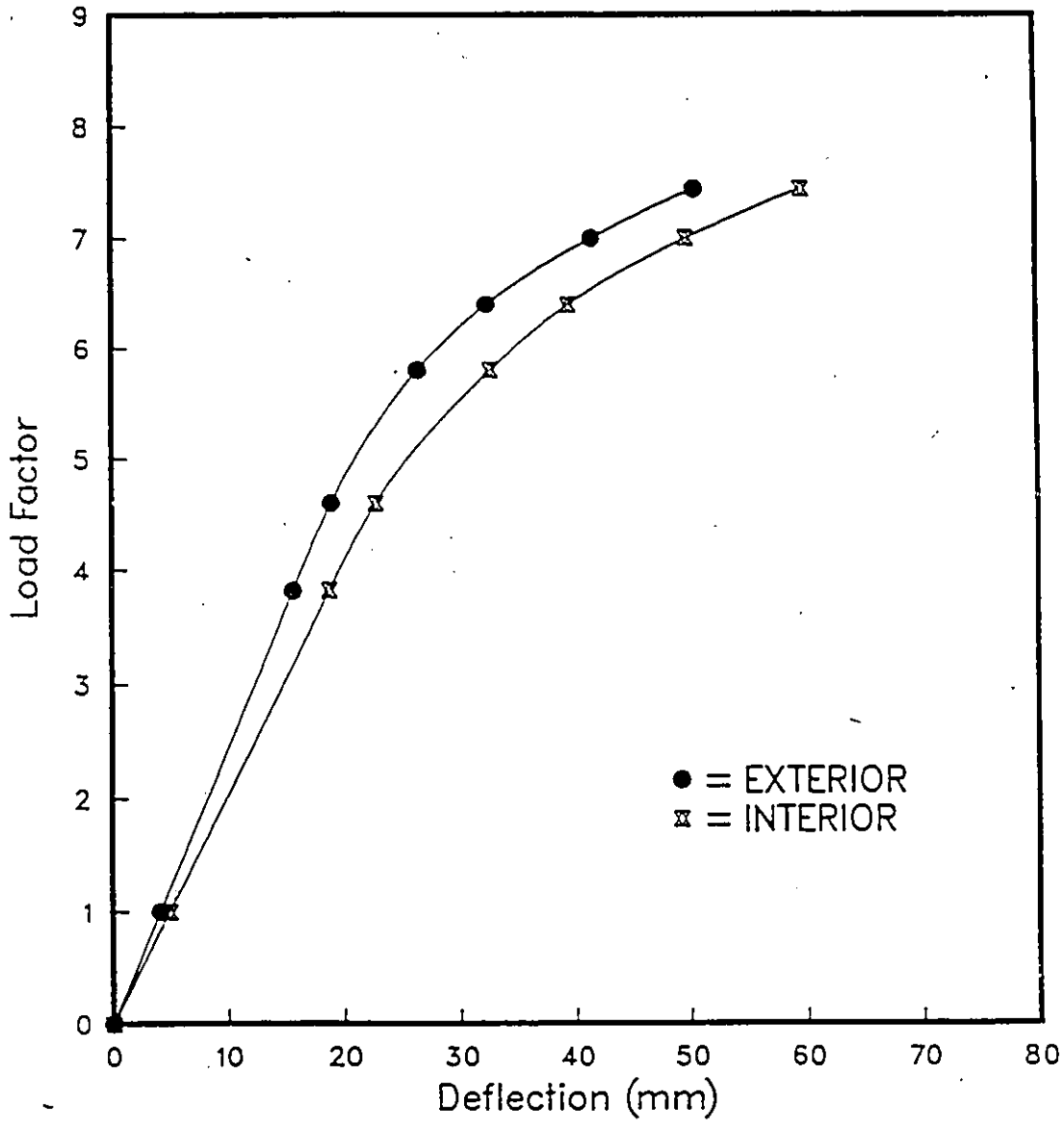

Figure 4.4: Load vs Maximum Deflection, case PTC.

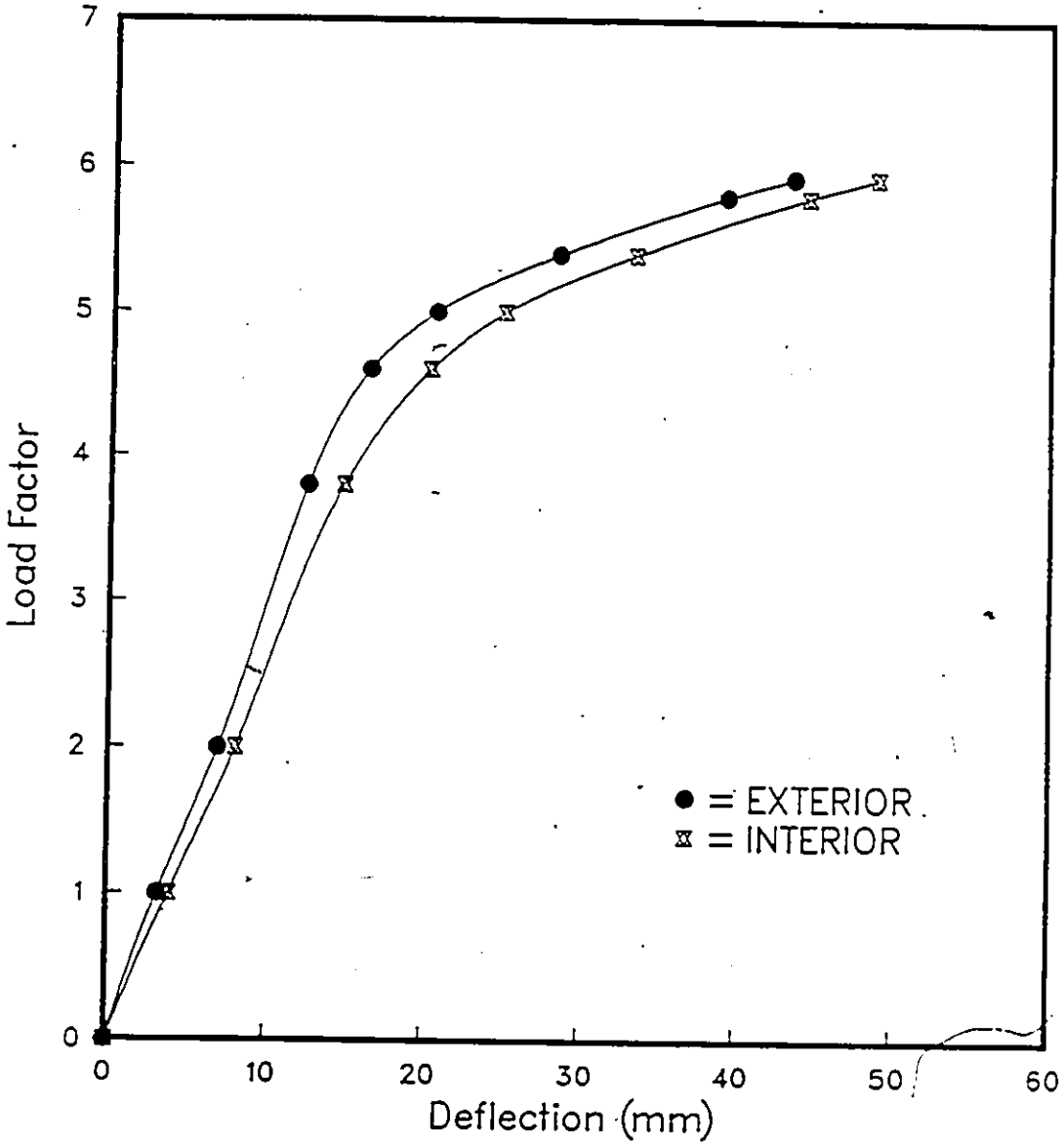

Figure 4.5: Load vs Maximum Deflection, case PTS-3L.

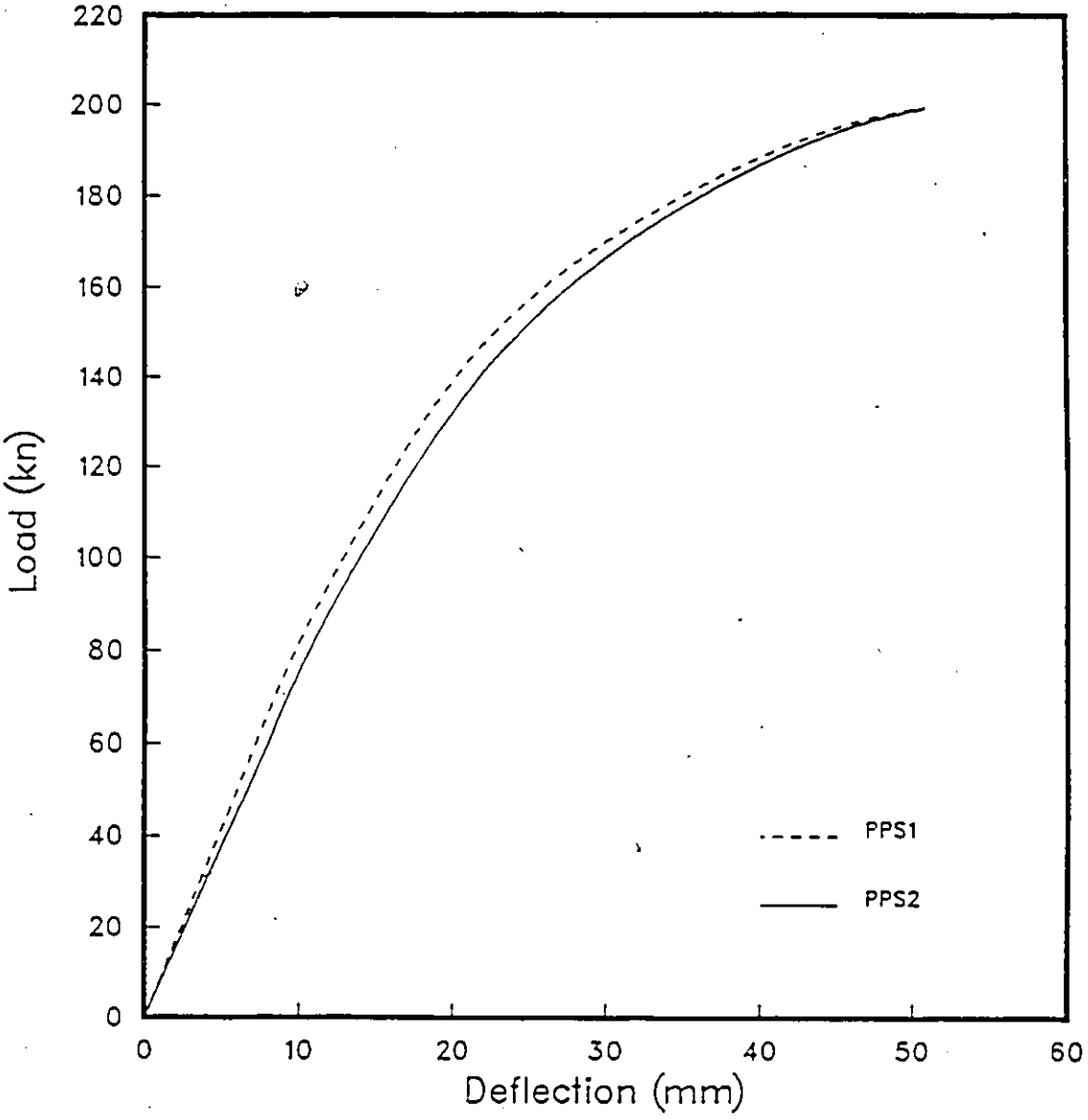

Figure 4.6: Load vs Maximum Deflection for the Exterior Girders, case PPS1 and PPS2 .

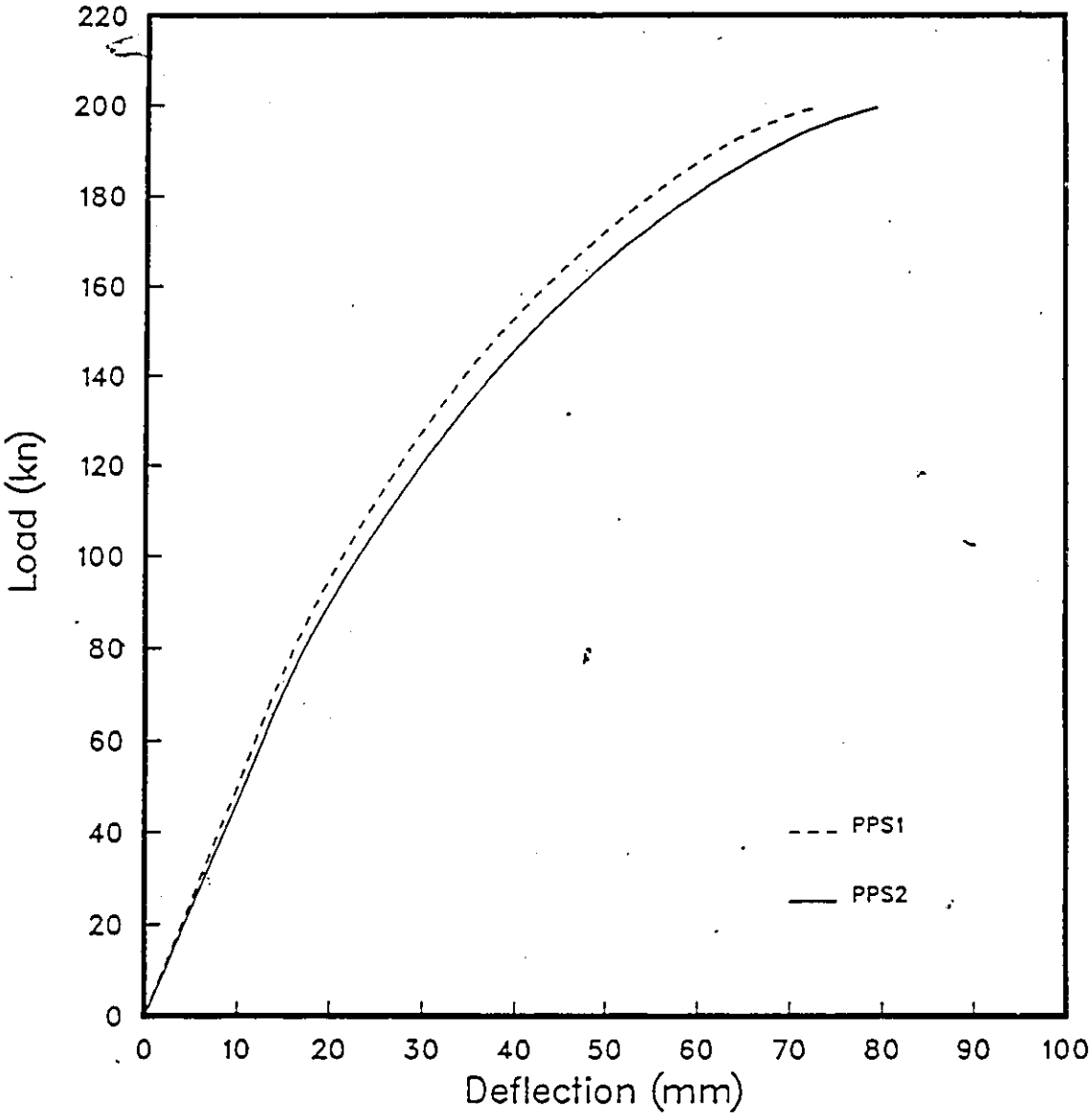

Figure 4.7: Load vs Maximum Deflection for the Interior Girders, case PPS1 and PPS2 .

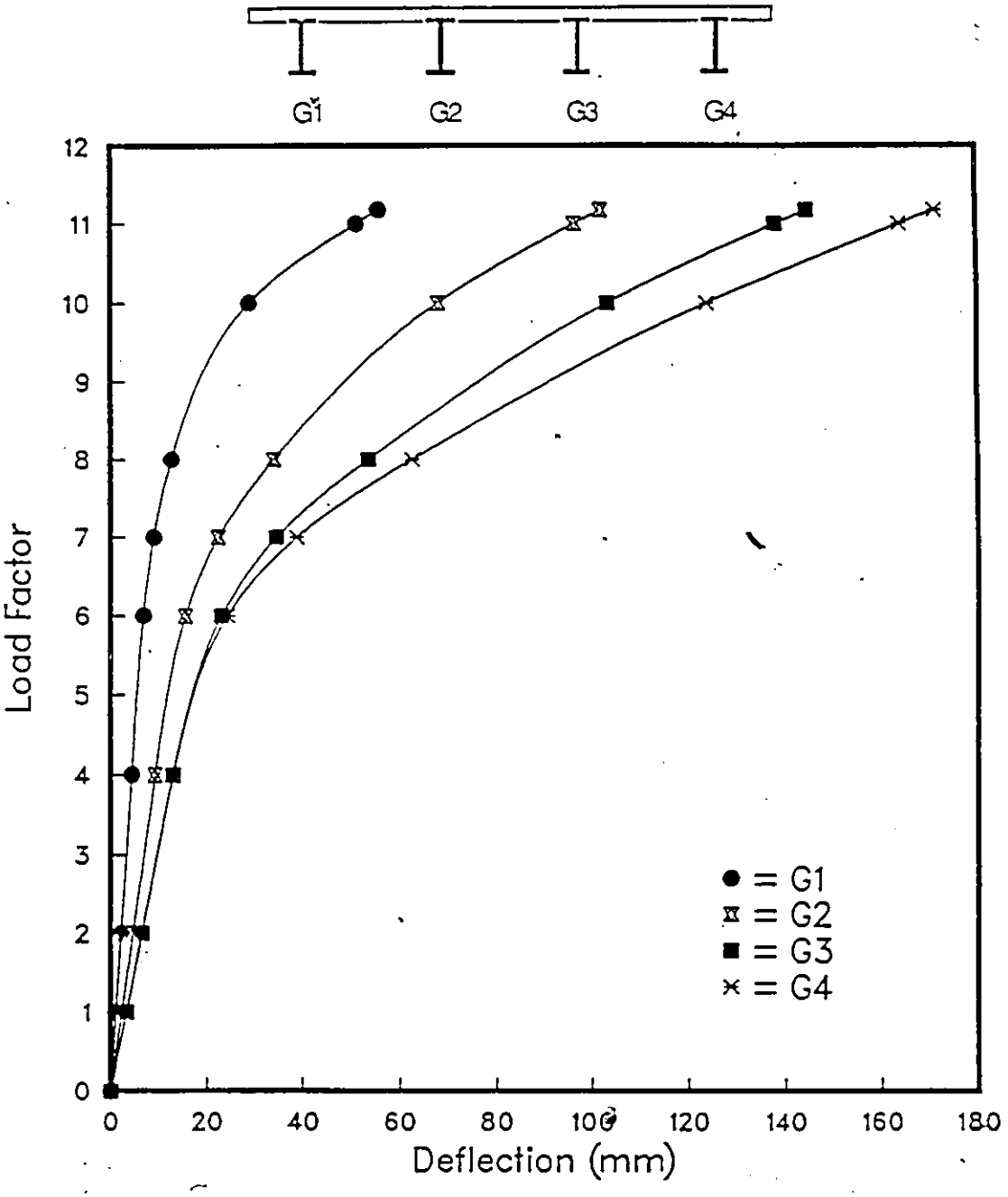

Figure 4.8: Load vs Maximum Deflection, case PTS-2L.

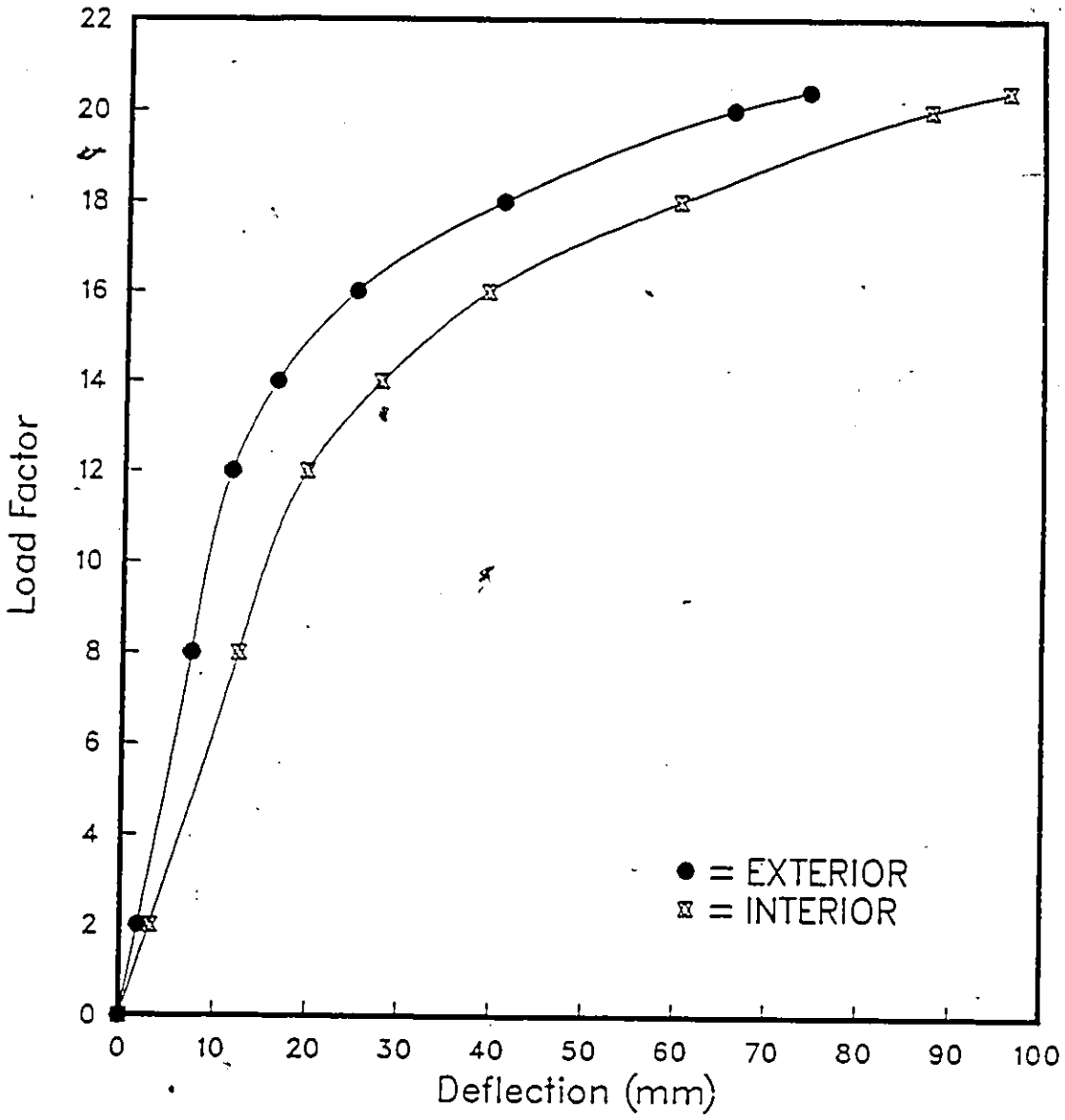

Figure 4.9: Load vs Maximum Deflection, case PTS-1L.

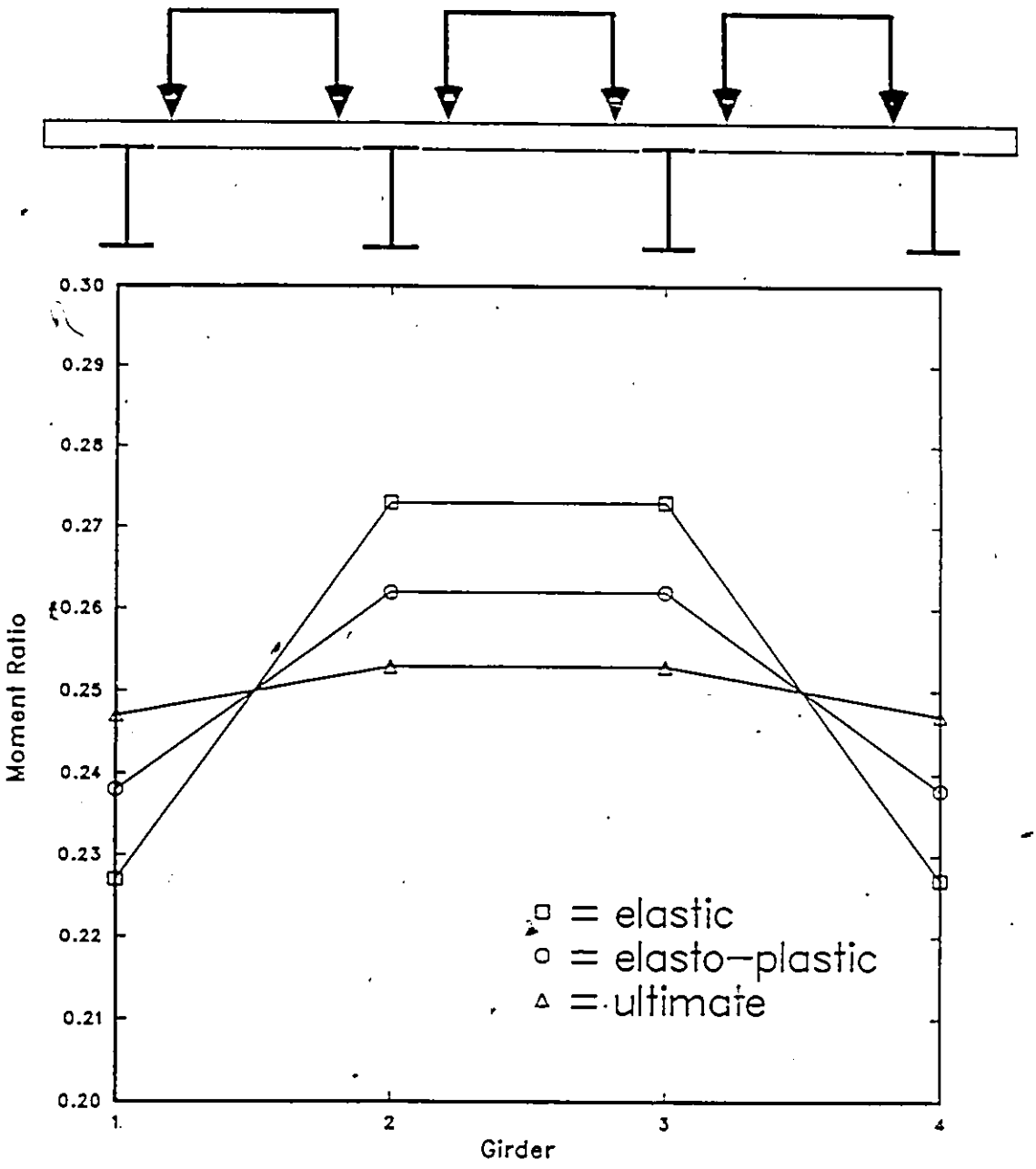

Figure 4.10: Transverse Moment Distribution, case NTC .

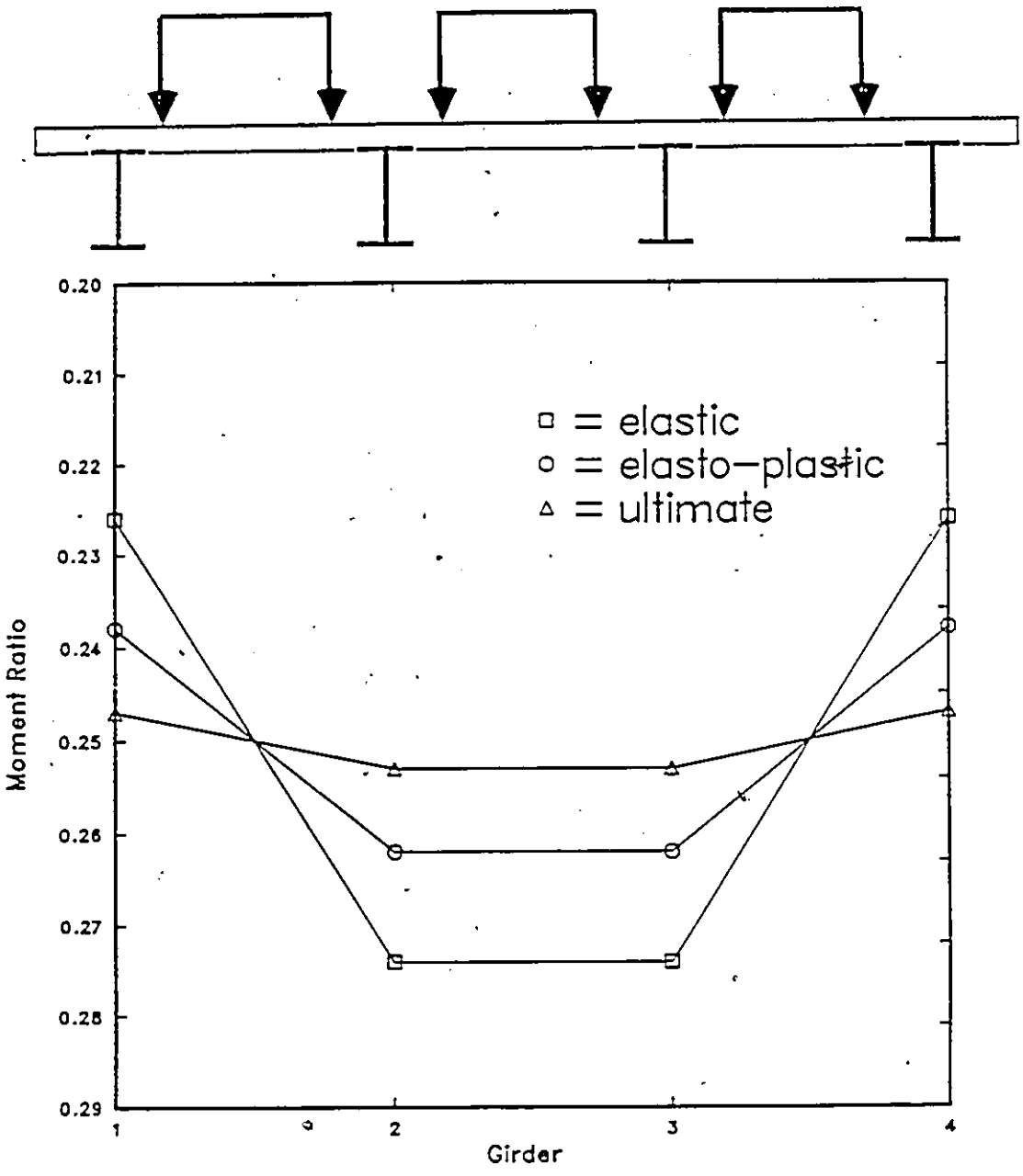

Figure 4.11: Transverse Moment Distribution, case PTC .

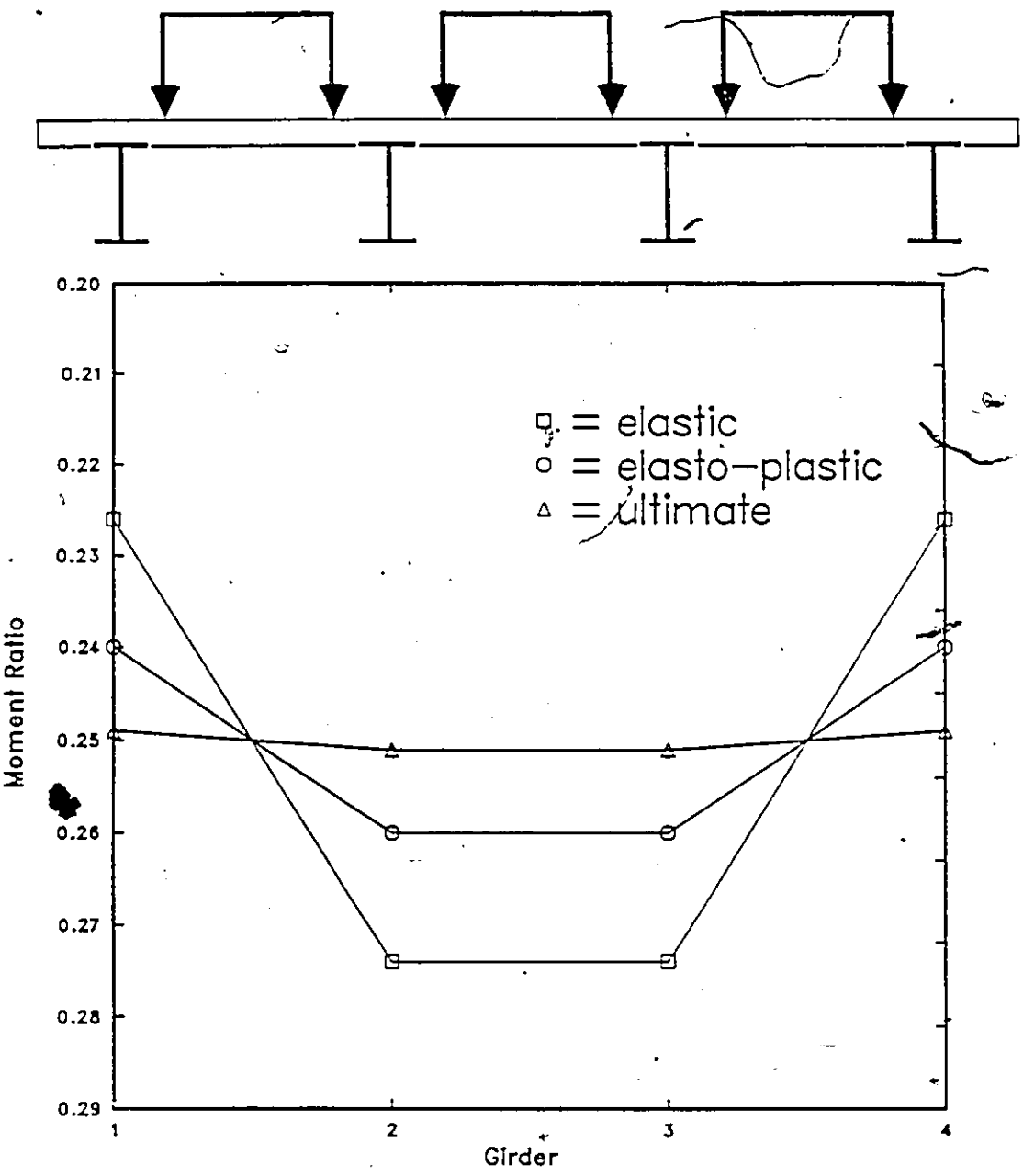

Figure 4.12: Transverse Moment Distribution, case PTS-3L .

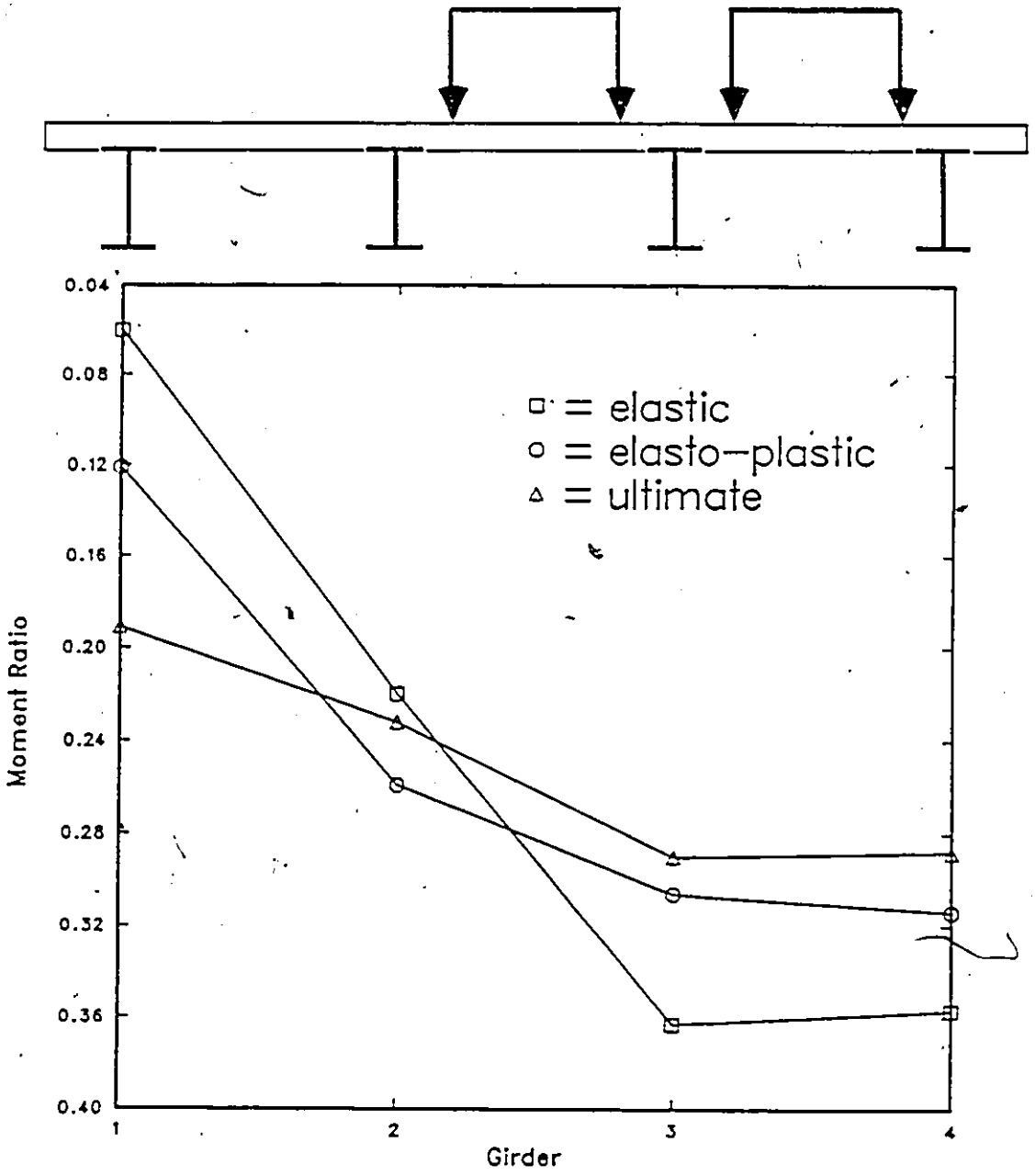

Figure 4.13: Transverse Moment Distribution, case PTS-2L .

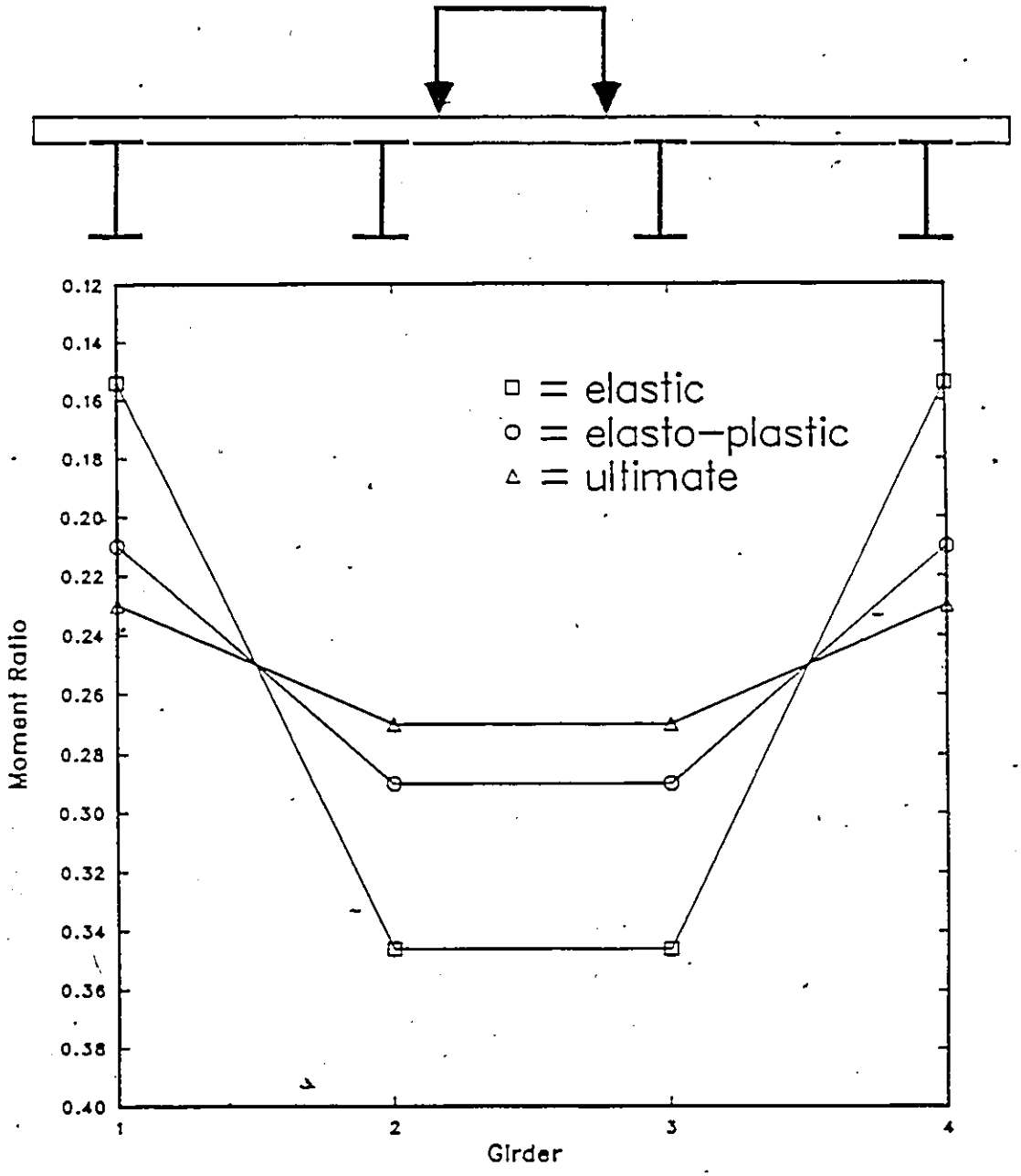

Figure 4.14: Transverse Moment Distribution, case PTS-1L .

Chapter 5

SUMMARY AND CONCLUSION

5.1 Summary

The objective of this thesis , given in chapter 1 , were as follow :

1. To study the elastic and inelastic behavior of the continuous slab-on-girder bridge model , in particular , the load distribution in both transverse and longitudinal directions.

2. To study the effect of diaphragms on the transverse load distribution.

3. To study the effect of the number of lanes loaded.

Background material on refined and simplified methods for the analysis of bridge superstructures was presented in chapter 2. Seven methods were briefly described, six refined methods and one simplified method. An analytical procedure including the loading system and idealization of the bridge was described in chapter 3.

In order to confirm the validity of "ADINA" that was used in the analysis, a simply supported span bridge of 18.29 m was compared with ADINA results presented in chapter 3 . Results were presented and discussed in chapter 4 . Finally ADINA-IN (input data) listings for the all cases are included in the appendix .

5.2 Conclusion

All conclusions made are restricted to the bridge model and those load configurations analyzed. Since only a few variations of a limited number of parameters were included, no design recommendation as such will be made. Only recommendations for future research will be offered.

1. The nonlinear finite element analysis program "ADINA" can be used efficiently and accurately in predicting stress distribution and complete nonlinear behavior of the composite slab-on-girder bridge. In applying ADINA to the analysis of the bridge , the numerical results will reflect the behavior of the bridge.

2. The distribution factors varied significantly from elastic stage to the ultimate stage. The transverse distribution factors started with a constant values in the elastic stage, after yielding occurred, a greater percentage of load was redistributed laterally to the exterior girders and longitudinally to the supports. In this manner, the structure attempts to utilize the full plastic capacity of all girders which , however , can only be achieved if the slab is capable of redistributing the load

3. The amount of longitudinal redistribution that will be required depends on the longitudinal position of the vehicle and the relative capacities of the bridge in sagging and hogging bending. These determine the ratios of live load flexural capacities to the elastic live load

more uniform these values are , the less longitudinal redistribution will be required.

4. Load distribution characteristics are dramatically improved when the number of the loaded lanes increased.

5. The load distribution factor, D, is improved between the elastic and the ultimate stages. For example, in the case of three lanes loaded, the D value at the interior girders improved by approximately 9%, this percentage increased up to 28% and 26% for the one and two lanes loaded respectively .

6. Significant reserve of capacity can exist between that based on elastic strength calculation for the most heavily loaded member and collapse of the entire structure. The magnitude of that reserve capacity for a specific positioning of the design vehicle will depend on the amount of longitudinal redistribution which is required before a collapse mechanism is complete.

7. The presence of the diaphragms will improve the transverse distribution factors.

8. One and two lane loaded cases would not govern the design of the bridge at ULS regardless of whether capacity is based on elastic strength calculations, plastic collapse, or any of the intermediate states identified as being critical .

9. The governing case for design purpose is generally a symmetrical one in which all lanes are loaded.

9. The governing case for design purpose is generally a symmetrical one in which all lanes are loaded.

5.3 Suggestion for Further Research

In this thesis, a number of questions arose which were not directly within the scope of this thesis . While time was not available to answer them here, the author feels that the following issues deserve further study :

1. Use of finite element procedures for design. Using parametric studies with finite element bridge models, it should be possible to develop design charts similar to, and perhaps more accurate than those currently used in the Ontario Code .

2. The ability of the slab to redistribute moments transversely while resisting the formation of longitudinal yield lines .

3. The effect of different transverse positions of the bridge vehicle on the redistribution patterns and the reserve capacities.

4. Additional variations in the bridge configurations considered, including the number and length of spans, the number of lanes, the number and spacing of girder, structure width, ...etc .

Bibliography

[1] ADINA-*A Finite Element Program for Automatic Dynamic Incremental Nonlinear Analysis*. Rep. ARD 84.6, ADINA-IN, Dec. 1984 .

[2] Ministry of Transportation and Communications:*Ontario Highway Bridge Design Code (OHBDC)*, 2nd edition, Downsview, Ont., 1983.

[3] American Association of State Highway and Transportation Officials (AASHTO), *Standared Specifications for Highway Bridges*, Washington, D.C. 1977.

[4] Canadian Institute of Steel Construction, *Handbook of Steel Construction*, 4th edition, Markham, Ont. 1950 .

[5] CSA, CAN3-S16.1-M78 : *Steel Structures for Buildings Limit States Design*, Rexdale, 1978 .

[6] Cheung, Y. K., *Finite Strip Method in Structural Analysis*, Oxford, Toronto, 1976 .

[7] Cusens, A.R. and Pama, R.P., *Bridge Deck Analysis*, Wiley, London, 1975 .

[8] Jaeger, L.G. and Bakht, B., The Grillage Analogy in Bridge Analysis, *Canadian Journal of Civil Engineering*, 1982, pp. 224-235 .

[9] W. W. Saders, Wheel Load Distribution in Highway and Railway Bridge, *Developement in Bridge Design and Construction.*

[10] Hendry, A. W. and Jaeger, L. G., *The Analysis of Grid Form Work and Related Structures*, Pretice-Hall, Englewood Cliff, N. J., 1958 .

[11] Yitahaki, D., *The Design of Prismatic and Cyinderical Shell Roofs* , Haifa Science Puplisher, 1958

[12] Robert D. Cook, *Concepts and Applications of Finite Element Analysis*, 2nd edition John and Sons Inc., Toronto, Canada, 1981.

[13] Zienkiewicz, O. C., *The Finite Element Method in Engineering Science*, McGraw Hill, New York, 1971 .

[14] Hambly, E. C., *Bridge Deck Behavior*, Champan and Hall, London, 1976 .

[15] Bakht, B. and Jaeger, L. G., *Bridge Analysis Simiplified*, McGraw Hill, 1985 .

[16] Conrad, P. and Heins, M., LFD Criteria for Composite Steel I-Beam Bridge, *Journal of The Structural Division*, Nov. 1980 .

[17] Gangarao, H. and Shakeri, A., Transverse load Distribution Factors for Rectangular Deck-Stringer Bridges, *Civil Engineering for Practicing and Design Engineers*, Vol. 4, pp.231-256, 1985 .

[18] Kennedy, J. B. and Grace, N. F., Load Distributioon in Continuous Composite Bridges, *Dep. of Civil Engineering, University of Windsor*, Windsor, Ont. 1983 .

[19] Dorton, R. A. and Csagrly, P. f., The development of The Ontario Bridge Code. Paper Prepared for the 1977 National Lecture Tour of Canadian Society for Civil Engineering, *Structural Division.*

[20] Bakht, B., Cheung, M. S. and Aziz, T. S., Application of a Simplified Method of Calculating Longitudinal Moments to the Ontario Highway Bridge Code, *Canadian Journal of Civil Engineering*, Vol. 6, No. 1, March 1979 .

[21] Conard, P., Heins, M. and Kuo, J. T., Ultimate Live Load Distribution Factor for Bridges, *Journal of The Structural Division*, ST7, July 1975

[22] Hondros, G. and Marsh, J. G., Load Distribution in Composite Girder-slab Systems, *Journal of Structural Division*, Vol. 86 No. ST11, 1960.

[23] Benjamin, C. F., Load Distribution of Diaphragms in I-Beam Bridges, *Journal of the Structural Division*, ST5 1959, pp. 17-55 .

[24] Hakala, M. K., A Nonlinear Finite Elemennt Analysis of Ice-strenghtened Ship Shell Structure,*Computers and Structures*, Vol. 12,

pp.541-547.

[25] Symko, Y., Transient Heat Conduction and Thermoelastic Analysis of Three-span Composite Highway Bridge,*Ph.D. Thesis, Civil Eng. Dep., University of Ottawa, 1980* .

[26] Amer, H. N. and Wegmuller, A. W., Nonlinear Response of Composite Factor for Bridges, *Journal of The Structural Division*, ST7, July 1975

[27] Kirkpatick, J., Long, A. E. and Thompson, A., Load Distribution Characteristics of M-Beam Bridge Decks, *The Structural engineer*, Vol. 6013 No. 2, June 1982 .

[28] Benjamin, C. F., Load Distribution of Diaphragms in I-Beam Bridges, Behavior of Concrete Beams, *St. Eng.*, Vol. 42, 1964, pp. 115-125.

[29] Chapman, J. C. and Balakrishman, S., Experiments on Composite Beams, *Str. Eng.*, Vol. 42, 1964, pp. 369-383 .

[30] Baranard, R. R. and Johnson, R. P., Ultimate Strength of Composite Beams, *PICE*, Part 2, Vol. 32, 1965 .

[31] Yam, L. C. and Chapman, J. C., The Inelastic Behavior of Simply-supported Composite Beams of Steel and Concrete, *PICE*, Part 2, Vol. 41, 1968 .

[32] Barnard, R. R. and Johnson, R. P., Plastic Behavior of Continuous Composite Beams, *PICE*, Part 2, Vol. 32, 1965, pp. 181-197 .

[33] Mallick, S. K. and Chattopadhyay, Ultimate Strength of Continuous Composite Beams, *Building Sceince*,Vol. 10, No.3, 1973, pp. 189-198.

[34] Lay, M. G., Flang Local Buckling in Wide-flange Shapes, Rectangular Plates: A Spline Technique Method of Solution. *ASCE*, Vol. 91, No. ST6, 1965, pp. 95-116 .

[35] Lukey, A. F., and Adams, P. F., Rotation Capacity of Beams Under Moment Gradient, *ASCE*, Vol. 95, n.ST6, 1969, pp. 1173-1188 .

[36] Lash, S. D. and Nagaraja, R., The Ultimate Load capacity of Beams and Slab Bridges, *Department of Highway Report No. RR-159*, Dep. of Highways, Ontario, 1970 .

[37] Heins, C. P. and Kuo, T. C., Ultimate Live Load Distribution Factors for Bridges, *ASCE*, Vol. 101, n.ST7, 1975, pp. 1481-1496 .

[38] Wegmuller, A. W., Overload behavior of Composite Steel-concrete Bridges, *ASCE*, vol. 103, n.ST9, 1977, pp.1799-1819 .

[39] Botzler, P. W. and Colville, J., Continuous Composite Bridge Model Test, *ASCE*, Vol.105, n.St9, 1979, pp. 1741-1755 .

[40] Cheung, M. S., Gardner, N. J. and Ng, S. F, Load Distribution Characteristics of Slab-on-girder Bridges at Ultimate, *Second International Conference on Short and Medium Span bridges, Proceedings*, Vol. 2, pp. 461-485, Ottawa, 1986 .

[41] Radkowski, A1, Bakht, B. and Billing, J. R, Design and Testing of 125 m Span Plate Girder bridge, *International Conference on Short and Medium Span bridges*, Toronto, 1982 .

[42] Mallick, S. K. and Chattopadhyay, Ultimate Strength of Continuous Composite Beams, *Building Sceince*,Vol. 10, No.3, 1973, pp. 189-198.

[43] Hamada, S. and Longworth, J., Ultimate Strength of Continuous Composite Beams, *ASCE*, Vol. 102, n.ST7, 1976, pp. 1463-1478 .

[44] Botzler, P. W., Colvill, J. and Heins, C. P., Ultimate Load Test of Continuous Composite Bridge Models, *Maryland University, College Park Dep. of Civil Engineering, C. E. Report no. 61*, June 1976 .

[45] Mahen, J. M., Redistribution of Moments in Slab-on-girder Bridge, *M.A.sc Thesis, University of Toronto, Dep. of Civil Eng., 1987* .

[46] Elling, C. W., Klingaer, R.E. and Burns, N. H., Distribution of Girder Loads in A Composite Highway Bridges,*Research Report 350-2, Reported for Fedral Highway Adminstration*, Austin, Tx., Dec. 1985 .

APPENDIX

```
'PLOTSIZE' 30 28
DATABASE CREATE
HEAD 'ADINA-IN for Case NTC'
MASTER IDOF=000C01 NSTEP=1
ITERATION M=BFGS
STIFFNESS-STEPS
EQUILIBRIUM-STEPS
PRINTOUT VOLUME=MIN IVC=0 IAC=0
TIMEFUNCTION 1
0 0.
1 1.0
PRINTNODES 1 1659 1
COORDINATES
ENTRIES NODE X Y Z
1 -1610 16186 277.75
21 -1610 11330 277.75
37 -1610 8317.4 277.75
49 -1610 5981 277.75
55 -1610 4856 277.75
63 -1610 3432.2 277.75
79 -1610 0 277.75
159 -1350 16186 277.75
237 -1350 0 277.75
633 0 16186 277.75
653 0 11330 277.75
669 0 8317.4 277.75
681 0 5981 277.75
687 0 4856 277.75
695 0 3432.2 277.75
711 0 0 277.75
949 -1401 16186 0
969 -1401 11330 0
985 -1401 8317.4 0
997 -1401 5981 0
1003 -1401 4856 0
1011 -1401 3432.2 0
1027 -1401 0 0
1107 -1299 16186 0
1127 -1299 11330 0
1143 -1299 8317.4 0
1155 -1299 5981 0
1161 -1299 4856 0
1169 -1299 3432.2 0
1185 -1299 0 0
1423 -501 16186 0
1443 -501 11330 0
1459 -501 8317.4 0
1471 -501 5981 0
1477 -501 4856 0
1485 -501 3432.2 0
```

```
1501 -501 0 0
1581 -399 16186 0
1601 -399 11330 0
1617 -399 8317.4 0
1629 -399 5981 0
1635 -399 4856 0
1643 -399 3432.2 0
1659 -399 0 0
LINE STRAIGHT N1=1 N2=21 EL=10 MID=1 NF=2 NS=1 R=1
LINE STRAIGHT N1=21 N2=37 EL=8 MID=1 NF=22 NS=1 R=1
LINE STRAIGHT N1=37 N2=49 EL=6 MID=1 NF=38
LINE STRAIGHT N1=49 N2=55 EL=3 MID=1 NF=50
LINE STRAIGHT N1=55 N2=63 EL=4 MID=1 NF=56
LINE STRAIGHT N1=63 N2=79 EL=8 MID=1 NF=64
LINE STRAIGHT N1=1 N2=159 EL=1 MID=1 NF=80 NS=79 R=1
LINE STRAIGHT N1=159 N2=633 EL=3 MID=1 NF=238 NS=79
LINE S N1=79 N2=237 EL=1 M=1 NF=158 NS=79
LINE S N1=237 N2=711 EL=3 M=1 NF=316 NS=79
LINE S N1=633 N2=653 EL=10 M=1 NF=634
LINE S N1=653 N2=669 EL=8 M=1 NF=654
LINE S N1=669 N2=681 EL=6 M=1 NF=670
LINE S N1=681 N2=687 EL=3 M=1 NF=682
LINE S N1=687 N2=695 EL=4 M=1 NF=688
LINE S N1=695 N2=711 EL=8 M=1 NF=696
LINE S N1=949 N2=969 EL=10 M=1 NF=950
LINE S N1=969 N2=985 EL=8 M=1 NF=970
LINE S N1=985 N2=997 EL=6 M=1 NF=986
LINE S N1=997 N2=1003 EL=3 M=1 NF=998
LINE S N1=1003 N2=1011 EL=4 M=1 NF=1004
LINE S N1=1011 N2=1027 EL=8 M=1 NF=1012
LINE S N1=1107 N2=1127 EL=10 M=1 NF=1108
LINE S N1=1127 N2=1143 EL=8 M=1 NF=1128
LINE S N1=1143 N2=1155 EL=6 M=1 NF=1144
LINE S N1=1155 N2=1161 EL=3 M=1 NF=1156
LINE S N1=1161 N2=1169 EL=4 MID=1 NF=1162
LINE STRAIGHT N1=1169 N2=1185 EL=8 MID=1 NF=1170
LINE STRAIGHT N1=1423 N2=1443 EL=10 MID=1 NF=1424
LINE STRAIGHT N1=1443 N2=1459 EL=8 MID=1 NF=1444
LINE STRAIGHT N1=1459 N2=1471 EL=6 MID=1 NF=1460
LINE STRAIGHT N1=1471 N2=1477 EL=3 MID=1 NF=1472
LINE S N1=1477 N2=1485 EL=4 M=1 NF=1478
LINE S N1=1485 N2=1501 EL=8 M=1 NF=1486
LINE S N1=1581 N2=1601 EL=10 M=1 NF=1582
LINE S N1=1601 N2=1617 EL=8 M=1 NF=1602
LINE S N1=1617 N2=1629 EL=6 M=1 NF=1618
LINE S N1=1629 N2=1635 EL=3 M=1 NF=1630
LINE S N1=1635 N2=1643 EL=4 M=1 NF=1636
LINE S N1=1643 N2=1659 EL=8 M=1 NF=1644
LINE COMBINED 1 79 21 37 49 55 63
LINE COMBINED 1 633 159
```

```
LINE C 79 711 237
LINE C 633 711 653 669 681 687 695
LINE C 949 1027 969 985 997 1003 1011
LINE C 1107 1185 1127 1143 1155 1161 1169
LINE C 1423 1501 1443 1459 1471 1477 1485
LINE C 1581 1659 1601 1617 1629 1635 1643
MATERIAL 1 ELASTIC E=4.358E4 NU=0.15 D=0. K=0.83333
MATERIAL 2 PLASTIC H=I E=2E5 NU=0.3 Y=304. ET=0. D=0.
EGROUP N=1 SHELL D=S M=1 RINT=3 SINT=3 TINT=2
GSURFACE 1 79 711 633 EL1=39 EL2=4 NO=9 NF=2 EF=1
THICKNESS 1 65.5
STRESSTABLE 1 1 2 3 4 5 6 7 8
EDATA
ENTRIES EL NTH TABLE
1 1 1
TO
156 1 1
EGROUP N=2 SHELL D=S M=2 RINT=3 SINT=5 TINT=2
GSURFACE 949 1027 1185 1107 EL1=39 EL2=1 NO=9 NF=950 EF=40
GSURFACE 1423 1501 1659 1581 EL1=39 EL2=1 NO=9 NF=1424 EF=118
COORDINATES
ENTRIES NODE X Y Z
712 -1350 16186 277.75
791 -1350 16186 138.875
870 -1350 16186 0
732 -1350 11330 277.75
811 -1350 11330 138.875
890 -1350 11330 0
748 -1350 8317.4 277.75
827 -1350 8317.4 138.875
906 -1350 8317.4 0
760 -1350 5981 277.75
839 -1350 5981 138.875
918 -1350 5981 0
766 -1350 4856 277.75
845 -1350 4856 138.875
924 -1350 4856 0
774 -1350 3432.2 277.75
853 -1350 3432.2 138.875
932 -1350 3432.2 0
1186 -450 16186 277.75
1265 -450 16186 138.875
1344 -450 16186 0
1206 -450 11330 277.75
1285 -450 11330 138.875
1364 -450 11330 0
1222 -450 8317.4 277.75
1301 -450 8317.4 138.875
1380 -450 8317.4 0
1234 -450 5981 277.75
```

```
1313 -450 5981 138.875
1392 -450 5981 0
1240 -450 4856 277.75
1319 -450 4856 138.875
1398 -450 4856 0
1248 -450 3432.2 277.75
1327 -450 3432.2 138.875
1406 -450 3432.2 0
NGENERATION TIMES=20 NSTEP=1 YSTEP=-242.8
712 STEP 79 TO 870
1186 STEP 79 TO 1344
ENODES
ENTRIES EL N1 N5 N2 N8 N13 N6 N4 N7 N3
1 712 713 714 791 792 793 870 871 872
79 1186 1187 1188 1265 1266 1267 1344 1345 1346
EGENERATION TIMES=9 ESTEP=1 NSTEP1=2
1 79
NGENERATION TIMES=16 NSTEP=1 YSTEP=-188.2875
732 STEP 79 TO 890
1206 STEP 79 TO 1364
ENODES
ENTRIES EL N1 N5 N2 N8 N13 N6 N4 N7 N3
11 732 733 734 811 812 813 890 891 892
89 1206 1207 1208 1285 1286 1287 1364 1365 1366
EGENERATION TIMES=7 ESTEP=1 NSTEP1=2
11 89
NGENERATION TIMES=12 NSTEP=1 YSTEP=-194.7
748 STEP 79 TO 906
1222 STEP 79 TO 1380
ENODES
ENTRIES EL N1 N5 N2 N8 N13 N6 N4 N7 N3
19 748 749 750 827 828 829 906 907 908
97 1222 1223 1224 1301 1302 1303 1380 1381 1382
EGENERATION TIMES=5 ESTEP=1 NSTEP1=2
19 97
NGENERATION TIMES=6 NSTEP=1 YSTEP=-187.5
760 STEP 79 TO 918
1234 STEP 79 TO 1392
ENODES
ENTRIES EL N1 N5 N2 N8 N13 N6 N4 N7 N3
25 760 761 762 839 840 841 918 919 920
103 1234 1235 1236 1313 1314 1315 1392 1393 1394
EGENERATION TIMES=2 ESTEP=1 NSTEP1=2
25 103
NGENERATION TIMES=8 NSTEP=1 YSTEP=-177.975
766 STEP 79 TO 924
1240 STEP 79 TO 1398
ENODES
ENTRIES EL N1 N5 N2 N8 N13 N6 N4 N7 N3
28 766 767 768 845 846 847 924 925 926
```

```
106 1240 1241 1242 1319 1320 1321 1398 1399 1400
EGENERATION TIMES=3 ESTEP=1 NSTEP1=2
28 106
NGENERATION TIMES=16 NSTEP=1 YSTEP=-214.5125
774 STEP 79 TO 932
1248 STEP 79 TO 1406
ENODES
ENTRIES EL N1 N5 N2 N8 N13 N6 N4 N7 N3
32 774 775 776 853 854 855 932 933 934
110 1248 1249 1250 1327 1328 1329 1406 1407 1408
EGENERATION TIMES=7 ESTEP=1 NSTEP1=2
32 110
THICKNESS 2 6.3
EDATA
ENTRIES EL NTH TABLE
1 2 2
TO
156 2 2
BOUNDARY IDOF=101001
949 STEP 79 TO 1107/870
1423 STEP 79 TO 1581/1344
969 STEP 79 TO 1127/890
1443 STEP 79 TO 1601/1364
1003 STEP 79 TO 1161/924
1477 STEP 79 TO 1635/1398
BOUNDARY IDOF=111001
1027 STEP 79 TO 1185/948
1501 STEP 79 TO 1659/1422
BOUNDARY IDOF=100011
633 TO 711
LIST BOUNDARY
CONSTRAINTS
712 1 159 1/TO/790 1 237 1
712 2 159 2/TO/790 2 237 2
712 3 159 3/TO/790 3 237 3
712 5 159 5/TO/790 5 237 5
1186 1 475 1/TO/1264 1 553 1
1186 2 475 2/TO/1264 2 553 2
1186 3 475 3/TO/1264 3 553 3
1186 5 475 5/TO/1264 5 553 5
871 1 1029 1/TO/947 1 1105 1
871 2 1029 2/TO/947 2 1105 2
871 3 1029 3/TO/947 3 1105 3
871 5 1029 5/TO/947 5 1105 5
DELETE 890 924
1345 1 1503 1/TO/1421 1 1579 1
1345 2 1503 2/TO/1421 2 1579 2
1345 3 1503 3/TO/1421 3 1579 3
1345 5 1503 5/TO/1421 5 1579 5
DELETE 1364 1398
```

```
870 2 1028 2
870 5 1028 5
890 2 1048 2
890 5 1048 5
924 2 1082 2
924 5 1082 5
948 5 1106 5
1344 2 1502 2
1344 5 1502 5
1364 2 1522 2
1364 5 1522 5
1398 2 1556 2
1398 5 1556 5
1422 5 1580 5
LOAD CONCENTRATED
195 3 -13150.
207 3 -9395.
221 3 -7515.
511 3 -29165.
525 3 -20830.
537 3 -16665.
FRAME
MESH NODES=11 ELEMENTS=1
ADINA
END
```

```
'PLOTSIZE' 30 28
DATABASE CREATE
HEAD 'ADINA-IN for Case PTC'
MASTER IDOF=000001 NSTEP=1
ITERATION M=BFGS
STIFFNESS-STEPS
EQUILIBRIUM-STEPS
PRINTOUT VOLUME=MIN IVC=0 IAC=0
TIMEFUNCTION 1
0 0.
1 7.44
PRINTNODES 1 1659 1
COORDINATES
ENTRIES NODE X Y Z
1 -1610 16186 277.75
21 -1610 11330 277.75
37 -1610 8534.6 277.75
49 -1610 6198.2 277.75
55 -1610 4856 277.75
63 -1610 3649.2 277.75
79 -1610 0 277.75
159 -1350 16186 277.75
237 -1350 0 277.75
633 0 16186 277.75
653 0 11330 277.75
669 0 8534.6 277.75
681 0 6198.2 277.75
687 0 4856 277.75
695 0 3649.2 277.75
711 0 0 277.75
949 -1401 16186 0
969 -1401 11330 0
985 -1401 8534.6 0
997 -1401 6198.2 0
1003 -1401 4856 0
1011 -1401 3649.2 0
1027 -1401 0 0
1107 -1299 16186 0
1127 -1299 11330 0
1143 -1299 8534.6 0
1155 -1299 6198.2 0
1161 -1299 4856 0
1169 -1299 3649.2 0
1185 -1299 0 0
1423 -501 16186 0
1443 -501 11330 0
1459 -501 8534.6 0
1471 -501 6198.2 0
1477 -501 4856 0
1485 -501 3649.2 0
```

```
1501 -501 0 0
1581 -399 16186 0
1601 -399 11330 0
1617 -399 8534.6 0
1629 -399 6198.2
1635 -399 4856 0
1643 -399 3649.2 0
1659 -399 0 0
LINE STRAIGHT N1=1 N2=21 EL=10 MID=1 NF=2 NS=1 R=1
LINE STRAIGHT N1=21 N2=37 EL=8 MID=1 NF=22 NS=1 R=1
LINE STRAIGHT N1=37 N2=49 EL=6 MID=1 NF=38
LINE STRAIGHT N1=49 N2=55 EL=3 MID=1 NF=50
LINE STRAIGHT N1=55 N2=63 EL=4 MID=1 NF=56
LINE STRAIGHT N1=63 N2=79 EL=8 MID=1 NF=64
LINE STRAIGHT N1=1 N2=159 EL=1 MID=1 NF=80 NS=79 R=1
LINE STRAIGHT N1=159 N2=633 EL=3 MID=1 NF=238 NS=79
LINE S N1=79 N2=237 EL=1 M=1 NF=158 NS=79
LINE S N1=237 N2=711 EL=3 M=1 NF=316 NS=79
LINE S N1=633 N2=653 EL=10 M=1 NF=634
LINE S N1=653 N2=669 EL=8 M=1 NF=654
LINE S N1=669 N2=681 EL=6 M=1 NF=670
LINE S N1=681 N2=687 EL=3 M=1 NF=682
LINE S N1=687 N2=695 EL=4 M=1 NF=688
LINE S N1=695 N2=711 EL=8 M=1 NF=696
LINE S N1=949 N2=969 EL=10 M=1 NF=950
LINE S N1=969 N2=985 EL=8 M=1 NF=970
LINE S N1=985 N2=997 EL=6 M=1 NF=986
LINE S N1=997 N2=1003 EL=3 M=1 NF=998
LINE S N1=1003 N2=1011 EL=4 M=1 NF=1004
LINE S N1=1011 N2=1027 EL=8 M=1 NF=1012
LINE S N1=1107 N2=1127 EL=10 M=1 NF=1108
LINE S N1=1127 N2=1143 EL=8 M=1 NF=1128
LINE S N1=1143 N2=1155 EL=6 M=1 NF=1144
LINE S N1=1155 N2=1161 EL=3 M=1 NF=1156
LINE S N1=1161 N2=1169 EL=4 MID=1 NF=1162
LINE STRAIGHT N1=1169 N2=1185 EL=8 MID=1 NF=1170
LINE STRAIGHT N1=1423 N2=1443 EL=10 MID=1 NF=1424
LINE STRAIGHT N1=1443 N2=1459 EL=8 MID=1 NF=1444
LINE STRAIGHT N1=1459 N2=1471 EL=6 MID=1 NF=1460
LINE STRAIGHT N1=1471 N2=1477 EL=3 MID=1 NF=1472
LINE S N1=1477 N2=1485 EL=4 M=1 NF=1478
LINE S N1=1485 N2=1501 EL=8 M=1 NF=1486
LINE S N1=1581 N2=1601 EL=10 M=1 NF=1582
LINE S N1=1601 N2=1617 EL=8 M=1 NF=1602
LINE S N1=1617 N2=1629 EL=6 M=1 NF=1618
LINE S N1=1629 N2=1635 EL=3 M=1 NF=1630
LINE S N1=1635 N2=1643 EL=4 M=1 NF=1636
LINE S N1=1643 N2=1659 EL=8 M=1 NF=1644
LINE COMBINED 1 79 21 37 49 55 63
LINE COMBINED 1 633 159
```

```
LINE C 79 711 237
LINE C 633 711 653 669 681 687 695
LINE C 949 1027 969 985 997 1003 1011
LINE C 1107 1185 1127 1143 1155 1161 1169
LINE C 1423 1501 1443 1459 1471 1477 1485
LINE C 1581 1659 1601 1617 1629 1635 1643
MATERIAL 1 ELASTIC E=4.358E4 NU=0.15 D=0. K=0.83333
MATERIAL 2 PLASTIC H=I E=2E5 NU=0.3 Y=304. ET=0. D=0.
EGROUP N=1 SHELL D=S M=1 RINT=3 SINT=3 TINT=2
GSURFACE 1 79 711 633 EL1=39 EL2=4 NO=9 NF=2 EF=1
THICKNESS 1 65.5
STRESSTABLE 1 1 2 3 4 5 6 7 8
EDATA
ENTRIES EL NTH TABLE
1 1 1
TO
156 1 1
EGROUP N=2 SHELL D=S M=2 RINT=3 SINT=5 TINT=2
GSURFACE 949 1027 1185 1107 EL1=39 EL2=1 NO=9 NF=950 EF=40
GSURFACE 1423 1501 1659 1581 EL1=39 EL2=1 NO=9 NF=1424 EF=118
COORDINATES
ENTRIES NODE X Y Z
712 -1350 16186 277.75
791 -1350 16186 138.875
870 -1350 16186 0
732 -1350 11330 277.75
811 -1350 11330 138.875
890 -1350 11330 0
748 -1350 8534.6 277.75
827 -1350 8534.6 138.875
906 -1350 8534.6 0
760 -1350 6198.2 277.75
839 -1350 6198.2 138.875
918 -1350 6198.2 0
766 -1350 4856 277.75
845 -1350 4856 138.875
924 -1350 4856 0
774 -1350 3649.2 277.75
853 -1350 3649.2 138.875
932 -1350 3649.2 0
1188 -450 16186 277.75
1265 -450 16186 138.875
1344 -450 16186 0
1206 -450 11330 277.75
1285 -450 11330 138.875
1364 -450 11330 0
1222 -450 8534.6 277.75
1301 -450 8534.6 138.875
1380 -450 8534.6 0
1234 -450 6198.2 277.75
```

```
1313 -450 6198.2 138.875
1392 -450 6198.2 0
1240 -450 4856 277.75
1319 -450 4856 138.875
1398 -450 4856 0
1248 -450 3649.2 277.75
1327 -450 3649.2 138.875
1406 -450 3649.2 0
NGENERATION TIMES=20 NSTEP=1 YSTEP=-242.8
712 STEP 79 TO 870
1186 STEP 79 TO 1344
ENODES
ENTRIES EL N1 N5 N2 N8 N13 N6 N4 N7 N3
1 712 713 714 791 792 793 870 871 872
79 1186 1187 1188 1265 1266 1267 1344 1345 1346
EGENERATION TIMES=9 ESTEP=1 NSTEP1=2
1 79
NGENERATION TIMES=16 NSTEP=1 YSTEP=-174.7125
732 STEP 79 TO 890
1206 STEP 79 TO 1364
ENODES
ENTRIES EL N1 N5 N2 N8 N13 N6 N4 N7 N3
11 732 733 734 811 812 813 890 891 892
89 1206 1207 1208 1285 1286 1287 1364 1365 1366
EGENERATION TIMES=7 ESTEP=1 NSTEP1=2
11 89
NGENERATION TIMES=12 NSTEP=1 YSTEP=-194.7
748 STEP 79 TO 906
1222 STEP 79 TO 1380
ENODES
ENTRIES EL N1 N5 N2 N8 N13 N6 N4 N7 N3
19 748 749 750 827 828 829 906 907 908
97 1222 1223 1224 1301 1302 1303 1380 1381 1382
EGENERATION TIMES=5 ESTEP=1 NSTEP1=2
19 97
NGENERATION TIMES=6 NSTEP=1 YSTEP=-223.7
760 STEP 79 TO 918
1234 STEP 79 TO 1392
ENODES
ENTRIES EL N1 N5 N2 N8 N13 N6 N4 N7 N3
25 760 761 762 839 840 841 918 919 920
103 1234 1235 1236 1313 1314 1315 1392 1393 1394
EGENERATION TIMES=2 ESTEP=1 NSTEP1=2
25 103
NGENERATION TIMES=8 NSTEP=1 YSTEP=-150.85
766 STEP 79 TO 924
1240 STEP 79 TO 1398
ENODES
ENTRIES EL N1 N5 N2 N8 N13 N6 N4 N7 N3
28 766 767 768 845 846 847 924 925 926
```

```
106 1240 1241 1242 1319 1320 1321 1398 1399 1400
EGENERATION TIMES=3 ESTEP=1 NSTEP1=2
28 106
NGENERATION TIMES=16 NSTEP=1 YSTEP=-228.075
774 STEP 79 TO 932
1248 STEP 79 TO 1406
ENODES
ENTRIES EL N1 N5 N2 N8 N13 N6 N4 N7 N3
32 774 775 776 853 854 855 932 933 934
110 1248 1249 1250 1327 1328 1329 1406 1407 1408
EGENERATION TIMES=7 ESTEP=1 NSTEP1=2
32 110
THICKNESS 2 6.3
EDATA
ENTRIES EL NTH TABLE
1 2 2
TO
156 2 2
BOUNDARY IDOF=101001
949 STEP 79 TO 1107/870
1423 STEP 79 TO 1581/1344
969 STEP 79 TO 1127/890
1443 STEP 79 TO 1601/1364
1003 STEP 79 TO 1161/924
1477 STEP 79 TO 1635/1398
BOUNDARY IDOF=111001
1027 STEP 79 TO 1185/948
1501 STEP 79 TO 1659/1422
BOUNDARY IDOF=100011
633 TO 711
LIST BOUNDARY
CONSTRAINTS
712 1 159 1/TO/790 1 237 1
712 2 159 2/TO/790 2 237 2
712 3 159 3/TO/790 3 237 3
712 5 159 5/TO/790 5 237 5
1186 1 475 1/TO/1264 1 553 1
1186 2 475 2/TO/1264 2 553 2
1186 3 475 3/TO/1264 3 553 3
1186 5 475 5/TO/1264 5 553 5
871 1 1029 1/TO/947 1 1105 1
871 2 1029 2/TO/947 2 1105 2
871 3 1029 3/TO/947 3 1105 3
871 5 1029 5/TO/947 5 1105 5
DELETE 890 924
1345 1 1503 1/TO/1421 1 1579 1
1345 2 1503 2/TO/1421 2 1579 2
1345 3 1503 3/TO/1421 3 1579 3
1345 5 1503 5/TO/1421 5 1579 5
DELETE 1364 1393
```

```
870 2 1028 2
870 5 1028 5
890 2 1048 2
890 5 1048 5
924 2 1082 2
924 5 1082 5
948 5 1106 5
1344 2 1502 2
1344 5 1502 5
1364 2 1522 2
1364 5 1522 5
1398 2 1556, 2
1398 5 1556 5
1422 5 1580 5
LOAD CONCENTRATED
195 3 -13150.
207 3 -9395.
221 3 -7515.
511 3 -29165.
523 3 -20830.
537 3 -16665.
FRAME
MESH NODES=11 ELEMENTS=1
ADINA
END
```

```
'PLOTSIZE' 30 28
DATABASE CREATE
HEAD 'ADINA-IN for Case PPS1'
MASTER IDOF=000001 NSTEP=1
ITERATION M=BFGS
STIFFNESS-STEPS
EQUILIBRIUM-STEPS
PRINTOUT VOLUME=MIN IPD=4 IDC=1 IVC=0 IAC=0
TIMEFUNCTION 1
0 0.
1 1.0
PRINTNODES 1 1100 1
COORDINATES
ENTRIES NODE X Y Z
1 -1610 8094 277.75
7 -1610 7015.5 277.75
17 -1610 4857 277.75
41 -1610 0 277.75
83 -1350 8094 277.75
123 -1350 0 277.75
329 0 8094 277.75
335 0 7015.5 277.75
345 0 4857 277.75
369 0 0 277.75
370 -1401 8094 0
376 -1401 7015.5 0
386 -1401 4857 0
410 -1401 0 0
452 -1299 8094 0
458 -1299 7015.5 0
468 -1299 4857 0
492 -1299 0 0
493 -501 8094 0
499 -501 7015.5 0
509 -501 4857 0
533 -501 0 0
575 -399 8094 0
581 -399 7015.5 0
591 -399 4857 0
615 -399 0 0
SHELLNODE DIRECTOR=-2 SYSTEM-D=L
83 -2 G TO 123 -2 G
247 -2 G TO 287 -2 G
411 -2 G TO 451 -2 G
534 -2 G TO 574 -2 G
697 -2 G STEP 41 TO 779 -2 G
689 -2 G STEP 41 TO 771 -2 G
681 -2 G STEP 41 TO 763 -2 G
673 -2 G STEP 41 TO 755 -2 G
663 -2 G STEP 41 TO 745 -2 G
```

```
902 -2 G STEP 41 TO 984 -2 G
894 -2 G STEP 41 TO 976 -2 G
886 -2 G STEP 41 TO 968 -2 G
878 -2 G STEP 41 TO 960 -2 G
868 -2 G STEP 41 TO 950 -2 G
LINE STRAIGHT N1=1 N2=7 EL=3 MID=1 NF=2 NS=1 R=1
LINE STRAIGHT N1=7 N2=17 EL=5 MID=1 NF=8 NS=1 R=1
LINE STRAIGHT N1=17 N2=41 EL=12 MID=1 NF=18
LINE STRAIGHT N1=1 N2=83 EL=1 MID=1 NF=42 NS=41 R=1
LINE STRAIGHT N1=83 N2=329 EL=3 MID=1 NF=124 NS=41
LINE S N1=41 N2=123 EL=1 M=1 NF=82 NS=41
LINE S N1=123 N2=369 EL=3 M=1 NF=164 NS=41
LINE S N1=329 N2=335 EL=3 M=1 NF=330
LINE S N1=335 N2=345 EL=5 M=1 NF=336
LINE S N1=345 N2=369 EL=12 M=1 NF=346
LINE S N1=370 N2=376 EL=3 M=1 NF=371
LINE S N1=376 N2=386 EL=5 M=1 NF=377
LINE S N1=386 N2=410 EL=12 M=1 NF=387
LINE S N1=452 N2=458 EL=3 M=1 NF=453
LINE S N1=458 N2=468 EL=5 M=1 NF=459
LINE S N1=468 N2=492 EL=12 M=1 NF=469
LINE S N1=493 N2=499 EL=3 M=1 NF=494
LINE S N1=499 N2=509 EL=5 M=1 NF=500
LINE S N1=509 N2=533 EL=12 M=1 NF=510
LINE S N1=575 N2=581 EL=3 M=1 NF=576
LINE S N1=581 N2=591 EL=5 M=1 NF=582
LINE S N1=591 N2=615 EL=12 M=1 NF=592
LINE COMBINED 1 41 7 17
LINE COMBINED 1 329 83
LINE C 41 369 123
LINE C 329 369 335 345
LINE C 370 410 376 386
LINE C 452 492 458 468
LINE C 493 533 499 509
LINE C 575 615 581 591
MATERIAL 1 ELASTIC E=4.358E4 NU=0.15 D=0. K=0.83333
MATERIAL 2 PLASTIC H=I E=2E5 NU=0.3 Y=304. ET=0. D=0.
MATERIAL 3 ELASTIC E=2E5 NU=.3 D=0. K=.83333
EGROUP N=1 SHELL D=S M=1 RINT=3 SINT=3 TINT=2
GSURFACE 1 41 369 329 EL1=20 EL2=4 NO=9 NF=2 EF=1
THICKNESS 1 65.5
STRESSTABLE 1 1 2 3 4 5 6 7 8
EDATA
ENTRIES EL NTH TABLE
1 1 1
TO
80 1 1
EGROUP N=2 SHELL D=S M=2 RINT=3 SINT=3 TINT=2
GSURFACE 370 410 492 452 EL1=20 EL2=1 NO=9 NF=371 EF=1
GSURFACE 493 533 615 575 EL1=20 EL2=1 NO=9 NF=494 EF=21
```

```
COORDINATES
ENTRIES NODE X Y Z
616 -1350 8094 243.03125
622 -1350 7015.5 243.03125
632 -1350 4857 243.03125
657 -1350 8094 208.3125
663 -1350 7015.5 208.3125
673 -1350 4857 208.3125
698 -1350 8094 138.875
704 -1350 7015.5 138.875
714 -1350 4857 138.875
739 -1350 8094 69.4375
745 -1350 7015.5 69.4375
755 -1350 4857 69.4375
780 -1350 8094 34.71875
786 -1350 7015.5 34.71875
796 -1350 4857 34.71875
411 -1350 8094 0
417 -1350 7015.5 0
427 -1350 4857 0
821 -450 8094 243.03125
827 -450 7015.5 243.03125
837 -450 4857 243.03125
862 -450 8094 208.3125
868 -450 7015.5 208.3125
878 -450 4857 208.3125
903 -450 8094 138.875
909 -450 7015.5 138.875
919 -450 4857 138.875
944 -450 8094 69.4375
950 -450 7015.5 69.4375
960 -450 4857 69.4375
985 -450 8094 34.71875
991 -450 7015.5 34.71875
1001 -450 4857 34.71875
534 -450 8094 0
540 -450 7015.5 0
550 -450 4857 0
NGENERATION TIMES=6 NSTEP=1 YSTEP=-179.75
83 247 411 534
616 STEP 41 TO 985
ENODES
ENTRIES EL N1 N5 N2 N8 N13 N6 N4 N7 N3
41 83 84 85 616 617 618 657 658 659
61 657 658 659 698 699 700 739 740 741
81 739 740 741 780 781 782 411 412 413
101 247 248 249 821 822 823 862 863 864
121 862 863 864 903 904 905 944 945 946
141 944 945 946 985 986 987 534 535 536
EGENERATION TIMES=2 ESTEP=1 NSTEP1=2
```

```
41 61 81 101 121 141
NGENERATION TIMES=10 NSTEP=1 YSTEP=-215.85
89 253 417 540
622 STEP 41 TO 991
ENODES
ENTRIES EL N1 N5 N2 N8 N13 N6 N4 N7 N3
44 89 90 91 622 623 624 663 664 665
64 663 664 665 704 705 706 745 746 747
84 745 746 747 786 787 788 417 418 419
104 253 254 255 827 828 829 868 869 870
124 868 869 870 909 910 911 950 951 952
144 950 951 952 991 992 993 540 541 542
EGENERATION TIMES=4 ESTEP=1 NSTEP1=2
44 64 84 104 124 144
NGENERATION TIMES=24 NSTEP=1 YSTEP=-202.375
99 263 427 550
632 STEP 41 TO 1001
ENODES
ENTRIES EL N1 N5 N2 N8 N13 N6 N4 N7 N3
49 99 100 101 632 633 634 673 674 675
69 673 674 675 714 715 716 755 756 757
89 755 756 757 796 797 798 427 428 429
109 263 264 265 837 838 839 878 879 880
129 878 879 880 919 920 921 960 961 962
149 960 961 962 1001 1002 1003 550 551 552
EGENERATION TIMES=11 ESTEP=1 NSTEP1=2
49 69 89 109 129 149
THICKNESS 2 6.3
STRESSTABLE 2 1 2 3 4
EDATA
ENTRIES EL NTH TABLE
1 2 2
TO
160 2 2
EGROUP N=3 SHELL D=S M=3 RINT=3 SINT=3 TINT=2
COORDINATES
ENTRIES NODE X Y Z
1026 -1125 0 208.3125
1031 -1125 0 138.875
1036 -1125 0 69.4375
1029 -225 0 208.3125
1034 -225 0 138.875
1039 -225 0 69.4375
1041 -1125 1619 208.3125
1046 -1125 1619 138.875
1051 -1125 1619 69.4375
1044 -225 1619 208.3125
1049 -225 1619 138.875
1054 -225 1619 69.4375
1056 -1125 3238 208.3125
```

```
1061 -1125 3238 138.875
1066 -1125 3238 69.4375
1059 -225 3238 208.3125
1064 -225 3238 138.875
1069 -225 3238 69.4375
1071 -1125 4857 208.3125
1076 -1125 4857 138.875
1081 -1125 4857 69.4375
1074 -225 4857 208.3125
1079 -225 4857 138.875
1084 -225 4857 69.4375
1086 -1125 7015.5 208.3125
1091 -1125 7015.5 138.875
1096 -1125 7015.5 69.4375
1089 -225 7015.5 208.3125
1094 -225 7015.5 138.875
1099 -225 7015.5 69.4375
NGENERATION TIMES=2 NSTEP=1 XSTEP=225.
1026 STEP 5 TO 1096
ENODES
ENTRIES EL N1 N5 N2 N8 N13 N6 N4 N7 N3
1 697 1026 1027 738 1031 1032 779 1036 1037
2 1027 1028 902 1032 1033 943 1037 1038 984
4 689 1041 1042 730 1046 1047 771 1051 1052
5 1042 1043 894 1047 1048 935 1052 1053 976
7 681 1056 1057 722 1061 1062 763 1066 1067
8 1057 1058 886 1062 1063 927 1067 1068 968
10 673 1071 1072 714 1076 1077 755 1081 1082
11 1072 1073 878 1077 1078 919 1082 1083 960
13 663 1086 1087 704 1091 1092 745 1096 1097
14 1087 1088 868 1092 1093 909 1097 1098 950
NGENERATION TIMES=1 NSTEP=1 XSTEP=225.
1029 STEP 5 TO 1099
ENODES
ENTRIES EL N1 N5 N2 N8 N13 N6 N4 N7 N3
3 902 1029 1030 943 1034 1035 984 1039 1040
6 894 1044 1045 935 1049 1050 976 1054 1055
9 886 1059 1060 927 1064 1065 968 1069 1070
12 878 1074 1075 919 1079 1080 960 1084 1085
15 868 1089 1090 909 1094 1095 950 1099 1100
THICKNESS 3 9.
THICKNESS 4 11.2
THICKNESS 5 16.4
STRESSTABLE 2 1 2 3 4
EDATA
ENTRIES EL NTH TABLE
1 3 2 TO 3 3 2
4 4 2 TO 9 4 2
10 5 2 TO 12 5 2
13 4 2 TO 15 4 2
```

```
BOUNDARY IDOF=101001
386 STEP 41 TO 468/427
509 STEP 41 TO 591/550
BOUNDARY IDOF=111001
410 STEP 41 TO 492/451
533 STEP 41 TO 615/574
BOUNDARY IDOF=100011
330 TO 369
1030 STEP 5 TO 1100
BOUNDARY IDOF=110111
329
BOUNDARY IDOF=010101
1 STEP 41 TO 288
370 STEP 41 TO 575
616 STEP 41 TO 985
LOAD CONCENTRATED
247 3 -72500. 1
FRAME
MESH NODES=11 ELEMENTS=1
ADINA
END
```

```
'PLOTSIZE' 30 28
DATABASE CREATE
HEAD 'ADINA-IN for Case PTS-2L'
MASTER IDOF=000001 NSTEP=1
ITERATION M=BFGS
STIFFNESS-STEPS
EQUILIBRIUM-STEPS
PRINTOUT VOLUME=MIN IVC=0 IAC=0
TIMEFUNCTION 1
0 0.
1 5.59
PRINTNODES 1 1517 1
COORDINATES
ENTRIES NODE X Y Z
1 -1610 4856 277.75
17 -1610 2914.6 277.75
33 -1610 578.4 277.75
37 -1610 0 277.75
75 -1350 4856 277.75
111 -1350 0 277.75
519 1350 4856 277.75
555 1350 0 277.75
593 1610 4856 277.75
609 1610 2914.6 277.75
625 1610 578.4 277.75
629 1610 0 277.75
741 -1401 4856 0
757 -1401 2914.6 0
773 -1401 578.4 0
777 -1401 0 0
815 -1299 4856 0
831 -1299 2914.6 0
847 -1299 578.4 0
851 -1299 0 0
963 -501 4856 0
979 -501 2914.6 0
995 -501 578.4 0
999 -501 0 0
1037 -399 4856 0
1053 -399 2914.6 0
1069 -399 578.4 0
1073 -399 0 0
1185 399 4856 0
1201 399 2914.6 0
1217 399 578.4 0
1221 399 0 0
1259 501 4856 0
1275 501 2914.6 0
1291 501 578.4
1295 501 0 0
```

```
1407 1299 4856 0
1423 1299 2914.6 0
1439 1299 578.4 0
1443 1299 0 0
1481 1401 4856 0
1497 1401 2914.6 0
1513 1401 578.4 0
1517 1401 0.0
LINE STRAIGHT N1=1 N2=17 EL=8 MID=1 NF=2 NS=1 R=1
LINE STRAIGHT N1=17 N2=33 EL=8 MID=1 NF=18 NS=1 R=1
LINE STRAIGHT N1=33 N2=37 EL=2 MID=1 NF=34
LINE STRAIGHT N1=1 N2=75 EL=1 MID=1 NF=38 NS=37 R=1
LINE STRAIGHT N1=75 N2=519 EL=6 MID=1 NF=112 NS=37
LINE S N1=519 N2=593 EL=1 M=1 NF=556 NS=37
LINE S N1=37 N2=111 EL=1 M=1 NF=74 NS=37
LINE S N1=111 N2=555 EL=6 M=1 NF=148 NS=37
LINE S N1=555 N2=629 EL=1 M=1 NF=592 NS=37
LINE S N1=593 N2=609 EL=8 M=1 NF=594 NS=1
LINE S N1=609 N2=625 EL=8 M=1 NF=610
LINE S N1=625 N2=629 EL=2 M=1 NF=626
LINE S N1=741 N2=757 EL=8 M=1 NF=742
LINE S N1=757 N2=773 EL=8 M=1 NF=758
LINE S N1=773 N2=777 EL=2 M=1 NF=774
LINE S N1=815 N2=831 EL=8 M=1 NF=816
LINE S N1=831 N2=847 EL=8 M=1 NF=832
LINE S N1=847 N2=851 EL=2 M=1 NF=848
LINE S N1=963 N2=979 EL=8 M=1 NF=964
LINE S N1=979 N2=995 EL=8 M=1 NF=980
LINE S N1=995 N2=999 EL=2 M=1 NF=996
LINE S N1=1037 N2=1053 EL=8 M=1 NF=1038
LINE S N1=1053 N2=1069 EL=8 M=1 NF=1054
LINE S N1=1069 N2=1073 EL=2 M=1 NF=1070
LINE S N1=1185 N2=1201 EL=8 M=1 NF=1186
LINE S N1=1201 N2=1217 EL=8 M=1 NF=1202
LINE S N1=1217 N2=1221 EL=2 M=1 NF=1218
LINE S N1=1259 N2=1275 EL=8 M=1 NF=1260
LINE S N1=1275 N2=1291 EL=8 M=1 NF=1276
LINE S N1=1291 N2=1295 EL=2 M=1 NF=1292
LINE S N1=1407 N2=1423 EL=8 M=1 NF=1408
LINE S N1=1423 N2=1439 EL=8 M=1 NF=1424
LINE S N1=1439 N2=1443 EL=2 M=1 NF=1440
LINE S N1=1481 N2=1497 EL=8 M=1 NF=1482
LINE S N1=1497 N2=1513 EL=8 M=1 NF=1498
LINE S N1=1513 N2=1517 EL=2 M=1 NF=1514
LINE COMBINED 1 37 17 33
LINE COMBINED 1 593 75 519
LINE C 37 629 111 555
LINE C 593 629 609 625
LINE C 741 777 757 773
LINE C 815 851 831 847
```

```
LINE C 963 999 979 995
LINE C 1037 1073 1053 1069
LINE C 1185 1221 1201 1217
LINE C 1259 1295 1275 1291
LINE C 1407 1443 1423 1439
LINE C 1481 1517 1497 1513
MATERIAL 1 ELASTIC E=4.358E4 NU=0.15 D=0. K=0.83333
MATERIAL 2 PLASTIC H=I E=2E5 NU=0.3 Y=304. ET=0. D=0.
EGROUP N=1 SHELL D=S M=1 RINT=3 SINT=3 TINT=2
GSURFACE 1 37 629 593 EL1=18 EL2=8 NO=9 NF=2 EF=1
THICKNESS 1 65.5
STRESSTABLE 1 1 2 3 4 5 6 7 8
EDATA
ENTRIES EL NTH TABLE
1 1 1
TO
144 1 1
EGROUP N=2 SHELL D=S M=2 RINT=3 SINT=5 TINT=2
GSURFACE 741 777 851 815 EL1=18 EL2=1 NO=9 NF=742 EF=19
GSURFACE 963 999 1073 1037 EL1=18 EL2=1 NO=9 NF=964 EF=55
GSURFACE 1185 1221 1295 1259 EL1=18 EL2=1 NO=9 NF=1186 EF=91
GSURFACE 1407 1443 1517 1481 EL1=18 EL2=1 NO=9 NF=1408 EF=127
COORDINATES
ENTRIES NODE X Y Z
630 -1350 4856 277.75
667 -1350 4856 138.875
704 -1350 4856 0
646 -1350 2914.6 277.75
683 -1350 2914.6 138.875
720 -1350 2914.6 0
662 -1350 578.4 277.75
699 -1350 578.4 138.875
736 -1350 578.4 0
852 -450 4856 277.75
889 -450 4856 138.875
926 -450 4856 0
868 -450 2914.6 277.75
905 -450 2914.6 138.875
942 -450 2914.6 0
884 -450 578.4 277.75
921 -450 578.4 138.875
958 -450 578.4 0
1074 450 4856 277.75
1111 450 4856 138.875
1148 450 4856 0
1090 450 2914.6 277.75
1127 450 2914.6 138.875
1164 450 2914.6 0
1106 450 578.4 277.75
1143 450 578.4 138.875
```

```
1180 450 578.4 0
1296 1350 4856 277.75
1333 1350 4856 138.875
1370 1350 4856 0
1312 1350 2914.6 277.75
1349 1350 2914.6 138.875
1386 1350 2914.6 0
1328 1350 578.4 277.75
1365 1350 578.4 138.875
1402 1350 578.4 0
NGENERATION TIMES=16 NSTEP=1 YSTEP=-121.3375
630 STEP 37 TO 704
852 STEP 37 TO 926
1074 STEP 37 TO 1148
1296 STEP 37 TO 1370
ENODES
ENTRIES EL N1 N5 N2 N8 N13 N6 N4 N7 N3
1 630 631 632 667 668 669 704 705 706
37 852 853 854 889 890 891 926 927 928
73 1074 1075 1076 1111 1112 1113 1148 1149 1150
109 1296 1297 1298 1333 1334 1335 1370 1371 1372
EGENERATION TIMES=7 ESTEP=1 NSTEP1=2
1 37 73 109
NGENERATION TIMES=16 NSTEP=1 YSTEP=-146.0125
646 STEP 37 TO 720
868 STEP 37 TO 942
1090 STEP 37 TO 1164
1312 STEP 37 TO 1386
ENODES
ENTRIES EL N1 N5 N2 N8 N13 N6 N4 N7 N3
9 646 647 648 683 684 685 720 721 722
45 868 869 870 905 906 907 942 943 944
81 1090 1091 1092 1127 1128 1129 1164 1165 1166
117 1312 1313 1314 1349 1350 1351 1386 1387 1388
EGENERATION TIMES=7 ESTEP=1 NSTEP1=2
9 45 81 117
NGENERATION TIMES=4 NSTEP=1 YSTEP=-144.6
662 STEP 37 TO 736
884 STEP 37 TO 958
1106 STEP 37 TO 1180
1328 STEP 37 TO 1402
ENODES
ENTRIES EL N1 N5 N2 N8 N13 N6 N4 N7 N3
17 662 663 664 699 700 701 736 737 738
53 884 885 886 921 922 923 958 959 960
89 1106 1107 1108 1143 1144 1145 1180 1181 1182
125 1328 1329 1330 1365 1366 1367 1402 1403 1404
EGENERATION TIMES=1 ESTEP=1 NSTEP1=2
17 53 89 125
THICKNESS 2 6.3
```

```
EDATA
ENTRIES EL NTH TABLE
1 2 2
TO
144 2 2
BOUNDARY IDOF=101001
741 STEP 37 TO 815/704
963 STEP 37 TO 1037/926
1185 STEP 37 TO 1259/1148
1407 STEP 37 TO 1481/1370
BOUNDARY IDOF=111001
777 STEP 37 TO 851/740
999 STEP 37 TO 1073/962
1221 STEP 37 TO 1295/1184
1443 STEP 37 TO 1517/1406
LIST BOUNDARY
CONSTRAINTS
630 1 75 1/TO/666 1 111 1
630 2 75 2/TO/666 2 111 2
630 3 75 3/TO/666 3 111 3
630 5 75 5/TO/666 5 111 5
852 1 223 1/TO/888 1 259 1
852 2 223 2/TO/888 2 259 2
852 3 223 3/TO/888 3 259 3
852 5 223 5/TO/888 5 259 5
1074 1 371 1/TO/1110 1 407 1
1074 2 371 2/TO/1110 2 407 2
1074 3 371 3/TO/1110 3 407 3
1074 5 371 5/TO/1110 5 407 5
1296 1 519 1/TO/1332 1 555 1
1296 2 519 2/TO/1332 2 555 2
1296 3 519 3/TO/1332 3 555 3
1296 5 519 5/TO/1332 5 555 5
705 1 779 1/TO/739 1 813 1
705 2 779 2/TO/739 2 813 2
705 3 779 3/TO/739 3 813 3
705 5 779 5/TO/739 5 813 5
927 1 1001 1/TO/961 1 1035 1
927 2 1001 2/TO/961 2 1035 2
927 3 1001 3/TO/961 3 1035 3
927 5 1001 5/TO/961 5 1035 5
1149 1 1223 1/TO/1183 1 1257 1
1149 2 1223 2/TO/1183 2 1257 2
1149 3 1223 3/TO/1183 3 1257 3
1149 5 1223 5/TO/1183 5 1257 5
1371 1 1445 1 /TO/1405 1 1479 1
1371 2 1445 2 /TO/1405 2 1479 2
1371 3 1445 3 /TO/1405 3 1479 3
1371 5 1445 5 /TO/1405 5 1479 5
704 2 778 2
```

```
704 5 778 5
926 2 1000 2
926 5 1000 5
1148 2 1222 2
1148 5 1222 5
1370 2 1444 2
1370 5 1444 5
740 5 814 5
962 5 1036 5
1184 5 1258 5
1406 5 1480 5
LOAD CONCENTRATED
91 3 700. 1
107 3 500. 1
239 3 -13020. 1
255 3 -37200. 1
387 3 -31305. 1
403 3 -22360. 1
535 3 -12795. 1
551 3 -9140. 1
FRAME
MESH NODES=11 ELEMENTS=1
ADINA
END
```

```
'PLOTSIZE' 30 28
DATABASE CREATE
HEAD 'ADINA-IN for Case PTS-1L and PTS-3L'
MASTER IDOF=000001 NSTEP=1
ITERATION M=BFGS
TOL E=.01 I=30
STIFFNESS-STEPS
EQUILIBRIUM-STEPS
PRINTOUT VOLUME=MIN IVC=0 IAC=0
TIMEFUNCTION 1
0 0.
1 1.
PRINTNODES 1 777 1
COORDINATES
ENTRIES NODE X Y Z
1 -1610 4856 277.75
17 -1610 2914.6 277.75
33 -1610 578.4 277.75
37 -1610 0 277.75
75 -1350 4856 277.75
111 -1350 0 277.75
297 0 4856 277.75
313 0 2914.6 277.75
329 0 578.4 277.75
333 0 0 277.75
445 -1401 4856 0
461 -1401 2914.6 0
477 -1401 578.4 0
481 -1401 0 0
519 -1299 4856 0
535 -1299 2914.6 0
551 -1299 578.4 0
555 -1299 0 0
667 -501 4856 0
683 -501 2914.6 0
699 -501 578.4 0
703 -501 0 0
741 -399 4856 0
757 -399 2914.6 0
773 -399 578.4 0
777 -399 0 0
LINE STRAIGHT N1=1 N2=17 EL=8 MID=1 NF=2 NS=1 R=1
LINE STRAIGHT N1=17 N2=33 EL=8 MID=1 NF=18 NS=1 R=1
LINE STRAIGHT N1=33 N2=37 EL=2 MID=1 NF=34
LINE STRAIGHT N1=1 N2=75 EL=1 MID=1 NF=38 NS=37 R=1
LINE STRAIGHT N1=75 N2=297 EL=3 MID=1 NF=112 NS=37
LINE S N1=37 N2=111 EL=1 M=1 NF=74 NS=37
LINE S N1=111 N2=333 EL=3 M=1 NF=148 NS=37
LINE S N1=297 N2=313 EL=8 M=1 NF=298
LINE S N1=313 N2=329 EL=8 M=1 NF=314
```

```
LINE S N1=329 N2=333 EL=2 M=1 NF=330
LINE S N1=445 N2=461 EL=8 M=1 NF=446
LINE S N1=461 N2=477 EL=8 M=1 NF=462
LINE S N1=477 N2=481 EL=2 M=1 NF=478
LINE S N1=519 N2=535 EL=8 M=1 NF=520
LINE S N1=535 N2=551 EL=8 M=1 NF=536
LINE S N1=551 N2=555 EL=2 M=1 NF=552
LINE S N1=667 N2=683 EL=8 M=1 NF=668
LINE S N1=683 N2=699 EL=8 M=1 NF=684
LINE S N1=699 N2=703 EL=2 M=1 NF=700
LINE S N1=741 N2=757 EL=8 M=1 NF=742
LINE S N1=757 N2=773 EL=8 M=1 NF=758
LINE S N1=773 N2=777 EL=2 M=1 NF=774
LINE COMBINED 1 37 17 33
LINE COMBINED 1 297 75
LINE C 37 333 111
LINE C 297 333 313 329
LINE C 445 481 461 477
LINE C 519 555 535 551
LINE C 667 703 683 699
LINE C 741 777 757 773
MATERIAL 1 ELASTIC E=4.358E4 NU=0.15 D=0. K=0.83333
MATERIAL 2 PLASTIC H=I E=2E5 NU=0.3 Y=304. ET=0. D=0.
EGROUP N=1 SHELL D=S M=1 RINT=3 SINT=3 TINT=2
GSURFACE 1 37 333 297 EL1=18 EL2=4 NO=9 NF=2 EF=1
THICKNESS 1 65.5
STRESSTABLE 1 1 2 3 4 5 6 7 8
EDATA
ENTRIES EL NTH TABLE
1 1 1
TO
72 1 1
EGROUP N=2 SHELL D=S M=2 RINT=3 SINT=5 TINT=2
GSURFACE 445 481 555 519 EL1=18 EL2=1 NO=9 NF=446 EF=19
GSURFACE 667 703 777 741 EL1=18 EL2=1 NO=9 NF=668 EF=55
COORDINATES
ENTRIES NODE X Y Z
334 -1350 4856 277.75
371 -1350 4856 138.875
408 -1350 4856 0
350 -1350 2914.6 277.75
387 -1350 2914.6 138.875
424 -1350 2914.6 0
366 -1350 578.4 277.75
403 -1350 578.4 138.875
440 -1350 578.4 0
556 -450 4856 277.75
593 -450 4856 138.875
630 -450 4856 0
572 -450 2914.6 277.75
```

```
609 -450 2914.6 138.875
646 -450 2914.6 0
588 -450 578.4 277.75
625 -450 578.4 138.875
662 -450 578.4 0
NGENERATION TIMES=16 NSTEP=1 YSTEP=-121.3375
334 STEP 37 TO 408
556 STEP 37 TO 630
ENODES
ENTRIES EL N1 N5 N2 N8 N13 N6 N4 N7 N3
1 334 335 336 371 372 373 408 409 410
37 556 557 558 593 594 595 630 631 632
EGENERATION TIMES=7 ESTEP=1 NSTEP1=2
1 37
NGENERATION TIMES=16 NSTEP=1 YSTEP=-146.0125
350 STEP 37 TO 424
572 STEP 37 TO 646
ENODES
ENTRIES EL N1 N5 N2 N8 N13 N6 N4 N7 N3
9 350 351 352 387 388 389 424 425 426
45 572 573 574 609 610 611 646 647 648
EGENERATION TIMES=7 ESTEP=1 NSTEP1=2
9 45
NGENERATION TIMES=4 NSTEP=1 YSTEP=-144.6
366 STEP 37 TO 440
588 STEP 37 TO 662
ENODES
ENTRIES EL N1 N5 N2 N8 N13 N6 N4 N7 N3
17 366 367 368 403 404 405 440 441 442
53 588 589 590 625 626 627 662 663 664
EGENERATION TIMES=1 ESTEP=1 NSTEP1=2
17 53
THICKNESS 2 6.3
EDATA
ENTRIES EL NTH TABLE
1 2 2
TO
72 2 2
BOUNDARY IDOF=101001
445 STEP 37 TO 519/408
667 STEP 37 TO 741/630
BOUNDARY IDOF=111001
481 STEP 37 TO 555/444
703 STEP 37 TO 777/666
BOUNDARY IDOF=100011
297 TO 333
LIST BOUNDARY
CONSTRAINTS
334 1 75 1/TO/370 1 111 1
334 2 75 2/TO/370 2 111 2
```

```
334 3 75 3/TO/370 3 111 3
334 5 75 5/TO/370 5 111 5
556 1 223 1/TO/592 1 259 1
556 2 223 2/TO/592 2 259 2
556 3 223 3/TO/592 3 259 3
556 5 223 5/TO/592 5 259 5
409 1 483 1/TO/443 1 517 1
409 2 483 2/TO/443 2 517 2
409 3 483 3/TO/443 3 517 3
409 5 483 5/TO/443 5 517 5
631 1 705 1/TO/665 1 739 1
631 2 705 2/TO/665 2 739 2
631 3 705 3/TO/665 3 739 3
631 5 705 5/TO/665 5 739 5
408 2 482 2
408 5 482 5
630 5 704 5
630 2 704 2
444 5 518 5
666 5 740 5
LOAD CONCENTRATED
91 3 1055. 1
107 3 755. 1
239 3 -15160. 1
255 3 -10830. 1
FRAME
MESH NODES=11 ELEMENTS=1
ADINA
END
```